Utrecht University
Faculty of Geosciences
Department of Earth Sciences

Elodie Duyck – Where does the freshwater go?

ISSN 2211-4335

USES 294

294

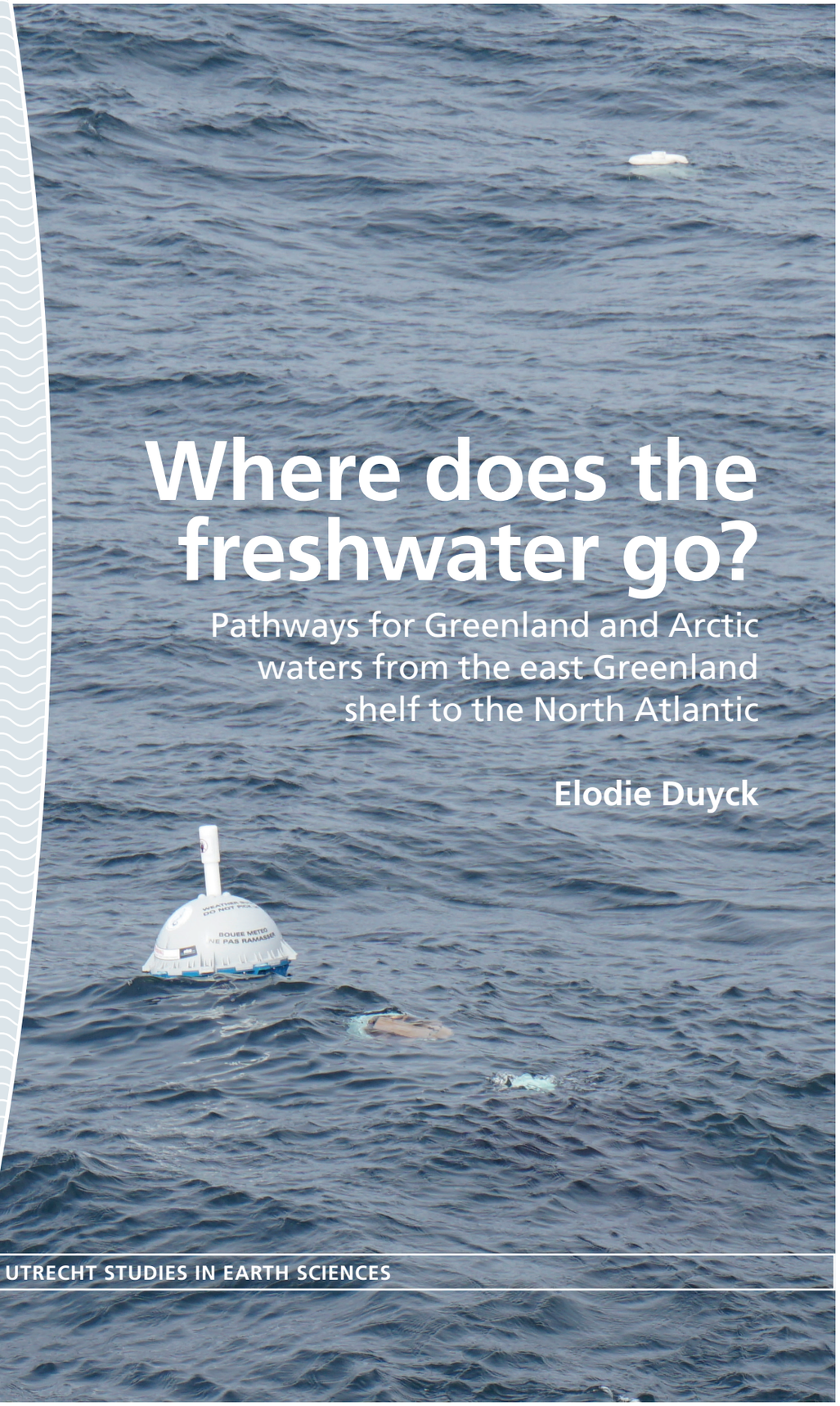

Where does the freshwater go?

Pathways for Greenland and Arctic waters from the east Greenland shelf to the North Atlantic

Elodie Duyck

UTRECHT STUDIES IN EARTH SCIENCES

Where does the freshwater go?

Pathways for Greenland and Arctic waters from the east Greenland shelf to the North Atlantic

Elodie Duyck

NIOZ, Royal Netherlands Institute for Sea Research

Author information: ORCID 0000-0001-9333-703X
elodie.duyck@uni-hamburg.de

Cover picture by Femke de Jong. Deployment of surface drifters at Cape Farewell from the R/V Pelagia in July 2020.
Cover design by Margot Stoete.

ISBN 978-90-6266-666-9
USES 294
https://doi.org/10.33540/1989

Printed in the Netherlands by Ipskamp.

Where does the freshwater go? Pathways for Greenland and Arctic waters from the east Greenland shelf to the North Atlantic

Het pad van zoetwater: trajecten van Groenlandse en Arctische wateren van de Groenlandse oostkust naar de Noord-Atlantische Oceaan
(met een samenvatting in het Nederlands)

De la côte est du Groënland jusqu'à l'Atlantique Nord: Où vont les eaux douces du Groënland et de l'Arctique?
(avec un résumé en français)

Proefschrift

ter verkrijging van de graad van doctor aan de
Universiteit Utrecht
op gezag van de
rector magnificus, prof.dr. H.R.B.M. Kummeling,
ingevolge het besluit van het college voor promoties
in het openbaar te verdedigen op

maandag 30 oktober 2023 des middags te 2.15 uur

door

Elodie Anne Marie Duyck

geboren op 10 september 1994
te Villeneuve d'Ascq, Frankrijk

Promotor:

Prof. dr. G.J. Reichart

Copromotor:

Dr. F. de Jong

Beoordelingscommissie:

Prof. dr. M.R. van den Broeke
Prof. dr. C.A. Katsman
Dr. T. Martin
Prof. dr. P.G. Myers
Prof. dr. E. van Sebille

The work presented in this thesis was supported by the NWO VIDI grant 016.Vidi.189.130

Table of Contents

Chapter 1

Introduction

"It is very likely that the Atlantic Meridional Overturning Circulation will decline in the 21st century, but there is low confidence in the model's projected timing and magnitude.
In addition, freshwater from the melting of the Greenland Ice Sheet could further enhance the future weakening of AMOC in the 21st century"
IPCC AR6 WG1 section 9.2.3.1, 2019

Illustration: SVP drifters waiting to be unpacked and deployed on the deck of the Adolph Jensen in August 2019. They will be deployed upstream of Sermilik Trough.

1.1 The Atlantic Meridional Overturning Circulation

In the Atlantic, the ocean circulation transports warm, light waters, northwards at the surface, and cold, dense waters, southwards at depth. This large-scale circulation is called Atlantic Meridional Overturning Circulation, or AMOC (Figure 1). It constitutes the Atlantic part of the global meridional overturning circulation that is often represented as a simplified conveyor belt, redistributing heat and freshwater across the ocean.

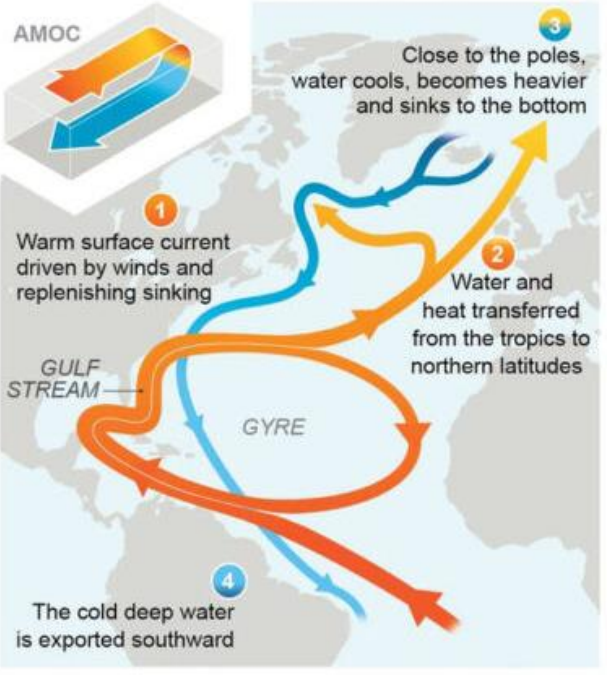

Figure 1.1: *Simplified schematic of the Atlantic Meridional Overturning Circulation in the North Atlantic. Red colors symbolize warm surface waters, and blue colors dense cold waters. From Fox-Kemper et al 2021.*

The AMOC is a key element of the climate system: It carries about 0.5 PW of heat across the equator (Buckley and Marshall 2016), leading to the northern hemisphere being warmer than the southern hemisphere, with consequences for instance on the location of tropical precipitations (Frierson et al 2013). Because it connects the surface and the deep circulation, the AMOC also contributes to storing excess heat and anthropogenic carbon to the deep ocean (Perez et al 2013, Kostov et al 2014). Climate change is predicted to lead to a weakening of the AMOC in the coming century, which would have a large impact on global and regional climates and could severely affect people and ecosystems (Fox-Kemper et al 2021, Collins et al 2019). A weaker AMOC could for

example lead to increased winter storms and changed precipitation patterns in Europe, and to reduced rainfall in the Sahel and south-Asian regions which could affect crop production (Jackson et al 2015, Collins et al 2019, Zhang et al 2019, figure 2).

Figure 1.2: *Potential global impacts of a weakening of the AMOC on the climate system, ecosystems, and people. From Collins et al 2019.*

A key driver of the AMOC is the formation of deep waters in the Subpolar North Atlantic (SPNA). As the warm, saline surface waters from the upper branch of the AMOC reach the SPNA, they lose heat to the atmosphere, thereby getting colder and denser. This leads to the formation of North Atlantic Deep Water, that is exported southwards at depth by the Deep Western Boundary Current, and by more complex interior pathways (Buckley and Marshall 2016). These deep waters reach the surface again many years later, far from the SPNA, in the Southern Ocean, Indian Ocean and Pacific Ocean, due to wind-driven upwelling and diapycnal mixing (Johnson et al 2019, Marshall and Speer 2012, Talley 2013). In the coming decades, climate change is expected to lead to a warming of the SPNA, an increase in net precipitations, and increasing freshwater input from the Greenland Ice Sheet (Goelzer et al 2020, Fox-Kemper et al 2021) and the Arctic (Holland et al 2006, Haine 2020). These changes will make surface waters lighter in the SPNA, which will lead to increased stratification of the upper ocean. The increased stratification of the upper layer of the SPNA could inhibit the formation of North Atlantic Deep Water, and weaken the overturning circulation.

Models from the 6th generation of the Coupled Model Intercomparison project (CMIP6) all show a decline of the AMOC in the 21st century as a response to increasing CO2 emissions (Weijer et al 2020, Fox-Kemper et al 2021, Figure 3). Additional freshwater input to the Subpolar North Atlantic from the Greenland ice sheet is neglected in these models and could lead to further weakening of the AMOC (Fox-Kemper et al 2021).

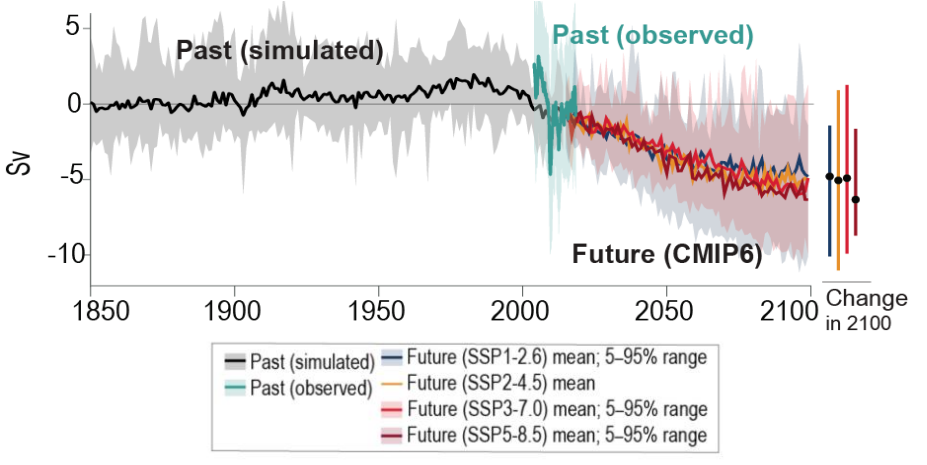

***Figure 1.3**: Evolution of AMOC transport at 26°N in four climate scenarios, relative to 1995-2014. The scenarios are the IPCC shared socioeconomic pathways, with SSP1-2.6 corresponding to low carbon emissions and SSP5-8.5 to high carbon emissions. The strength of the AMOC corresponds to the vertical maximum of the northward volume transport across the Atlantic and is here given in Sverdrups (1Sv=1e6m3s-1). From Chen et al 2021.*

The sensitivity of the AMOC to freshwater in the SPNA has been the focus of a range of studies arguing that a sudden increase of freshwater to the SPNA, for instance due to an accelerated melt of the Greenland ice sheet, could lead to an abrupt weakening of the AMOC, potentially even its collapse and tipping to another state (e.g Stommel et al 1961, Manabe and Stouffer 1988, Weijer et al 2019). Paleoclimate studies suggest that such transitions happened in the past and were associated with abrupt climate changes (Broeker et al 1985, Rahmstorf 2002, Lynch-Stieglietz et al 2017). The stability of the AMOC and the climate response to an AMOC shutdown have been investigated by modelling experiments called hosing (e.g Stouffer et al 2006, Jackson and Wood 2018, Jackson et al 2023), in which large amounts of freshwater are released over the subpolar region, inhibiting the formation of deep waters. Meltwater from Greenland is however released in much smaller amounts, around the coast of Greenland, and is advected over the Greenland continental shelf in narrow western boundary currents. To impact the formation of deep waters, Greenland meltwater first needs to leave the boundary current and enter the interior of the SPNA (Marsh et al 2010, Condron and Windsor 2011). Studies that released more realistic amounts of freshwater at the coast found a

limited impact of Greenland melt on AMOC weakening (Bakker et al 2016, Weijer et al 2012). There are however remaining uncertainties on the exact pathways of fresh waters from the Greenland continental shelf to the interior of the SPNA, and on how well these are represented in models at different resolutions.

1.2. The Subpolar North Atlantic

To better constrain the future evolution of the AMOC, we need to understand how waters originating from the Arctic and Greenland circulate around the SPNA and how they reach deep convection regions.

1.2.1 Surface circulation in the SPNA

Warm, saline, subtropical waters enter the SPNA via the North Atlantic Current. A part of these waters continues north over the Greenland Scotland ridge, towards the Nordic Seas (Iceland Sea, Greenland Sea, Norwegian Sea) and Fram Strait, while the rest (re)circulates within the subpolar gyre, in the rim currents of the Iceland Basin, Irminger Sea and Labrador Sea (Hansen and Østerhus 2000, Daniault et al 2016, Holiday et al 2018). Relatively fresh Polar Surface Water (Rudels 2002) enters the SPNA via Fram Strait, to the northeast of Greenland, and the Canadian Arctic Archipelago and Davis Strait, to the west of Greenland (e.g Aagard and Carmack 1988, Haine et al 2015). These waters circulate over the continental shelf of Greenland and over the Labrador shelf, and there is a sharp temperature and salinity front between the cold and relatively fresh waters found over the continental shelf and the warmer, saltier waters of the interior seas. Surface shelf waters are transported downstream by the East Greenland Current (EGC), West Greenland Current (WGC) and Labrador Current, which are all surface intensified, buoyant, western boundary currents. The Labrador Current joins the Gulf Stream south of the Subpolar Gyre to form the North Atlantic Current. Figure 4 summarizes the surface circulation of the SPNA and important topographic features.

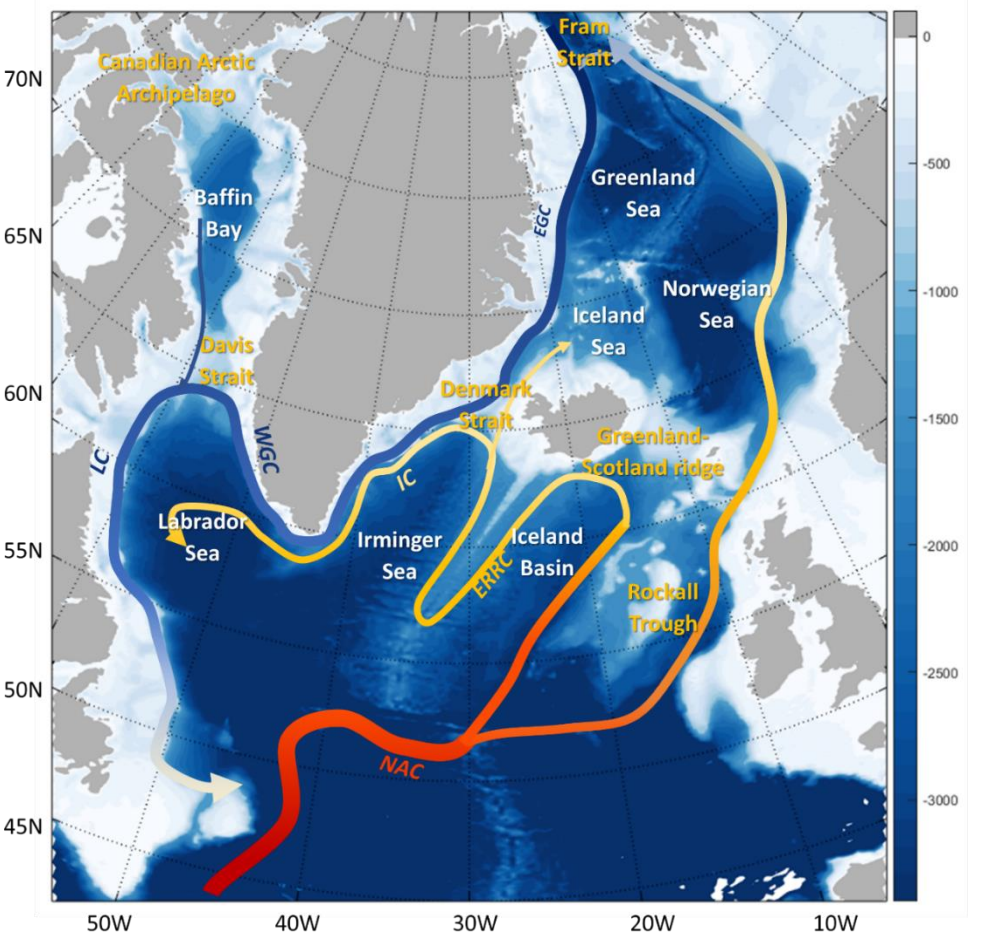

Figure 1.4: *Simplified surface circulation map of the SPNA. EGC: East Greenland Current, WGC: West Greenland Current. LC: Labrador Current. NAC: North Atlantic Current. ERRC: East Reykjanes Ridge Current. IC: Irminger Current.*

1.2.2 Deep water formation and overturning in the SPNA

The formation of dense, deep waters takes place in the interior seas of the SPNA and in their boundary currents. In these interior seas, a cyclonic circulation and Ekman pumping create doming isopycnals that lower the stratification in the center of the gyre. In winter, storms generate strong heat fluxes and erode the remaining stratification, creating increasingly deeper mixed layer and increasingly denser waters. This process is called deep convection (Marshall and Schott 1999) and has been documented in the Labrador Sea (Lazier 1980, Lazier et al 2002), the Nordic Seas (Swift and Aagard 1981, Brakstad et

al 2019) and the Irminger Sea (Pickart et al 2003, De Jong et al 2012). After winter, the interior seas are restratified with lighter waters from the boundary currents (Sterl and De Jong 2022). Part of the convective waters are then exchanged with the boundary current (Le Bras et al 2020) where they sink along the deepening isopycnals (Katsman et al 2018). The newly formed deep waters join the Deep Western Boundary Current and are exported away from the SPNA.

Changes in the stratification of interior seas ahead of winter could limit or even shut down deep convection and the formation of deep waters. Recent observations showed that the subpolar overturning is dominated by overturning east of Greenland, and therefore mostly due to the formation and export of deep waters in the eastern SPNA (Lozier et al 2019, Li et al 2021). This led to an important change in our understanding of overturning, which used to be focused on the role of deep convection and deep water formation in the Labrador Sea (e.g, Yeager and Danabasoglu 2014, Thornalley et al 2018). These new insights motivate a better understanding of how shelf waters can enter the Nordic Seas and Irminger Sea more specifically.

1.2.3 Increasing freshwater inputs to the SPNA

In the last two decades, the Greenland ice sheet has been melting at an increasing rate (Bamber et al 2018, Mouginot et al 2019, The IMBIE team 2020). This is due both to increasing air surface temperatures (Hanna et al 2012, Trusel et al 2018), that enhance surface meltwater runoff, and to submarine melt due to increasing ocean temperatures (Holland et al 2008, Straneo et al 2013). Greenland mass loss rate increased sixfold between 1992-1999 and 2010-2019 (from on average 39Gt/yr for 1992-1999 to 243 Gt/yr over 2010-2019, Fox-Kemper et al 2021), and is predicted to continue increasing in the future, with the magnitude of the decrease depending on emission pathways (Pattyn et al 2018, Goelzer et al 2020, Fox-Kemper et al 2021). Most of that mass loss took place in the southeast and west of Greenland (Mouginot et al 2019), where marine terminating glaciers release freshwater as surface runoff, subglacial discharge, submarine melt, and as icebergs calving into fjords. This meltwater is transformed in fjords before reaching the Greenland shelf at the coast (Straneo and Cenedese 2015).

The other possible source of increasing freshwater input to the SPNA is the Arctic Ocean. Both anthropogenic climate change and natural modes of variability can affect freshwater storage in the Arctic (Timmermans and Marshall 2020). Climate models predict an increase in liquid freshwater in the Arctic, due to increasing river runoffs and net precipitations, as well as decreasing sea ice volume (Haine et al 2015, Holland et al 2007, Shu et al 2018). Freshwater storage in the Arctic and export through Fram Strait also depend on natural variability: Since the 1990s, liquid freshwater storage in the Arctic has been increasing (Rabe et al 2014, Jahn and Laiho 2020), as more freshwater was stored in the Beaufort Gyre (Proshutinsky et al 2009, Giles et al 2012, Proshutinsky et al 2019). A future release of the Beaufort Gyre could add to the anthropogenic freshening signal and lead to large freshwater export via Fram Strait and Davis Strait (Zhang et al 2021, Lin et al 2023).

1.3. Pathways of Arctic and Greenland waters into the interior SPNA

Increasing freshwater runoff from Greenland and the freshening of the Arctic will lead to additional freshwater input over the Greenland shelf in the future. However, there is a sharp salinity front between the shelf and interior seas where deep convection takes place, and it is not clear where, how much or how the additional freshwater would reach deep convection regions.

1.3.1 Circulation over the Greenland shelf

The Greenland shelf is a wide continental shelf, that is on average 200-400m deep. The width of the shelf varies from 250km in the north-east to 50km at its narrowest point over the south-eastern shelf. At the shelf edge, the sea floor drops from 400 to 2000m over only a few kilometres. This very steep slope is referred to as the shelfbreak. The topography of the shelf is complex, with for instance deep troughs reaching up to 1000m deep that cut across the shelf in the extensions of inland fjords (Figure 5).

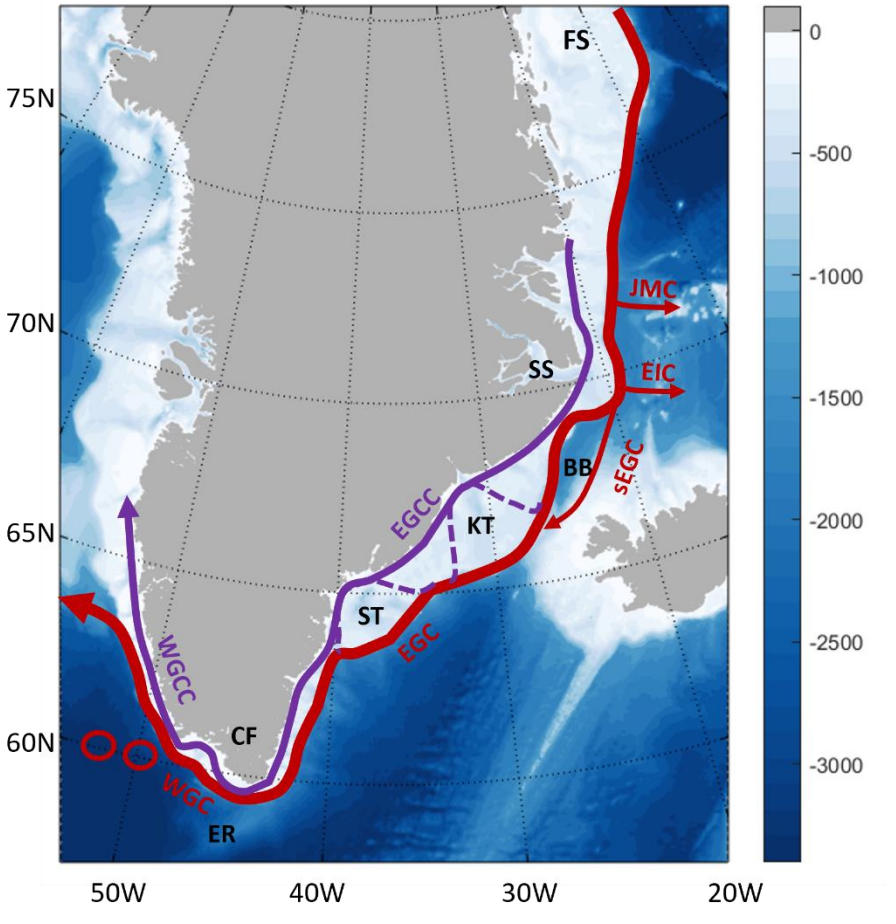

Figure 1.5: *Topography of the Greenland shelf and adjacent seas, and circulation over the east Greenland shelf. Circulation: EGC: East Greenland Current; EGCC: East Greenland Coastal Current, sEGC: Separated East Greenland Current; JMC: Jan Mayen Current; EIC: East Icelandic Current; WGC: West Greenland Current; WGCC: West Greenland Coastal Current. Main topographic features: FS: Fram Strait. SS: Scoresby Sund. BB: Blosseville Basin. KT: Kangerdlussuaq Trough. ST: Sermilik Trough. DS: Denmark Strait. CF: Cape Farewell. ER: Eirik Ridge.*

Polar Surface Water (Rudels et al 2002) enter the shelf from the Arctic via Fram Strait. These cold and relatively fresh surface waters are transported southwards by the EGC (e.g, Sutherland and Pickart 2008, Håvik et al 2017a), a surface-intensified, buoyant western boundary current, that flows all along the shelfbreak from Fram Strait to Cape Farewell. A coastal, fresher core, the East Greenland Coastal Current (EGCC, Bacon 2002, Sutherland and Pickart 2008, Foukal et al 2020) flows closer to the coast and carries the freshest waters southwards, including runoff from Greenland.

North of Denmark Strait, offshore branches bring some of the EGC waters into the Nordic Seas: At 73°N, the Jan Mayen Current separates from the EGC over the Jan Mayen fracture zone (Bourke et al 1992) and diverts shelf waters into the Greenland Sea. At 70°N the East Icelandic Current branches off from the EGC at the latitude of Scoresby Sund into the southern Iceland sea (Jónsson, 2007, Casanova et al 2020). At 69°N, a separated branch of the EGC is formed that flows into Denmark Strait alongside the Iceland continental shelf (Våge et al 2013, Havik et al 2017b).

South of Denmark Strait, the EGC flows alongside the warm and salty Irminger Current, and there are no clear pathways from the shelf into the Irminger Sea. The EGC and EGCC are two clearly separate cores, but the bathymetry of the shelf leads to exchanges between the two: At the deep Kangerdlussuaq and Sermilik troughs part of the shelfbreak EGC is driven along the topography of the troughs and interacts with the EGCC (Sutherland et al 2008, Sutherland and Cenedese 2009).

As they round Cape Farewell, the EGC and EGCC become the WGC and WGCC (Pacini et al 2020). In that region, the coastal current is brought closer to the shelfbreak current, potentially leading to exchanges between the two (Lin et al 2018). The WGC and WGCC then flow northwards along the Labrador Sea. Part of the WGC water is exported into the Labrador Sea by eddies at 60°N (Prater et al 2002, Lilly et al 2003, Chanut et al 2008). The other part of the WGC and the WGCC continues into the Labrador Current or enters Baffin Bay.

1.3.2 Freshwater pathways from the Greenland shelf to interior seas

There is only limited connection between the shelf waters and the interior seas where deep convection takes place. The cold and relatively fresh waters found on the shelf are separated from warmer and saltier waters of the interior seas by a strong hydrographic front situated at the shelfbreak. On the eastern side of Greenland, consistent north-easterly winds driven by the high topography of Greenland (Moore and Renfrew 2005,

Harden et al 2011) tend to constrain shelf waters further towards the coast. North of Denmark Strait, the JMC and EIC branch off the EGC, but there is no consensus on how much freshwater is then exported into the Nordic Seas (Bourke et al 1992, Macrander et al 2014). On the western side of Greenland, both winds (Schulze-Chrétien and Frajka-Williams 2019) and eddies (Lilly et al 2003, Chanut et al 2008) are known to stir shelf waters into the Labrador Sea. Similar mechanisms, related to strong wind events (Oltmans et al 2014), or eddies (Våge et al 2013), could also lead to exchanges on the eastern side of Greenland.

Modelling studies that released tracers to track the fate of Greenland meltwater show that it follows the boundary currents along the Greenland shelf and subpolar gyre, and that a part of it is stirred into the Labrador Sea (Dukhovskoy et al 2016, 2019, Gillard et al 2016). The amount of freshwater entering the Labrador Sea is dependent on model resolution, with higher resolution models showing most intense eddy activity, leading to more shelf water stirred into the Labrador Sea (Dukhovskoy et al 2016). Over the course of several years, Greenland meltwater recirculates over the Subpolar Gyre and the SPNA, reaching the Irminger Sea first, and then the Nordic Seas. Some of the models do show a more direct pathway for tracers into the Nordic Seas via the Jan Mayen and East Icelandic currents (Dukhovskoy et al 2016). Meltwater from Greenland first enters the shelf at the coast, leading to low density of tracers at the shelfbreak in the north-east part of Greenland for models that represent the coastal current (Dukhovskoy et al 2019). This suggests that freshwater coming from the Arctic, that is more evenly distributed over the north-east shelf, could show slightly different pathways. Most of the Greenland waters exported to the Labrador Sea originate from the east of Greenland, as meltwater from west Greenland glaciers enter the WGCC and are fluxed northwards towards Baffin (Gillard et al 2016, Luo et al 2016).

1.3.3 Investigating freshwater export east of Greenland

Though most studies so far have focused on investigating how Greenland and Arctic waters could enter the Labrador Sea and affect deep convection in that region (Böning et al 2016, Yang et al 2016), recent observational studies highlighted the importance the Irminger Sea and the Nordic Seas regions for the subpolar overturning (Lozier et al 2019). Though less freshwater export is expected to take place east than west of Greenland, both sea ice and liquid freshwater are fluxed from the shelf towards the Nordic Seas (Dickson et al 2007, Dodd et al 2009, Le bras et al 2021), and some shelf waters could enter the Irminger Sea near Cape Farewell (Holiday et al 2007).

Investigating freshwater pathways over the Greenland shelf is challenging due to the small scale and possible intermittence of exchange processes and to the paucity of observations. One degree climate models for instance, cannot realistically represent narrow boundary currents (Marzocchi et al 2015) and therefore the EGC and the front between the shelf and interior seas. Models with ¼ degree resolution better represent circulation over the shelf but cannot represent the distinct coastal current (Marsh et al

2010). The small-scale exchanges at the shelfbreak can only be realistically resolved by higher resolution models that resolve the Rossby radius of deformation (Swingedouw et al 2022, Martin et al 2023).

Observations of the east Greenland shelf are sparse and challenging to carry out. Mooring arrays at Fram Strait and Cape Farewell have been monitoring volume and freshwater transport since respectively 1997 and 2014 (Fahrbach et al 2001, Le Bras et al 2018), but they do not extend all the way to the coast nor to the surface, where most of the freshwater is found. Repeated sections have also been carried out along the coast (e.g, Havik et al 2017a, Sutherland and Pickart 2008), but they only provide snapshots of water properties and velocities and it is not always possible to cover all the way to the coast because of sea ice and icebergs, in particular in the northernmost areas. Satellite sea surface salinity is of poor quality near the coast and at high latitudes (Vinogradova et al 2019), and frequent cloud cover often prevents the collection of good quality high resolution SST data near Greenland (Chin et al 2017). Argo floats, which have been instrumental in improving our understanding of ocean circulation in the last decade, do not enter the shallow shelf (Riser et al 2016).

One instrument that is particularly well suited to the study of surface current and pathways is surface drifters. Drifters are Lagrangian oceanographic instruments that follow surface waters. Modern drifters transmit their position in real time and can also collect and transmit ocean and atmospheric data such as sea surface temperature or atmospheric pressure (Lumpkin et al 2017). Numerous types of surface drifters have been developed in the last decade, with different characteristics and for different applications in mind. The most used drifter currently is the Surface Velocity Program (SVP) drifter (Figure 6B). It is composed of a surface float and a holey sock drogue, that anchors it at 15m depth. The drogue also serves to minimize the impact of winds and waves on the drifter trajectory (Niiler et al 1995, Poulain et al 2009). The Global Drifter Program monitors an array of about 1250 SVP drifters (Lumpkin et al 2013) spread over most of the oceans. This large drifter dataset has been instrumental in advancing our understanding of large-scale ocean circulation and its variability (Lumpkin and Johnson 2013, Maximenko et al 2013) and has also been used to investigate regional and small-scale processes. An example of another type of drifter is the CARTHE drifter. CARTHE drifters were initially developed for understanding the propagation of oil spills in the Gulf of Mexico, an application which required the launch of a very high number of drifters (Novelli et al 2017, Lumpkin et al 2017). They are composed of a buoyant torus and a drogue that is anchoring it at 40cm, both made of biodegradable plastic (Figure 6C).

There is limited existing drifter coverage over the east Greenland, in particular north of Denmark Strait and close to the coast (Figure 6A). A thorough investigation of surface freshwater pathways from the shelf to the interior seas of the SPNA with surface drifters therefore necessitates the deployment of additional drifters over the east Greenland shelf.

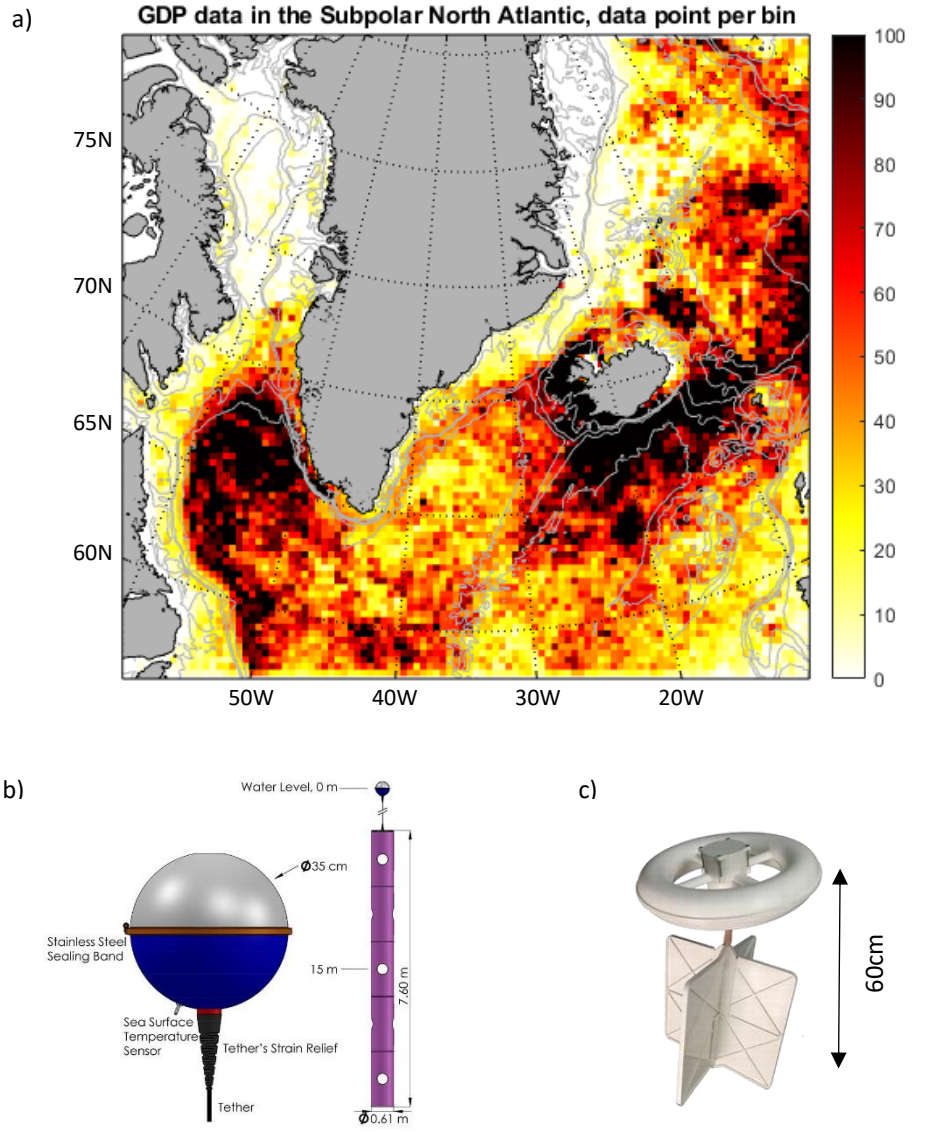

Figure 1.6: *A. Existing drifter coverage in the SPNA from the Global Drifter Program. B. Illustration of a SVP drifter hull and with its drogue deployed. From Centurioni et al 2019 . C. Illustration of a CARTHE drifter, from Pacific Gyre.*

1.4. Aims and scope of this thesis

To predict how the AMOC will evolve under anthropogenic climate change, it is necessary to better understand the processes that can influence deep water formation in the SPNA and how it will change in a warming climate. Additional freshwater input to the SPNA from Greenland and the Arctic could contribute to the freshening of convection regions, which has the potential to affect the overturning circulation. However, Greenland runoff and Arctic waters first enter the Greenland shelf and are advected around the SPNA in narrow boundary currents. It is unclear how much shelf water is stirred into the interior seas of the SPNA where deep waters are formed. Most studies of freshwater pathways into the SPNA have focused on freshwater export to the Labrador Sea, as deep convection in that region was thought to be key to AMOC variability. However, recent observations have shown that the subpolar overturning is dominated by overturning east rather than west of Greenland, shedding a new light on the role of the Irminger Sea and Nordic Seas. This motivates a better understanding of freshwater pathways from the east Greenland shelf to the Irminger Sea and Nordic Seas.

This thesis aims to answer the following question:

Where does cold and fresh water from the east Greenland shelf enter the interior seas of the subpolar north Atlantic?

To respond to this question, 120 surface drifters were deployed along the East Greenland during the summers of 2019, 2020 and 2021 as part of the East Greenland Current Drifter Investigation of Freshwater Transport (EGC-DrIFT) project. These deployments provided new data in areas with previously poor drifter coverage, such as the Greenland coast and north of Denmark Strait. I combined results from these deployments with data from existing drifters, satellite data, ocean and atmospheric reanalyses, a high-resolution model, and results from a coupled climate model at three different resolutions. This allowed me to investigate where exchanges take place, but also what are the mechanisms driving these exchanges, and what is the impact of model resolution on the representation of these mechanisms.

Chapter 2 explores results from the first deployment of the EGC-Drift dataset. Using this dataset, I present an improved understanding of the circulation over the south-east Greenland shelf, including exchanges between the coastal and shelfbreak current cores in the south-east part of the east Greenland shelf, and as drifters round Cape Farewell. The first drifter deployment revealed enhanced cross-shelf exchanges close to Cape Farewell, associated with westerly wind events.

The role of winds at Cape Farewell is further investigated in **Chapter 3**. In this chapter, I use a high-resolution regional model to examine whether strong westerly wind events

named Tip Jets could be a driver for freshwater export at Cape Farewell. Using composites of wind events, I show that Tip Jets do lead to increased freshwater export at Cape Farewell, and that moderate westerly winds can also contribute to enhanced freshwater export. Additionally, I show that westerly wind events lead to sea ice export, though there is only little ice cover in the Cape Farewell area.

In **Chapter 4**, I combine the full EGC-Drift dataset with other drifter datasets, to identify where most of the cross-shelf exchanges take place, and what drives these exchanges. No clear advective pathway is identified east of Greenland from that drifter dataset, though small-scale intermittent processes lead to exchanges at the shelfbreak. Two regions where identified where topography, eddies, and intermittent wind events lead to cross-shelf exchanges: The Blosseville Basin area and Cape Farewell.

Chapter 5 investigates to what extent the circulation over the east Greenland shelf and exchange processes identified in the previous chapters are realistically represented in the HadGEM3-GC3.1 coupled climate model at 1, 0.25 and 0.12 degrees resolution. The analysis suggests that while higher resolution models allow to better represent the upper layer circulation of the SPNA, increasing resolution does not necessarily solve all issues related to shelf-interior exchanges. I also show that, in the models that represent the boundary current correctly, most of the freshwater export from the shelf to the interior seas takes place north of Denmark Strait, both as liquid freshwater and sea ice export.

Chapter 6 concludes this thesis, reflecting on what we learned about pathways of Greenland and Arctic waters into the SPNA and sketching future research outlooks.

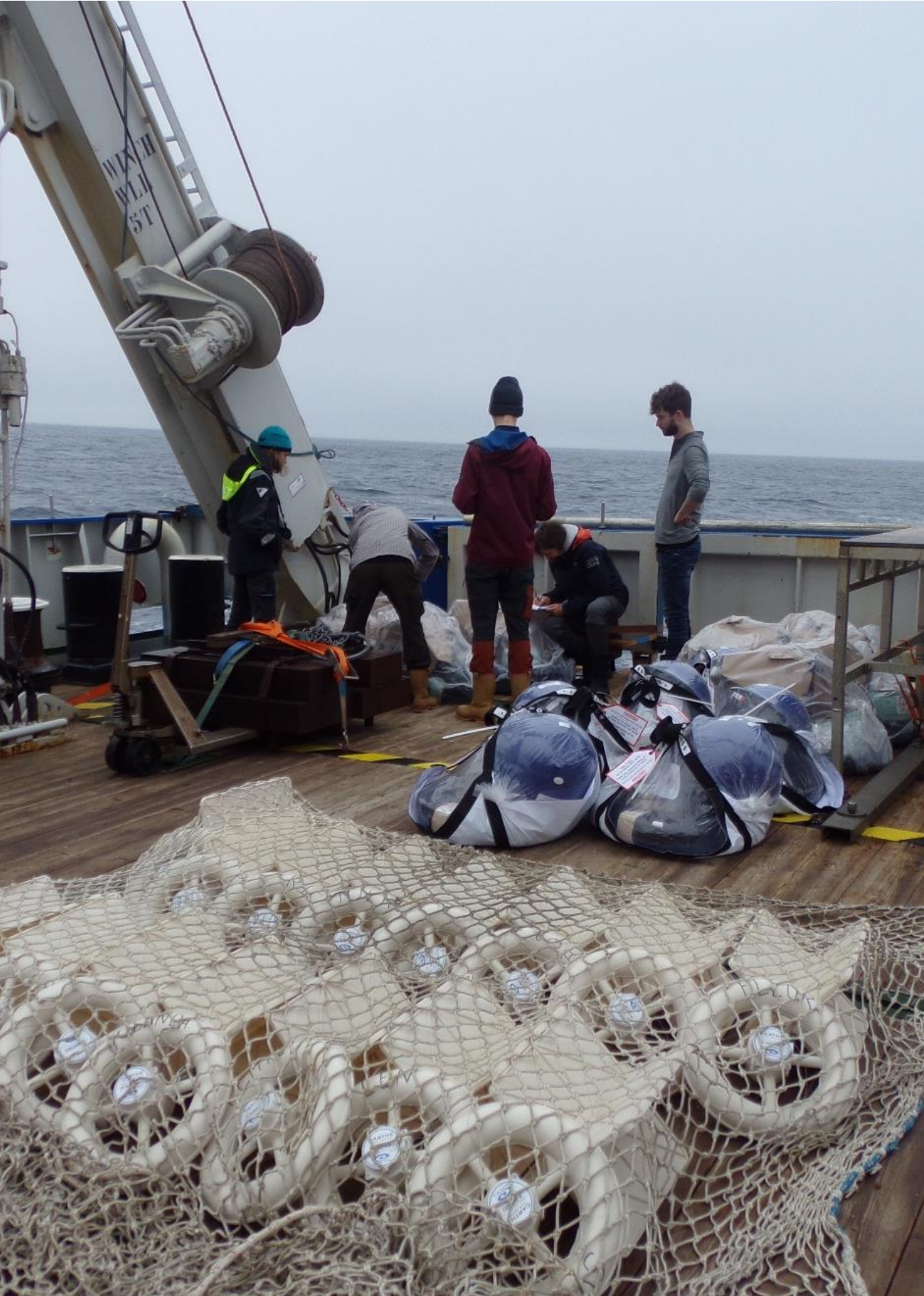

Chapter 2

Circulation over the South-East Greenland Shelf and Potential for Liquid Freshwater Export: A Drifter Study

This chapter was published as:

Duyck, E., & De Jong, M. F. (2021). Circulation over the south-east Greenland shelf and potential for liquid freshwater export: A drifter study. *Geophysical Research Letters,* 48*, e2020JB020886.* https://doi.org/10.1029/2020GL091948

Illustration: Getting ready for deployment. The scientific team of the OSNAP PE473 expedition is activating and verifying SVP drifters before their deployment at Cape Farewell. In the foreground, CARTHE drifters are secured to prevent them from rolling with the ship.

Abstract

Freshwater input into deep convection regions could affect the overturning circulation. With a set of 15 CARTHE and 15 SVP drifters, we investigate the circulation over the south-east Greenland shelf and the potential for off-shelf freshwater export. Part of the East Greenland Current flow is steered into the East Greenland Coastal Current immediately upstream of Sermilik Trough. Between the trough and Cape Farewell, two separate cores are visible. Just past Cape Farewell drifters are redistributed into a shelfbreak core and a slow eddying shelf flow. A coastal core is reestablished downstream. Exchanges between the shelfbreak and coastal flows take place both on the east and west Greenland shelf, allowing fresher water to be diverted away from the coast. Five of 15 shallower CARTHE drifters were exported, mainly at Cape Farewell. CARTHE motion shows a higher correlation with local winds, which are more favorable for off-shelf transport in this area.

2.1 Introduction

Atmospheric and oceanic warming of the Arctic and Subarctic regions results in enhanced Greenland Ice Sheet melt and freshening of the Arctic Ocean, leading to increased discharge of freshwater into the East Greenland Current (EGC) (Bamber et al., 2018; Haine et al., 2015). Additional freshwater input into the convective regions of the Subpolar North Atlantic could strengthen watercolumn stratification and weaken deep mixing (Aagaard & Carmack, 1989), in turn affecting the strength of the Atlantic Meridional Overturning Circulation (Bakker et al., 2016; Böning et al., 2016; Manabe & Stouffer, 1994). Recent findings argue for a more important role of the overturning east of Greenland (Lozier et al., 2019), highlighting the particular climatic importance of freshwater export from the east Greenland Shelf. This study investigates the fate of liquid freshwater from the EGC system, notably potential export into the deep convection region of the central Irminger Sea (de Jong et al., 2018).

South of Denmark Strait (DS), the EGC system (Figure 1A) consists of a main branch located at the shelf-break (EGC), and a coastal branch referred to as the East Greenland Coastal Current (EGCC). The EGC is found at the front between the colder, fresher waters flowing south from Fram Strait and the warmer, saltier Irminger Current waters. The EGCC (Malmberg, 1967; Bacon, 2002) is a fresh (practical salinity < 34), 20 km-wide, surface-intensified current, with a high-velocity core (speeds > 1 m s^{-1}) carrying arctic waters and Greenland runoff equatorwards (Bacon et al., 2014; le Bras et al., 2018). Recent work (Foukal et al, 2020) showed that the EGCC extends along the whole east Greenland coast, while confirming that deep troughs south of Denmark strait divert part of the EGC into the coastal current (Sutherland & Pickart, 2008; Sutherland & Cenedese, 2009). Past Cape Farewell (CF), the EGC and EGCC were first thought to merge into the West Greenland Current (WGC) (Bacon, 2002), but more recent studies argue that the EGCC keeps its identity as a coastal core to become the West Greenland Coastal Current (WGCC) (Lin et al., 2018).

The cold and fresh Polar Surface Water found over most of the east Greenland shelf (Rudels et al., 2002) is isolated from interior seas by the sharp hydrographic front associated with the EGC. It is pushed towards the coast by the onshore Ekman transport caused by south-westward barrier winds (Moore & Renfrew, 2005). However, the complex bathymetry of the shelf, meandering of the front, wind strength and variability, create opportunities for export of surface waters towards the interior seas, notably at CF (Holliday et al., 2007). While export of fresh waters from the west Greenland shelf into the Labrador Sea is already well documented (Schulze Chretien & Frajka-Williams, 2018; Wolfe & Cenedese, 2006), there is still little insight into surface water export from the east Greenland shelf into the Irminger Sea.

Despite renewed interest in the EGC system, our understanding of the liquid freshwater circulation over the east Greenland shelf remains sparse. Insight into the properties and structure of the EGC is provided by synoptic sections, mooring arrays in select locations and isolated drifters (Bacon 2002, Reverdin 2003). In this study, we present a set of 30

drifters deployed at the east Greenland continental shelf-break at approximately 65°N. Drifter deployments and data processing are described in Section 2. Drifter trajectories and insights from additional datasets are presented in Section 3. Section 4 discusses the results and possible implications for liquid freshwater export.

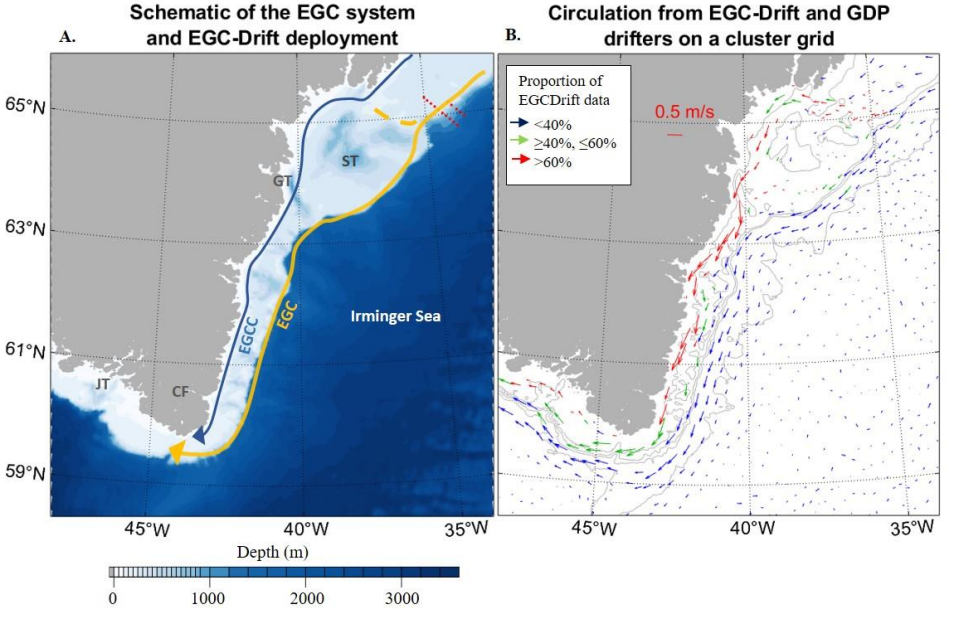

Figure 2.1: *Schematic of the surface circulation over the east Greenland shelf with drifter deployment location and drifter data overview:* ***A.*** *EGC System, and main topographic features. EGC: East Greenland Current, EGCC: East Greenland Coastal Current, ST: Sermilik Trough, GT: Gyldenlove Trough, CF: Cape Farewell, JT: Julianehåb Trough; Drifters were deployed at two shelfbreak sections at 65°N (red dots).* ***B.*** *Circulation inferred from the Global Drifter Program and our EGC-DrIFT datasets combined on a cluster grid (see methods in Section 2). Arrows are colored depending on the percentage of EGC-DrIFT data in each cluster as defined in the legend. Isobaths (in grey) are drawn at 2000, 1000, 500 and 200 m depth.*

2.2 Materials and Methods

We present the first results from the East Greenland Current Drifter Investigation of Freshwater Transport (EGC-DrIFT) campaign. This study aims to elucidate possible pathways for freshwater exchanges east of Greenland with surface drifter deployments planned in the summers of 2019, 2020 and 2021. The dataset discussed here consists of two types of drifters. Surface Velocity Program (SVP) drifters are composed of a spherical buoy and a holey sock drogue centred at 15 m below sea level (Lumpkin et al., 2017). Two models of SVP drifters are used: SVP-T, fitted with a temperature sensor measuring sea surface temperature (SST) at 0.5 m depth, and SVP-S fitted with an additional conductivity sensor to measure salinity. GPS positions and data are transmitted to shore

via iridium at hourly intervals for SVP-T drifters and 3-hourly intervals for SVP-S drifters. CARTHE drifters (Consortium for Advanced Research for the Transport of Hydrocarbon in the Environment, Novelli et al., 2017) are shallower drifters, composed of a floating torus sitting low above water and a drogue at 0.4 m depth. They provide GPS tracking at 3-hourly intervals.

In total, 15 CARTHEs and 15 SVPs (seven SVP-Ts, eight SVP-Ss) were deployed along two lines perpendicular to the shelf-break and 40 km apart (Figure 1A) on the 14th August 2019. The southern line extended from 1200 to 250 m depth and the northern line from 1300 to 250 m depth. Drifters were released 9 km apart, in pairs of one SVP and one CARTHE drifter, as to elucidate the behaviour of different extents of the surface water layer. We present here their trajectories until 1st December 2019 and up to 48°W.

One SVP drifter stopped working upon launch, but the remaining 14 functioned properly. By the 1st December 2019, 12 SVPs and four CARTHEs (that have a shorter expected lifetime) were still active. SVP-Ts occasionally (4% of dataset) display repeated positions, mostly corresponding to one to two hours GPS gaps. SVP-Ss do not experience similar issues. CARTHEs display GPS gaps that can last for several days. Temperature and conductivity timeseries are despiked and other hydrographic properties, such as absolute salinity and density are derived using the TEOS10 toolbox (Mc Dougall and Barker, 2011). Drifter velocities, computed from displacement, are filtered with a 25-hour centered Butterworth filter to remove high-frequency components. The presence of the drogues on SVP drifters is monitored from a submergence sensor and the time to first GPS fix, both of which exhibit drastic changes when a drogue is lost. No SVP drifter seems to have lost its drogue before 1st December 2019. Finally, the dataset is resampled using linear interpolation on a 3-hour regular grid, not interpolating data gaps longer than 12h.

We use the Global Drifter Program (GDP) quality-controlled 6-hour interpolated dataset (Lumpkin & Centurioni, 2019) to contextualize our results. GDP and EGC-DrIFT data are non-uniformly distributed in the region, and therefore less suitable for regular spatial gridding. Instead, we combine EGC-DrIFT and GDP drifter data on an irregular grid built with a clustering method using a k-mean algorithm. This algorithm groups neighboring observations in clusters with an iterative assignment/update mechanism, in order to find a solution minimizing the distance between observations and cluster centers. See McKay (2003) for more details on the algorithm, or Koszalka and LaCasce (2010) for an example of its application to drifter data. We choose a k number of clusters so that the mean amount of observations per cluster is 80, and do not take into account clusters with less than 20 data points

Surface winds from 1993 to 2020 are retrieved from the ERA5 atmospheric reanalysis hourly data on single levels (Copernicus Climate Change Service, 2017). Wind data are used to compute the correlation coefficient between wind and drifter motion. This coefficient is the magnitude of the complex correlation between wind and drifter velocities ($u(t)+i\cdot v(t)$) (Poulain 2009). Wind data are also used to evaluate potential for

off-shelf Ekman transport along the east greenland shelf. Wind components are interpolated along the shelfbreak, defined as the 500 m isobath, and Ekman transport is computed from wind stress as:

$$\begin{cases} U_{ek} = \dfrac{T_y}{f * \rho} \\ V_{ek} = \dfrac{-T_x}{f * \rho} \end{cases}$$

Tx, Ty being wind stress components, ρ=1027 kg m^{-3} and f=10^{-4} s^{-1}. Along and across shelf Ekman transports are then derived using the local angle of the 500 m isobath, and used to compute the proportion of days with positive off-shelf Ekman transport along the shelf.

SST is retrieved from the GHRSST Level 4 MUR Global Foundation SST Analysis (JPL MUR MEaSUREs Project, 2015), a data blend of microwave, infrared, ice fraction and in situ measurements, with a very high resolution (1 km) in cloudless conditions (Chin et al., 2017). Cloud cover sometimes diminishes the real resolution of the MUR dataset and can cause artifacts. The quality of the MUR SST data at times of interest is verified by comparing it to the GHRSST Level 4 OSTIA Global Foundation SST Analysis (UK MetOffice, 2012).

2.3 Results

The trajectories of the EGC-DrIFT SVP buoys are consistent with existing GDP trajectories, while providing extended coverage close to the coast and a denser sampling of the circulation over the shelf (Figure 1B). Although the EGC-DrIFT drifters are limited in numbers they close an important data gap in the inner shelf region and provide coverage of the EGC and EGCC simultaneously, allowing comparison of properties and insight into exchanges taking place between these two cores.

The drifters take one to two months to reach the southern tip of Greenland. They quickly separate into three groups after deployment (figures 2B and 2C): 1) following the EGC, 2) steering around Sermilik Trough (ST) into the EGCC, and 3) entering the trough before joining the EGCC.

The first group follows the EGC and is composed of 12 drifters, among those deployed the furthest offshore (seven out of 15 (7/15) CARTHEs and 5/14 SVPs). In the EGC core, SVPs measure temperatures about 10°C and absolute salinities between 34.6 and 35.2 g kg^{-1} (Figures 2E and F). Speeds do not exceed 0.6 m s^{-1} as the EGC is steered around ST (Figure 2D). The three SVP drifters from the northern line first head offshore, but loop around and come back on the inshore side of the EGC. Three SVPs and one CARTHE re-

enter the shelf at different points along the trough. Out of the core, their motion becomes very slow (<0.1 m s^{-1}) and inertial. They join the EGCC just downstream of ST, measuring a sharp decrease in temperature as they enter the coastal core.

Ten drifters (2/15 CARTHEs, 8/14 SVP drifters) belong to the second group, which is steered around ST directly towards the EGCC. They are initially slow (<0.1 m s^{-1}) but accelerate as they get closer to the coast, eventually reaching speeds up to 0.8 m s^{-1} as they enter the EGCC core. Inside the core, they measure a large range of salinities (29 to 34 g kg^{-1}) and temperatures between 3 and 5.5°C, the coldest and freshest waters being closest to the coast.

Finally, seven drifters (6/15 CARTHEs and 1/14 SVPs) move across the trough before joining the EGCC. They all follow similar trajectories as they flow from their deployment area, close to the shelf-break, into the trough and later into the EGCC. Their speed inside the trough does not exceed 0.2 m s^{-1}. The SVP drifter measures temperatures around 7°C , and salinities around 34.5 g kg^{-1} in the middle of ST.

South of ST, only two groups are identifiable, associated with the two current cores. As the Greenland shelf narrows downstream of ST, drifters in the EGCC are steered along the Gyldenløve Trough and accelerate, reaching speeds of more than 1 m s^{-1}. The EGCC remains faster than the EGC until they reach CF. The cores are well defined but exchanges take place between them. As was previously observed with a CTD section by Sutherland & Pickart (2008), the two cores come closer together just downstream of ST, at the narrowest part of the shelf. There, four of the CARTHEs are deviated from the EGCC to the EGC. Further downstream, two SVPs and one CARTHE also leave the EGCC for the EGC. As the drifters near CF, seven SVPs and no CARTHE remain in the EGCC, four SVPs and six CARTHEs in the EGC.

Four of these CARTHEs are exported into the Irminger Sea just before rounding CF. The two others round the cape and enter the west Greenland shelf. Another CARTHE drifter had been exported earlier at a bathymetric bend downstream of ST. The others stopped functioning.

West of CF, only one strong (1 m s^{-1}) velocity core is visible, at the shelf-break, with a slower, less laminar flow over the shelf. As illustrated in Figure 2A, SVPs originating from the EGCC (green) spread over the shelf as they round the cape. Two SVPs remain close to the shore, showing slow and eddying motions, while five SVPs approach the shelfbreak, two of which enter the WGC. Similarly, two of the EGC-origin SVPs (red) enter the shelf on the western side of Greenland. Most shelf SVPs are then steered along Julianehåb Trough. This redistribution of coastal and shelfbreak floats suggests that the WGC and WGCC are not as clearly separated as the EGC and EGCC, enhancing potential for freshwater exchange away from the inner shelf west of CF.

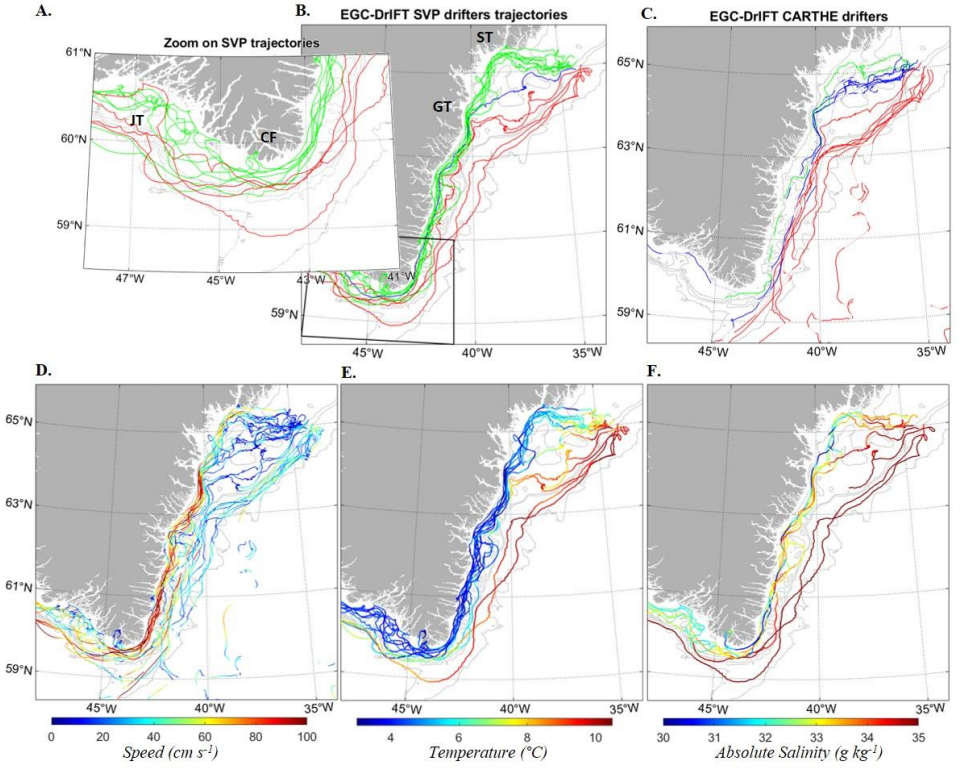

Figure 2.2: *Overview of drifter trajectories and along-track properties. A. Zoom on SVP trajectories at CF, distinguishing origin from the EGC (red) and EGCC (green) B. SVP trajectories, coloured in three groups (EGCC: green, ST: Blue, EGC: Red); ; C. Same as B for CARTHEs; D. Drifter speed in cm s^{-1}; E. Temperature in °C from SVP-S and SVP-Ts; F. Absolute salinity from SVP-Ss in g kg^{-1}. Isobaths (in grey) are drawn at 2000, 1000, 500 and 200 m depth.*

CARTHE and SVP drifters display different behaviours: As they approach ST, nearly all SVPs join either the EGC or the EGCC, when nearly half of the CARTHEs cut across the trough. A majority of CARTHEs remain in or re-enter the EGC when most SVP drifters are part of the EGCC. Most of the exchanges between the EGC and EGCC cores, and all the export into the Irminger Sea, are observed with CARTHE drifters. Though CARTHEs and SVPs are both built to minimize wind drag and have similar water following capabilities (Novelli et al, 2017), CARTHEs have shallower anchors (0.4 m against 15 m), and are therefore more directly influenced by wind forcing. This is confirmed by computing the correlation between drifter and wind velocities, reaching 0.66 for CARTHEs, against 0.23 for SVPs, a value that is consistent with existing studies (Poulain 2009).

Drifter data are limited in space and time and therefore only provide a limited overview of processes at the front. We investigate the correspondence between very-high resolution satellite SST measurements (1 km) and drifter tracks to assess the use of

satellite SST as a source of information for surface circulation over the shelf when no drifter data is available. The SST snapshots (Figure 3A-F) show the concurrent evolution of drifter tracks and MUR SST at ST, from deployment until the beginning of September. Two temperature fronts are visible in the snapshots, which coincide well with the EGC and EGCC as inferred from drifter tracks. Drifters that move across ST closely follow warm water entering the trough from the north-east (24th - 27th August). South of the trough, a second warm-water intrusion is visible, coincident with drifters from the EGC re-entering the shelf (4th-11th September). Both SVPs and CARTHEs trajectories are consistent with the MUR SST patterns, suggesting the satellite data reflects the surface circulation well. Looking at the complete MUR (2002-2020) and OSTIA (2007-2020) SST time series, we repetitively find the same patterns in ST suggesting that the circulation observed with the drifters is typical of the area.

The agreement between drifter tracks and SST patterns suggests that high resolution SST data can help infer variability of the location of the front over the East Greenland shelf. We use the MUR SST data to further investigate potential for freshwater export at CF. Figures 3G-I show a cold water tongue exiting the shelf at CF in early September 2019. Similar features are visible at CF at other times and could be markers of an export pathway for fresh and cold surface shelf waters towards the Irminger Sea. Due to cloud cover at the exact time when the CARTHE drifters were exported, it is not possible to investigate that specific event with the MUR SST data. Further observations or model analysis are necessary to verify the link between such cold water signature in the SST data and surface water export.

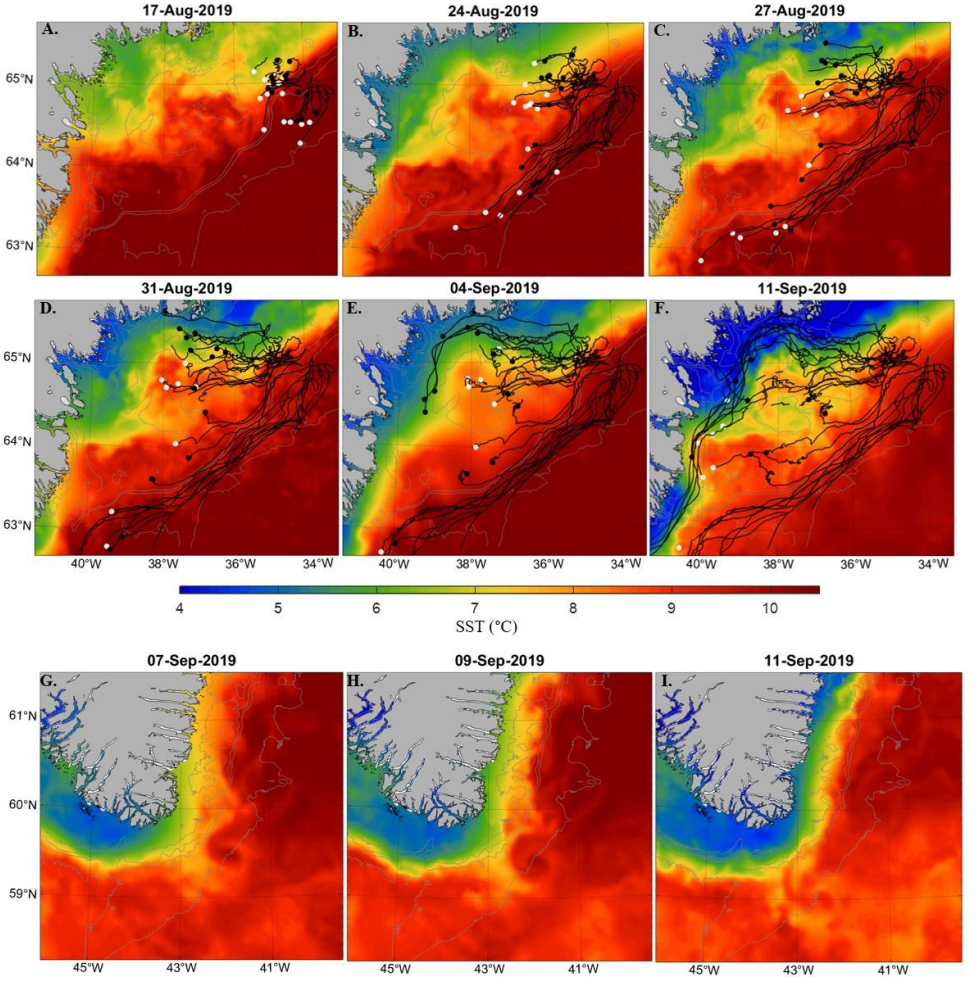

Figure 2.3: *Sea surface temperature snapshots from MUR at ST and CF.* ***A-F.*** *Co-evolution of SST with SVPs (Black) and CARTHEs (White) drifters from deployment through 11 September. Dots indicate drifter position at the time of the snapshots, with tracks shown since deployment.* ***G-I.*** *Instability at the EGC front at CF forming a cold water tongue, likely a marker of shelf water export. Isobaths (in grey) are drawn at 2000, 1000, 500 and 200 m depth.*

2.4 Discussion and conclusion

The circulation of freshwater over the south-east Greenland shelf and its potential export into the Irminger Sea are of particular climatic importance. In this study, we presented observations from drifters deployed during the EGC-DrIFT campaign, in August 2019. Our results generally agree with existing literature regarding the position,

speed and properties of the EGC and EGCC cores (Harden et al., 2014; Sutherland & Pickart, 2008), and extend existing drifter coverage closer to the coast.

The new drifter dataset shows exchanges between the East and West Greenland shelf and shelfbreak cores, suggesting that Greenland meltwater is not solely confined to the inner shelf. Past CF, earlier studies suggested that the EGC and EGCC merge into the WGC (Bacon 2002). Recent results (Lin et al 2018) argue that the coastal core keeps its identity to become the WGCC, although local bathymetry does divert part of the flow to the outer shelf, causing loss of freshwater to the WGC. In this study, coastal drifters show a stark behaviour change as they round the cape. While drifters in the EGCC showed fast, nearly straight tracks, no clearly defined coastal velocity core is visible between CF and 46°W. Part of the drifters from the EGCC are deviated towards the outer shelf and the WGC. The drifters that stay on the inner shelf slow down substiantially (Fig. 2D), displaying eddying or meandering motions, likely due to the widening of the shelf in this area. As drifters are steered along Julianehab Trough, a well defined coastal core reappears. The low velocities and meandering tracks on the inner shelf between Cape Farewell and Julianehåb Trough suggest there was no coherent WGCC velocity core in this section of the shelf at the time the drifters were there. Tracks from GDP drifters also do not show a coherent WGCC core in that area, only downstream of Julianehab Trough (Fig. 4A). The location of the WGCC core may be time variable, as could be interpreted from Pacini et al (2020). The combination of EGC-DrIFT and GDP datasets (Fig. 4A) shows that most drifters originating from the EGCC (red) spread over the western shelf, while most EGC-origin drifters (blue) flow along the western shelfbreak, with exchanges taking place between the two. Past 48°W, the position of drifters with respect to the shelfbreak is not indicative of their origin in either the EGCC or EGC. These exchanges contribute to the export of freshwater from the inner shelf to the central Labrador Sea, as a well known eddy shedding region is located shortly downstream (Lilly et al., 2003; Bracco et al., 2008; de Jong et al., 2014).

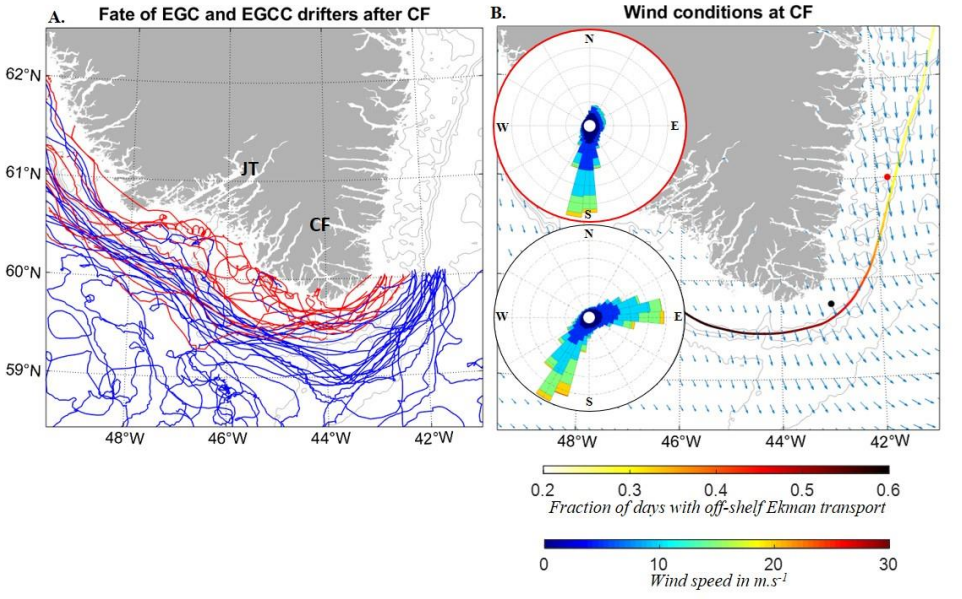

Figure 2.4: *Drifter tracks and wind conditions around CF. A. EGC-Drift (SVPs) and GDP drifter tracks originating from the EGC (blue) and EGCC (red) cores. B. Mean winds and fraction of days with positive off-shelf wind-driven transport (as defined in Methods, section 2). Wind roses show speed and direction of winds at the red and black dots during 1993-2020. Isobaths (in grey) are drawn at 2000, 1000, 500 and 200 m depth.*

Out of 15 SVP and 15 CARTHE drifters, five CARTHEs were exported into the Irminger Sea, including four at CF. The motion of these shallow drifters is more strongly correlated with wind forcing, suggesting that wind could be a primary driver for export away from the east Greenland shelf into the Irminger Sea, similar to what Schulze Chretien and Frajka-Williams (2018) found for export off the west Greenland shelf. The fraction of days with positive off-shelf Ekman transport (as defined in Methods, section 2), shows a sharp transition to more off-shelf transport favourable conditions near CF (Figure 4B). This is both due to the bend in the shelf and to strong eastward wind events such as tip jets (Moore & Renfrew, 2005), opposed to the dominance of strong and persistent barrier winds along the eastern shelf, as shown by the wind-roses in Figure 4B. Satellite SST snapshots at CF (Figure 3G-I) confirm that CF could be an enhanced export area for cold and fresh surface shelf waters. These export events could contribute to the low salinity surface waters extending away from the shelf as found by Sutherland and Pickart (2008). Whether bathymetry driven instabilities, possibly related to the subsurface retroflection of the EGC (Holliday et al, 2007), contribute these surface features is currently not clear. A more quantitative study of the wind driven cross-shelf freshwater export east of Greenland is ongoing.

Acknowledgments and Open Research

The EGC-DrIFT project is financially supported by the Innovational Research Incentives Scheme of the Netherlands Organisation for Scientific Research (NWO) under grant agreement nos. 016.Vidi.189.130.

The drifter dataset presented in this study is available at : Duyck, E., & de Jong, M.F. (2020), EGC-DrIFT drifter dataset Kulusuk deployment 2019, doi:10.25850/nioz/7b.b.4 We thank the captain and crew of the M/V Adolph Jansen, from which drifters were deployed

Chapter 3

Wind-driven freshwater export at Cape Farewell

This chapter was published as:

Duyck, E., Gelderloos, R., & de Jong, M. F. (2022). Wind-Driven Freshwater Export at Cape Farewell. Journal of Geophysical Research: Oceans, 127(5), e2021JC018309. https://doi.org/10.1029/2021JC018309

Illustration: Unpacking a SVP drifter under the snow before launch at Fram Strait. September 2019, R/V Kronprins Haakon. Picture: Lawrence Hislop

Abstract

Increased freshwater input to the Subpolar North Atlantic from Greenland ice melt and the Arctic could strengthen stratification in deep convection regions and impact the overturning circulation. However, freshwater pathways from the east Greenland shelf to deep convection regions are not fully understood. We investigate the role of strong wind events at Cape Farewell in driving surface freshwaters from the East Greenland Current to the Irminger Sea. Using a high-resolution model and an atmospheric reanalysis, we identify strong wind events and investigate their impact on freshwater export. Westerly tip jets are associated with the strongest and deepest freshwater export across the shelfbreak, with a mean of 37.5 mSv of freshwater in the first 100 m (with reference salinity 34.9). These wind events tilt isohalines and extend the front offshore, especially over Eirik Ridge. Moderate westerly events are associated with weaker export across the shelfbreak (mean of 15.9 mSv) but overall contribute to more freshwater export throughout the year, including in summer, when the shelf is particularly fresh. Particle tracking shows that half of the surface waters crossing the shelfbreak during tip jet events are exported away from the shelf, either entering the Irminger Gyre, or being driven over Eirik Ridge. During strong westerly wind events, sea ice detaches from the coast and veers towards the Irminger Sea, but the contribution of sea ice to freshwater export at the shelfbreak is minimal compared to liquid freshwater export due to limited sea-ice cover at Cape Farewell.

3.1. Introduction

The Atlantic Meridional Overturning Circulation (AMOC) is a critical element of the climate system. It redistributes heat and freshwater across the Atlantic and stores carbon in the deep ocean (Buckley and Marshall 2016). With continued global warming, the overturning circulation is predicted to weaken, possibly leading to large-scale remote impacts (Collins et al 2019).

One mechanism that could lead to a slow-down of the AMOC is an increase in freshwater input to the Subpolar North Atlantic deep convection regions (Manabe and Stouffer 1995, Weijer et al 2019). The freshening of the Arctic, predicted to strengthen in the coming decades (Haine et al 2015), and the accelerated melt of the Greenland ice sheet (Bamber et al 2018, Shepherd et al 2020), can lead to increasing freshwater input to the Greenland shelf. If this additional freshwater reaches the deep convection regions of the Subpolar North Atlantic, it could strengthen stratification in these regions, thereby dampening deep convection and impacting the overturning circulation (Aaagaard and Carmack 1989). This mechanism was observed in the Labrador Sea during the Great Salinity Anomaly of 1969-1972 (Gelderloos et al 2012), which originated from Fram Strait and led to an extra 10,000 km^3 of freshwater circulating in the North Atlantic (Dickson et al 1988). Freshwater pathways from the boundary current on the Greenland shelf to convection regions are however still unclear, and model studies disagree on the timescale at which additional freshwater input from Greenland and the Arctic could have a significant impact on the overturning circulation (Böning et al 2016, Bakker et al 2016, Dukhovskoy et al 2015). In particular, there is only little understanding of possible freshwater pathways from the south-eastern Greenland shelf into the Irminger Sea. Recent results found the Irminger Sea to be of greater importance than the Labrador Sea in driving variability of the overturning circulation (Lozier et al 2019, Petit et al 2020, Li et al 2021), but most studies to date have focused on freshwater export in the Labrador Sea and its impact in this region (Pennelly et al 2019, Yang et al 2016).

On the east Greenland shelf, freshwater is contained within the East Greenland Current (EGC), which flows along the east Greenland coast from Fram Strait to Cape Farewell. The main branch is located at the shelfbreak and separates the cold and fresh waters flowing south from Fram Strait from the warmer and saltier Irminger Current waters (Figure 1a). An even fresher coastal branch, referred to as the East Greenland Coastal Current, is located over the shelf, carrying Greenland meltwater and Arctic waters equatorwards (Bacon et al 2014, Le Bras et al 2018, Foukal et al 2020). At Cape Farewell, the EGC rounds the cape to become the West Greenland Current. Freshwater export from the boundary current to interior seas is well documented on the western side of Greenland, where both eddies (Hátún et al 2007, Lilly et al 2003) and winds (Schulze Chretien and Frajka-Williams 2018) bring fresh surface waters to the Labrador Sea. On the eastern side of Greenland, surface freshwater is exported from the Greenland shelf north of Denmark Strait to the Nordic Seas, mainly via the Jan Mayen and East Icelandic Current (Håvik et al 2017, Dodd et al 2009). Freshwater export from the south-east

Greenland shelf to the Irminger Sea is expected to be much weaker and is not well documented.

A drifter deployment conducted on the eastern Greenland shelf in August 2019 suggested that wind events at Cape Farewell could lead to short lived freshwater export towards the Irminger Sea (Duyck and De Jong 2021). The Cape Farewell region is the windiest location of the world's oceans (Sampe and Xie 2007). The interaction of synoptic scale cyclones with the high topography of southern Greenland creates strong wind events called tip jets (Moore 2003, Moore and Renfrew 2005). Westerly tip jets are meso-scale (200-400km) events that are usually short in duration (1 day), and can reach 30 m s^{-1} at the surface. They result from the deflection and acceleration of westerly flow at the tip of Greenland, as well as acceleration down the slope at Cape Farewell (Doyle and Shapiro 1999, Moore 2003, Våge et al 2009). They are characterized by a strong westerly flow over the Irminger Sea, that creates heat fluxes of up to 600 W m^{-2} and contributes to deep convection (Våge et al 2009, Våge et al 2008, Pickart et al 2003). Easterly, or reverse tip-jets are strong north-easterly wind events (Moore 2012, Moore 2003) that can also reach 30 m s^{-1} at the surface and flow along and south of the east Greenland shelf (Renfrew et al 2009, Outten et al 2009). North-easterly events result from barrier flows adjusting to the loss of the barrier at the tip of Greenland (Moore and Renfrew 2005, Renfrew et al 2009). In the following, these two types of extreme wind events occurring at Cape Farewell will be referred to as tip jets and strong north-easterlies. The occurrence of these winds is strongly dependent on background synoptic conditions, and the position of the cyclone center, to the north-east or south of Cape Farewell, respectively allowing for the generation of tip-jets and strong north-easterly wind events (Moore 2003, Bakalian et al 2007). These strong wind events are likely to influence surface waters at Cape Farewell, as well as sea-ice cover, and maybe drive fresh waters and sea ice off the shelf, into the Irminger Sea. Deep convection takes place within the Irminger Gyre, both in the gyre center situated east of Cape Farewell (Våge et al 2011, De Jong et al 2012, 2018) as well as south of Cape Farewell (de Jong et al 2012, Piron et al 2016, 2017). Liquid or solid freshwater export off the shelf in this area could impact the stratification of this deep convection region.

The study presented here investigates wind-driven export events in the Cape Farewell area using results from a high-resolution simulation of the area (Almansi et al 2017), atmospheric reanalysis data and satellite observations. Section 2 will describe the datasets used, as well as the methods employed to identify extreme wind events and to compute freshwater export. Section 3 presents the wind events identified using the above method. Section 4 investigates the wind-driven liquid freshwater export and Section 5 expands this to sea-ice export. Finally, Section 6 discusses the relevance of these results for convection regions.

3.2. Data and Methods

3.2.1 Data description

Wind-driven freshwater export at Cape Farewell is investigated using results from a high-resolution simulation based on the Massachusetts Institute of Technology General Circulation Model (MITgcm; Marshall et al., 1997). The configuration and forcing are described in Almansi et al (2017), and updated as in Almansi et al (2020). The horizontal domain covers 47°W-1°E and 57-76°N, discretized with an unevenly spaced grid with resolution of 2 km at the center and 4 km in peripheral areas (including our study area at Cape Farewell). The vertical domain consists of 216 levels, with resolution linearly increasing from 1-15 m in the first 120 m and equal to 15 m beyond 120 m depth. The model is forced with the 15-km resolution Arctic System Reanalysis version 2 (ASR-2; Bromwich et al., 2018). Due to its high resolution, the model was run for only one year, from September 2007 to August 2008. The output is available at 6-hr resolution and retrieved from SciServer (Medvedev et al., 2016). We retrieve the 10-m wind fields, ocean velocity fields, ocean salinity and temperature fields, and ice thickness and concentration fields. The salinity field is practical salinity, and practical salinity is used throughout the paper. Additional fields and computations, as presented in Section 2.2, can be reproduced using the OceanSpy v0.1 python package (Almansi et al 2019). To avoid confusion with other datasets, we will refer to this simulation as MITgcm in the rest of the manuscript.

In addition to MITgcm, we use the CARRA (Copernicus Climate Data Store Arctic Regional Reanalysis on single levels) atmospheric reanalysis in order to put the wind conditions of the MITgcm year (September 2007 – August 2008) in the context of a longer time series. The reanalysis data covers the period from 1998 to 2019 with a 3h temporal resolution and a 2.5 km spatial resolution, currently the best available time-coverage with high-resolution in the area. We also use the sea-ice product from CARRA, derived from two satellite sea-ice concentration products: the European Space Agency Climate Change Initiative (ESA CCI) sea-ice concentration product (SICCI; Toudal Pedersen et al., 2017), which has a 15-25 km resolution and is used whenever available, and the EUMETSAT OSISAF sea-ice concentration product OSI-450 (Tonboe et al., 2016), which has a 30-60 km resolution and is used to fill gaps in the SICCI product.

Snapshots of the MODIS true color reflectance from the TERRA satellite are retrieved at times of extreme wind events to investigate the sea-ice response to extreme winds. The MODIS data has a maximal resolution of 250 m, which allows detection of smaller details in sea-ice behavior than with MITgcm and the satellite sea-ice concentration product from CARRA. However, good data is limited to satellite passes with clear skies.

3.2.2 Description of methods

3.2.2.1 Definition and detection of wind events

The wind analysis at Cape Farewell focuses on the region defined in Figure 1b, corresponding to the southernmost part of the east Greenland shelf, where strong winds are most likely to bring fresh surface waters to the Irminger Sea. Two main types of winds are dominant in that area; westerly winds and north-easterly winds (Figure 1c), and we are interested in the extreme manifestation of those winds.

Identification methods based on time series of average wind direction and speed in the area of interest are designed to detect the strongest events for both types of winds. Tip jets are defined as strong (> 17 m s^{-1}), westerly winds (mean wind direction towards the 45° to 135° quadrant with respect to north), lasting for more than 12 h. Strong north-easterly events are defined as strong (> 17 m s^{-1}) north-easterly winds (mean wind direction towards the 180° to 270° quadrant with respect to north) lasting more than 12 h. Two separate events of the same type must be at least 12 h apart, and are otherwise considered as a single event.

Our identification method and chosen threshold are similar to the ones used in previous studies identifying extreme wind events near Greenland (Harden et al 2011, Moore 2012). The 17 m s^{-1} threshold corresponds to the 10% strongest westerly winds in the ASR2 data of the MITgcm year, and to gale force wind. The choice of other thresholds modify the number of detected events, but not the conclusions regarding the impact of strong wind events on the ocean at Cape Farewell. In this study, the mean winds in the area of interest at a given time are used to identify the extreme wind events. Using maximum winds in the area rather than mean winds, as done in Moore (2014) has the same effect as changing the threshold: It changes the number of detected events but not their characteristics nor the conclusions regarding their impact.

Though tip jets are the most likely to cause the strongest freshwater export at Cape Farewell, more moderate westerly winds are also likely to play a role. To identify moderate westerly winds, we use the same direction constraints than for tip jets, but with a threshold of 10 m s^{-1} in place of 17 m s^{-1}.

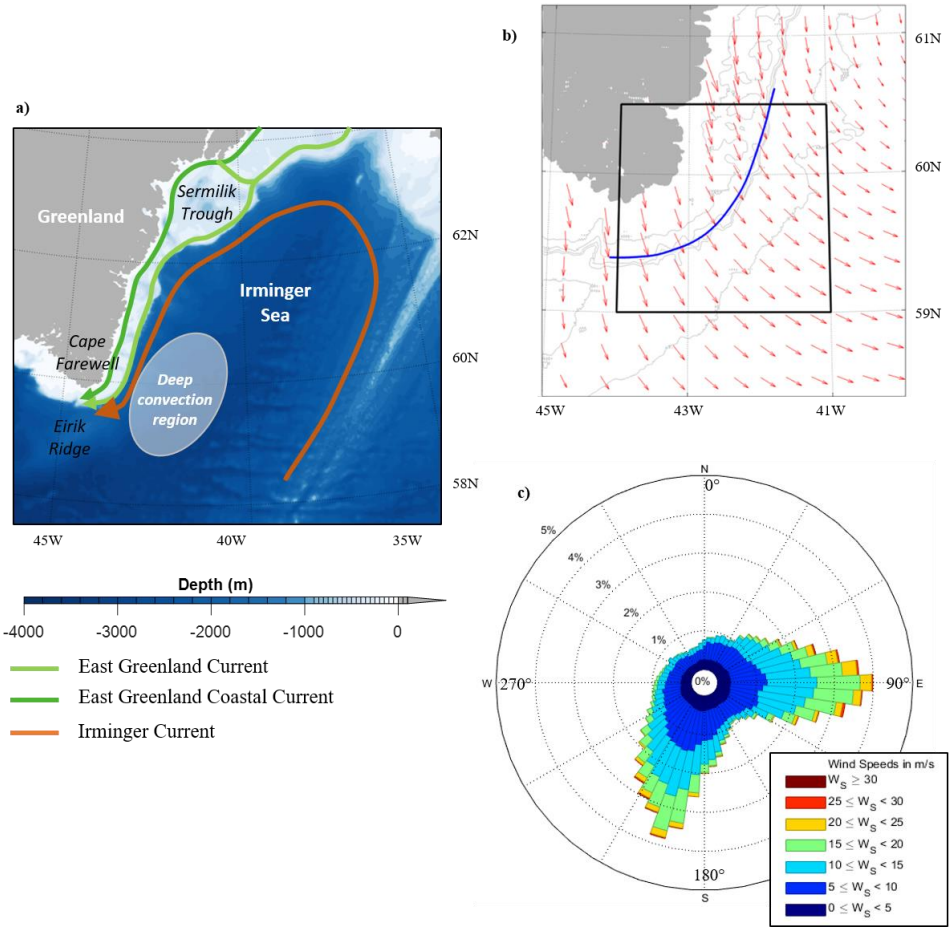

***Figure 3.1**: (a) Overview of surface currents and topographic features along the south-east Greenland shelf; (b) Mean winds at Cape Farewell (red arrows), area of interest for wind computations (black), and shelfbreak defined as the smoothed 800 m isobath (blue), bathymetry in grey: 2000m, 1000m, 800m, 500m and 200m; (c) Wind rose for the area of interest*

3.2.2.2 Computation of transports across the shelfbreak

We compute volume and freshwater transports across the shelfbreak at Cape Farewell. The shelfbreak is defined as the smoothed 800 m isobath, as shown Figure 1b. The isobath is extracted from the etopo2 bathymetric data and smoothed with a 50 km window. Points along the shelfbreak are spaced two to three kilometers apart.

Transports across each section of this line are obtained using the OceanSpy python toolbox (Almansi et al 2019) “Survey” tool. Velocities at the shelfbreak are projected

using the local shelf angle to compute the orthogonal velocity, which is then used to compute volume transport. Freshwater transport is computed with a reference salinity of 34.9 PSU, chosen because it is a good indication of the position of the salinity front and for consistency with previous studies. The cell thickness in MITgcm varies with depth. In order to make export values comparable at different depths, we compute the freshwater and volume transport per meter of the water column.

To compute across-shelf sea-ice transport, sea-ice velocities at the shelfbreak are extracted with the Survey tool, and projected to obtain the orthogonal velocity. The sea-ice volume transport is then computed as:

$$T_{ice} = v_{\perp ice} * H_{eff} * d_x,$$

where $v_{\perp ice}$ (in m s^{-1}) is the ice velocity across the section, H_{eff} (in m) is the effective thickness of sea-ice (thickness of the ice if it were homogeneously distributed over the cell), and d_x (in m) is the cell width.

In order to compare sea-ice export to liquid freshwater export, we compute the freshwater transport equivalent of across-shelf sea-ice export. First, the water volume transport equivalent is computed as:

$$T_{ice/water} = T_{ice} * \frac{\rho_{ice}}{\rho_{water}},$$

With ρ_{water} = 1027 kg m^{-3} the density of seawater and ρ_{ice} = 917 kg m^{-3} the density of sea-ice.

Finally, we compute the freshwater transport equivalent of sea-ice transport. Sea-ice is not pure freshwater, and we compute the freshwater transport as for liquid freshwater transport:

$$T_{ice\_FWT} = T_{ice/water} * \left(\frac{S_{Ref} - \frac{S_{eff}}{H_{eff} * \rho_{ice}}}{S_{Ref}}\right),$$

with S_{Ref} the reference salinity, and S_{eff} the effective salinity, retrieved from MITgcm. The effective salinity is given in g m^{-2}, the amount of salt in grams in a given sea-ice cell, and is thus divided by the effective thickness and the density of ice to obtain sea-ice salinity.

Theoretical Ekman transport across the shelfbreak is computed using wind stress from MITgcm projected similarly along the shelfbreak as:

$$\begin{cases} T_{ekx} = \dfrac{\tau_y}{f * \rho_{water}} \\ T_{eky} = \dfrac{-\tau_x}{f * \rho_{water}} \end{cases}$$

τx, τy being the horizontal wind stress components, and the Coriolis parameter f = 10^{-4} s^{-1}.

3.2.2.3 Particle release

To investigate the fate of freshwater during extreme wind events, numerical particle trajectories are simulated using MITgcm and the particle-tracking algorithm presented in Koszalka et al (2013) and Gelderloos et al (2016). Particles were released during 11 tip jets and five strong north-easterly wind events. The particles were released every 6h, at all times identified as belonging to these events. The size of the ensemble of particle releases varied between two and 14 ensemble members, depending on the duration of the wind event. Each ensemble member contained 8106 particles seeded between 0.5 m and 100 m depth, at 0.5 km spacing along the smoothed 800-m isobath. Each ensemble member was run for 90 days. Since 90% of the particles took less than seven days to reach the western side of Greenland, this is more than enough time for robust statistics.

Additionally, two sets of ensembles were run in 2D mode to mimick the behavior of floats in the real ocean, using only horizontal velocities. In the 2D simulations, particles were seeded at 0.5 m and 15 m depth. The simulated trajectories in the 2D simulations were not significantly different from the 3D simulations. Therefore, only the 3D simulation results will be discussed in this manuscript.

3.3 Extreme wind events at Cape Farewell

3.3.1 Identified extreme wind events in MITgcm

Using the method presented in Section 2.2, we identify eleven tip jets and five strong north-easterly wind events during the MITgcm year. Figure 2a shows the timeseries of wind speed averaged over the area of interest (black line), with identified tip jets (red shade) and strong north-easterly (blue shade) events. In the MITgcm year, tip jets occur mainly in winter, from the end of October to early March, whereas the strong north-easterly events take place outside of that period in fall and spring. In the summer months (June to September), the mean wind is much weaker and no extreme events are identified.

Figure 2b shows mean winds during all events identified as tip jets and strong north-easterlies in MITgcm. During tip jets, westerly winds extend offshore from Cape Farewell, with the strongest winds (>20 m s^{-1}) over the Irminger Sea, and only weak winds (< 5 m s^{-1}) north of Cape Farewell. Strong north-easterly events are associated with wind speeds between 15-20 m s^{-1} along the southeast shelf, and weak winds on the western side of Greenland. The structure and magnitude of these wind events is consistent with existing studies (Moore and Renfrew 2005, Renfrew et al 2009). Most detected events last between ½ day and a day, with three exceptions during which gale force winds last two

or three days. On average, the time evolution of tip jets shows a clear peak shape, with winds reaching 20 m s^{-1} at peak, from 10 m s^{-1} 30 h before and after the peak. For north easterlies, the curve is similar, but with stronger winds before the event and a weaker peak.

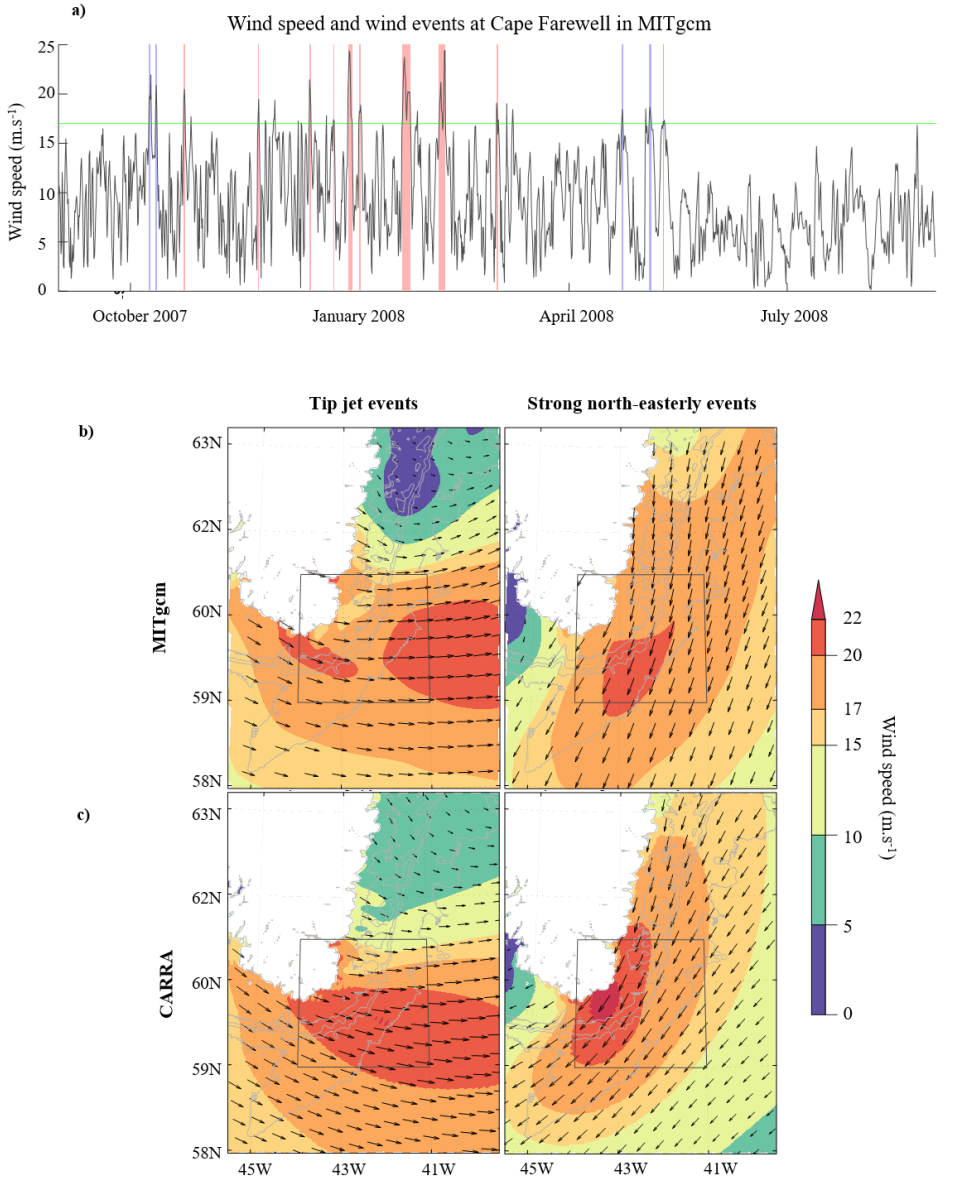

Figure 3.2: *(a) Wind speed time series in the region of interest for MITgcm (black), detected tip jets (red shade) and north-easterly events (blue shade). The green line indicates the 17 m* s^{-1}

threshold value for extreme wind events; (b) Average wind speed and direction during tip jet and strong north-easterly events in MITgcm; (c) Average wind speed and direction during tip jet and strong north-easterly events in CARRA

3.3.2 Comparison to wind events identified in the 1998-2019 CARRA time series

The same detection method is applied to surface winds from the CARRA reanalysis, which spans 22 years from 1998 to 2019. In total, 240 tip jets and 289 strong north-easterly events are detected during that period.

Characteristics of tip jet and strong north-easterly events are similar between CARRA and the ASR-2 reanalysis used in MITgcm, with a few differences. As visible in the composites Figure 2c, the north-easterly events are stronger in the CARRA reanalysis, and both tip jets and north-easterly events show strong winds closer to the coast in CARRA reanalysis than in ASR-2. In CARRA, most events last between 0.5 day and a day (205 north-easterly events, 183 tip jets), some events last between 1.5 and 2.5 days (70 north-easterly events, 50 tip jets) and only very few last for a longer time (less than 10 of each). Mean wind speeds in the area are mostly between 18 and 25 m s^{-1} with a long tail distribution of more extreme events up to 32 m s^{-1}, with similar magnitude for tip jets and strong north-easterlies.

The seasonal distribution of wind events in CARRA is very similar than in MITgcm: Most wind events are observed in the winter months, especially tip jets. A few strong north-easterly events are detected in summer, but most of them also take place in the winter months. In total, more than 90% of tip jets and 80% of strong north-easterlies take place between October and April. The composite of mean wind speeds in the area, centered on the peak wind of each event, shows a similar behavior as in MITgcm. The temporal evolution of wind speeds during strong north-easterly and tip jet events are here much more alike, with similar initial and peak speeds. The number of events varies from year to year (Figure 3), with a minimum of two tip jet events in the winter 2009-2010, and a maximum of 21 in 2014-2015. This year-to-year variability between the number of tip jets and north-eastly events is due to variability of background atmospheric conditions, that can be linked to the phase of the North Atlantic Oscillation (NAO, Hurrell 1995), and in particular the position of the Icelandic low. During positive NAO phases, the North Atlantic storm track shifts northward, which favors the occurrence of tip jet enabling conditions, while during negative NAO phases the contrary happens (Bakalian et al 2007, Våge et al 2009, Josey et al 2019), hence the correlation between the number of tip jets and the NAO index, visible Figure 3.

On average, 13 strong north-easterly events and 11 tip jet events were detected each year in CARRA. In the winter 2007-2008, 13 tip jet events and 12 strong north-easterly events were detected, close to the multiyear average. This makes 2007-2008 an adequate period to study the impact of wind events on freshwater export. As mentioned

above, the mean wind speeds during strong north easterlies is higher in CARRA than MITgcm, which explains why more north-easterly events are identified as strong wind events in the reanalysis.

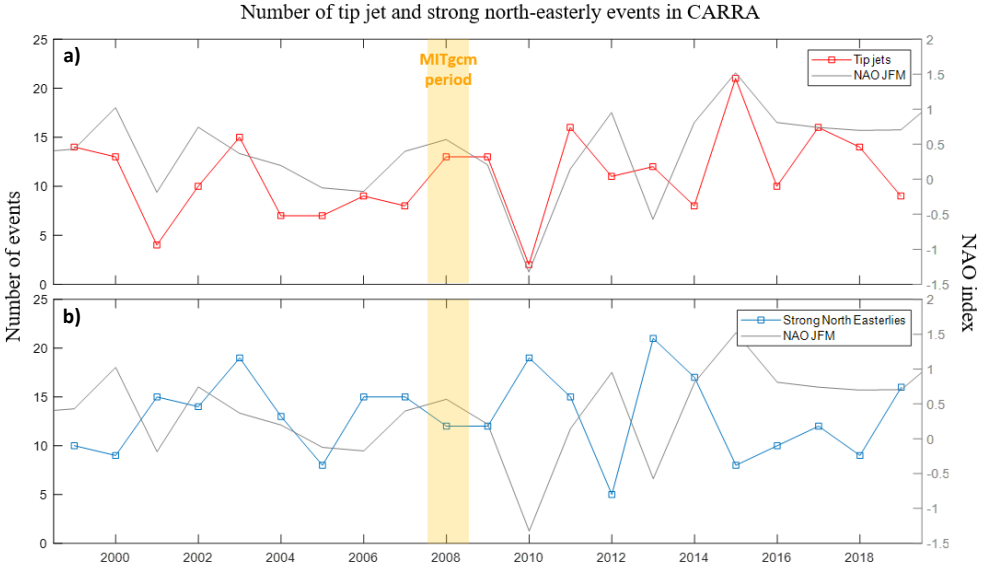

Figure 3.3: (a) *Time series of number of tip jets per year in the CARRA reanalysis, and seasonal mean (January, February, March) NAO index; (b) Time series of number of strong north-easterlies per year in the CARRA reanalysis, and seasonal mean (January, February, March) NAO index; The number of wind events per year is computed from summer to summer so that the whole winter is included in the yearly means.*

3.4 Impact on liquid freshwater export

3.4.1 Export across the shelfbreak

The strong wind patterns presented in Section 3 can impact the top layer of the shelf waters. In particular, strong westerly winds such as tip jets have the potential to drive freshwater export away from the shelf. To investigate this process, the shelfbreak at Cape Farewell is defined as the 800 m smoothed isobath, and time series of volume and freshwater export across the shelfbreak are computed as presented in Section 2.2. Figure 4 displays time series of volume, Ekman and freshwater transport, together with identified tip jet events (dark grey shade) and moderate westerly wind events (light gray shade).

Figure 4a shows the time series of shelfbreak volume transport in the first 100 m and Ekman transport, both filtered with a one day low-pass 2nd order Butterworth filter. The two time series show a strong correlation (Pearson's correlation coefficient > 0.8), suggesting that export in the top layer of the water column is predominantly wind-driven. Times identified as tip jets are associated with the strongest export at the shelfbreak. Moderate westerlies are also associated with export, though weaker.

Figure 4b and Figure 4c show respectively volume and freshwater transport at the shelfbreak, at the surface and at 25 m depth, also filtered with a one day low-pass 2nd order Butterworth filter. Volume and freshwater transports are strongest at the surface, and surface export peaks occur both during tip jets and moderate westerlies. At 25 m depth, only tip jets have a clear impact on volume and freshwater export. The strongest wind and export events take place in winter, but moderate westerly events in summer can also lead to non-negligible freshwater export at the surface, especially due to fresher waters being present over the shelf in summer. For instance, a moderate westerly event on the 15th August led to surface freshwater export comparable in intensity to the one happening on the 6th February, associated with the most intense winter tip jet.

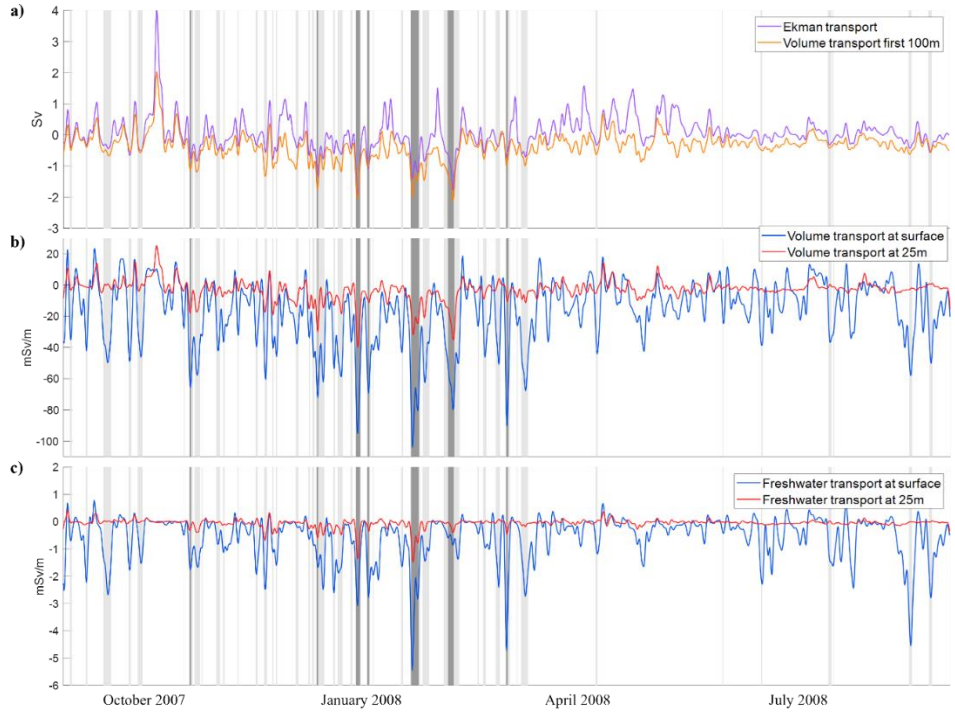

Figure 3.4: *(a) Time series of Ekman transport (yellow) and volume transport in the first 100m (red); (b) Time series of volume transport at the surface and 25m; (c) Time series of freshwater*

transport at the surface and 25 m. Light gray lines correspond to moderate westerlies, dark gray lines to tip jets. All time series are filtered with a one day low-pass 2nd order Butterworth filter.

3.4.2 Salinity changes during different wind events

The previous section showed that westerly winds, and tip jets in particular, lead to freshwater export across the shelfbreak (defined as the 800 m isobath). To investigate in more detail what happens during these export events, salinity composites for different wind events are displayed in Figure 5 (tip jets as defined section 2.2 in red, moderate westerlies ≥ 10 m s^{-1} and < 17 m s^{-1} in light red, north-easterlies ≥ 10 m s^{-1} in blue and weak winds < 10 m s^{-1} in black). To avoid artifacts due to high seasonal variability in salinity and the uneven distribution of tip jets compared to the other wind events considered, only the winter months are taken into account when computing the composites (December to April). North-easterlies stronger than 10 m s^{-1} are used instead of the strong north-easterlies defined earlier due to the low amount of such events detected during these months.

Figure 5a shows contours of the salinity composites for the surface layer. During tip jets, fresher waters extend away from the coast south of Cape Farewell. The 32.5 isohaline then shows very fresh waters extending towards the shelfbreak, while the 34.9 isohaline shows that the salinity front situated at the shelfbreak moves slightly offshore. At Eirik Ridge, tip jets drive an extension of the fresher waters over the ridge. During north-easterly winds, the front moves in the opposite direction and fresher waters are brought closer to the coast than during weak winds.

Figures 5b and 5c show the vertical sections corresponding to the green lines on Figure 5a, with contours of salinity composites for the same wind events. Both sections show that tip jet events, and to a lesser extent moderate westerlies, are associated with an offshore extension of fresh shelf waters. During tip jets, the extension is visible up to 100 m deep. On the contrary, north-easterly events are associated with a vertical straightening of the isohalines compared to the weak-winds situation. This behavior is clearest for section 2, which is located at Eirik Ridge, where most freshwater is exported during tip jet events.

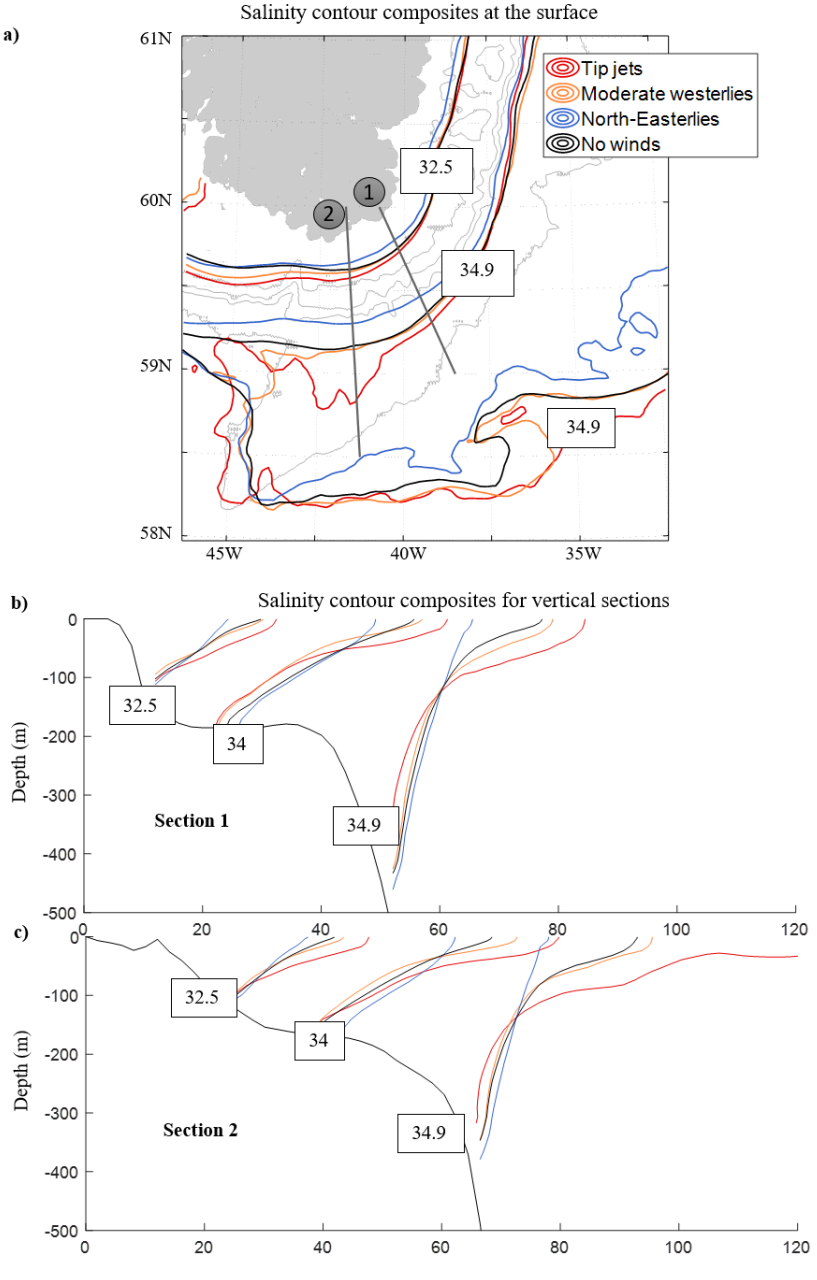

***Figure 3.5**: (a) Salinity composites at the surface, (b) Salinity composites along section 1 in green on panel a. (c) Same for section 2. For composites, colors are: tip jets (red), moderate westerlies ≥ 10 m s^{-1} and < 17 m s^{-1} (light red), north-easterlies ≥ 10 m s^{-1} (blue), and weak winds < 10 m s^{-1} (black)*

3.4.3 Trajectories of particles released during extreme wind events

The salinity composites show that strong wind events impact the EGC front at Eirik Ridge, with fresher waters in the upper 100 m pushed offshore during tip jets (Figure 5). This also agrees with the peaks in off-shelf freshwater transport in our time series presented in Figure 4. However, these analyses do not reveal whether freshwater is then exported to neighboring seas, or rejoins the EGC after the wind event. To further investigate where the freshwater goes during and after wind events, particles were released at the shelfbreak at all times identified as part of tip jets and strong north-easterly wind events, as described in the methods section 2.2.3.

Figure 6 shows the resulting particle distribution density maps, for the first 2 weeks after particle release. The maps are shown for events classified as tip jets and events classified as strong north-easterlies, for particles released at the surface and at 25 m depth. Particles that were released during strong north-easterly events (Figure 6b and 6d) follow the shelfbreak towards the western side of Greenland. While the particles deployed at the surface tend to flow on the offshore side of the shelfbreak, a minority of the particles deployed at 25 m spread out onto the shelf.

Particles deployed during tip jets (Figure 6a and 6c) show a different behavior. Particles deployed at the surface are pushed offshore by the strong westerly winds. In the first two weeks after their release during tip jet events, these particles are found in the EGC, but also in the Western Irminger Sea and over Eirik Ridge. Particles released at 25 m during tip jets mostly follow the shelfbreak into the West Greenland Current with only a minority of particles driven over Eirik Ridge, and nearly none exported to the Irminger Sea. Only the two most intense tip jet events (starting on the 22nd of January and the 6th of February) are associated with particle export at 25 m, which leads to the signal of export being fairly faint in the particle density distribution plot. This is consistent with the export time series presented Figure 4, which show that strong export at 25 m depth only occurs during the most intense and longest tip jet events. In panels a, b and c, a return flow of particles is visible at the MITgcm western boundary. This recirculation is also visible in the mean surface circulation in MITgcm, and therefore not due to wind events. It could be related to previously identified recirculation in the area (Fischer et al 2018), but this is beyond the scope of this study, and because it takes place so close to the boundary, this setup of the MITgcm is not adapted to investigate it.

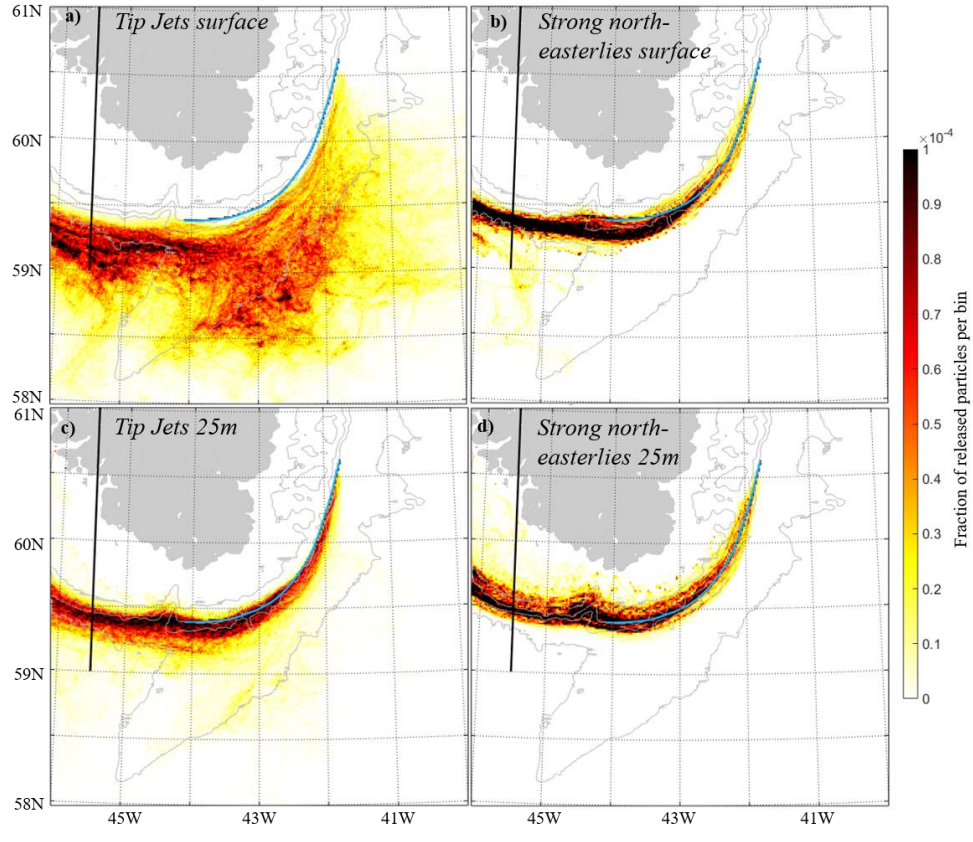

Figure 3.6: *Density maps of particles within two weeks after release, with a bin size of 0.025 decimal degrees of longitude and 0.0125 decimal degrees latitude. The colorbar corresponds to the fraction of released particles found in each bin. (a) Particles released at 0.5 m depth during tip jet events; (b) Particles released at 25 m depth during tip jet events; (c) Particles released at 0.5 m depth during strong north-easterly events; (d) Particles released at 25 m depth during strong north-easterly events; For all figures, the deployment line (blue) and the crossing line to the western side of Greenland (black) are shown.*

To quantify the fraction of particles exported during each type of wind event, we compute the number of particles crossing the 45.5°W line to west Greenland between 59-61°N (black line Figure 6), as a function of release depth. During strong north-easterly events, all particles crossed that line within two weeks (less than 1% of the particles released at the surface stayed on the eastern side of Greenland). During tip jets, the number of particles staying on the eastern side of Greenland depended on the depth at which they were released, but also on the intensity of the tip jet event. Figure 7 shows the fraction of particles deployed during tip jets that do not cross the line to west Greenland as a function of their release depth (in blue). Forty-seven percent of the particles released at the surface did not cross the line to west Greenland, meaning they were exported to the Irminger Sea or driven over Eirik Ridge. The percentage of exported

particles decreases with the release depth to 18% for 5 m, 10% for 10 m and only 3% for 25 m. The same analysis is made for the most intense tip jet event, taking place from the 6th to 9th February (in red on Figure 7). Fifty-three percent of the particles released at the surface during that event did not cross the line to west Greenland, 25% at 5 m, down to 16% at 10 m and 7% at 25 m. More particles are exported at the surface during this strong event, and the fraction of particles exported decreases slower with depth compared to the ensemble of tip-jet events.

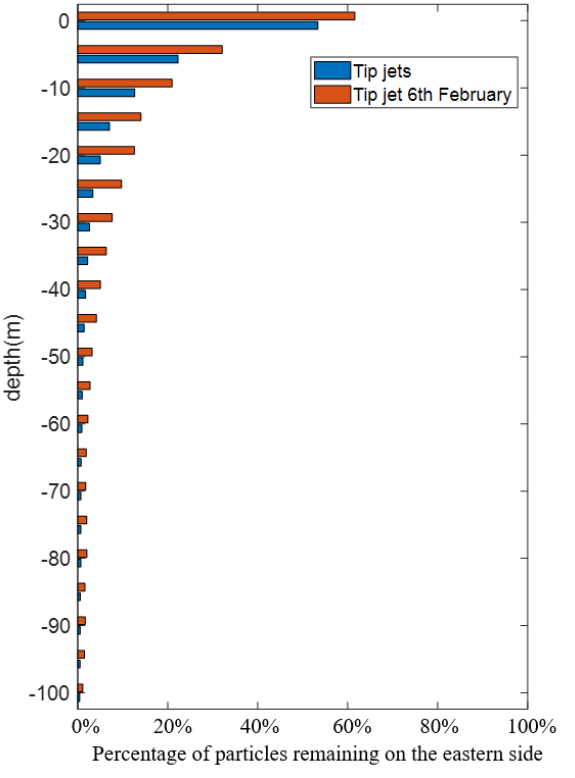

Figure 3.7: *Fraction of particles that do not cross the 45.5W, 59-61N line to west Greenland within two weeks as a function of release depth, for particles released during all tip jets, and particles released during the strongest tip jet identified, which started on the 6th of February*

3.5 Wind-driven solid freshwater export

3.5.1 Wind-driven ice export in MITgcm

Strong wind events at Cape Farewell are likely to not only impact liquid freshwater export, but also sea-ice cover, and lead to export of sea-ice that then melts in the Irminger Sea. To evaluate the impact of westerlies on ice export at Cape Farewell, the

freshwater equivalent of sea-ice transport across the shelfbreak is computed from MITgcm using the methods described in section 2.2.2. Figure 8a shows the resulting across-shelf transport together with identified tip jet (red) and moderate westerly (light red) events. Some sea-ice export events seem associated with wind events, such as the moderate westerlies of mid-January and late February; however, tip jets are not associated with the strongest export, and there is no clear correlation between sea ice export and the intensity of westerly winds. Ice cover at Cape Farewell is highly variable throughout the winter, and in general ice concentration is very low in the area, as shown with the blue line in Figure 8a. It is therefore likely that even if sea ice responds to westerly wind events by veering eastwards, it does not reach the shelfbreak, and computed export depends as much on how much sea ice is present at the time of the wind event as on the wind event itself.

The impact of tip jets on sea-ice cover is investigated using sea-ice composites at the peak of each wind event, 24 h before and 24 h after. Tip jet events are considered only if ice concentration is above 5% in the area of interest 24h before peak winds. Figure 8b shows the resulting composite ice-concentration maps. As westerly winds increase, the sea ice moves away from the coast and towards the Irminger Sea. Overall, ice concentrations decrease significantly south of 61°N during the wind event. As the wind calms down, very low concentrations of sea ice re-enter the shelf. The decrease in sea-ice concentration is likely due to enhanced melting past the front, as the ice enters the warmer waters offshore, but also to the ice breaking up in strong waves during peak winds. Even though the response of sea ice to tip jets is clear, the ice only rarely crosses the shelfbreak, which could also contribute to the low level of ice export and lack of correlation with wind events mentioned above.

3.5.2 Effect of tip jets on sea ice in CARRA

In order to investigate the impact of westerlies on sea ice at Cape Farewell over a longer time period, we apply the same analysis to the CARRA sea-ice concentration data, derived from satellite observations. Figure 8c shows composites of sea-ice concentration anomaly 24 h before, during, and 24 h after a tip jet event as detected in the CARRA time series. As for the analysis presented above, wind events are only considered if ice concentration is above 5% in the area of interest 24 h before peak wind. This corresponds to 19 tip jets, less than 10% of all tip jets detected in CARRA.

The results are similar to what we obtained with MITgcm, although the satellite products used in the CARRA reanalysis for sea-ice have a lower resolution (15 to 60 km depending on conditions and what product can be used). During tip jets, ice concentration decreases close to the coast, sea-ice at Cape Farewell detaches from the coast and forms a tongue along the shelfbreak. A general reduction in sea-ice concentrations is seen south of 61°N indicating a loss of ice on the shelf. Similarly as in MITgcm, the ice stays mostly confined over the shelf even though it veers eastwards as a response to tip jets.

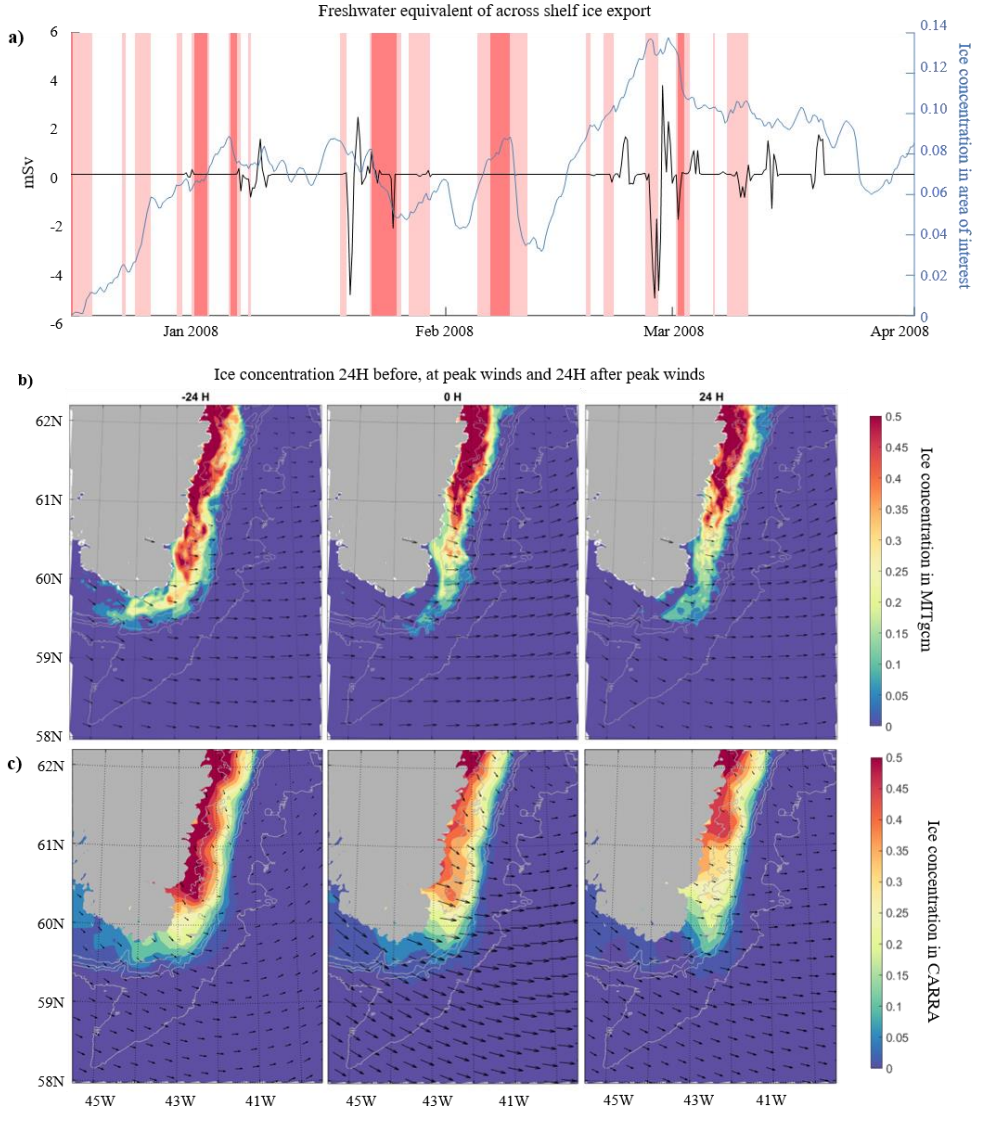

Figure 3.8: *(a) Time series of sea-ice freshwater equivalent transport (black) and sea-ice concentration (blue) in the area of interest. Tip jet events are indicated in red and moderate westerlies in light red. Negative transport is directed off-shelf. (b) Composite of ice concentration and 10 m winds during tip jet events from MITgcm, 24 h before, during, and 24 h after peak tip jet winds; (c) Composite of ice concentration and 10 m winds from CARRA during tip jet events, 24h before, during, and 24 h after peak tip jet winds.*

3.5.3 Sea-ice response to tip jets as seen with MODIS

Tip jet events lead to a decrease in sea-ice cover at Cape Farewell both in the MITgcm simulation, and in the satellite derived sea-ice product retrieved from the CARRA reanalysis. Sea-ice however remains mostly on the shelf, even as it turns eastward in response to wind forcing. This leads to only a few sea-ice across-shelf export events throughout the year. We investigate whether this result is consistent with higher resolution observations using the MODIS true-color imagery at Cape Farewell. Figure 9 shows MODIS snapshots retrieved for two tip jet events, starting on the 28th of January and on the 6th of February, with CARRA winds at the time of the event superimposed over the imagery in red, and the bathymetry in white. These two tip jet events were detected both in MITgcm and in CARRA, and selected based on ice cover and the absence of clouds.

The MODIS snapshots show sea ice responding in a similar way as outlined earlier, but also reveal details that were not visible in MITgcm and the satellite sea ice concentration products from CARRA. During both tip-jet events, sea ice is pushed away from the coast, forming a tongue at Cape Farewell that fans out into the Irminger Sea. On the day following the strongest winds the sea ice is further dispersed, broken up into smaller pieces and much less concentrated, likely melting as it enters the warmer waters in the Irminger Sea. The bathymetry shows that the ice extends further off the shelfbreak than in all the export events investigated in MITgcm, suggesting that the model-based export might be an underestimate.

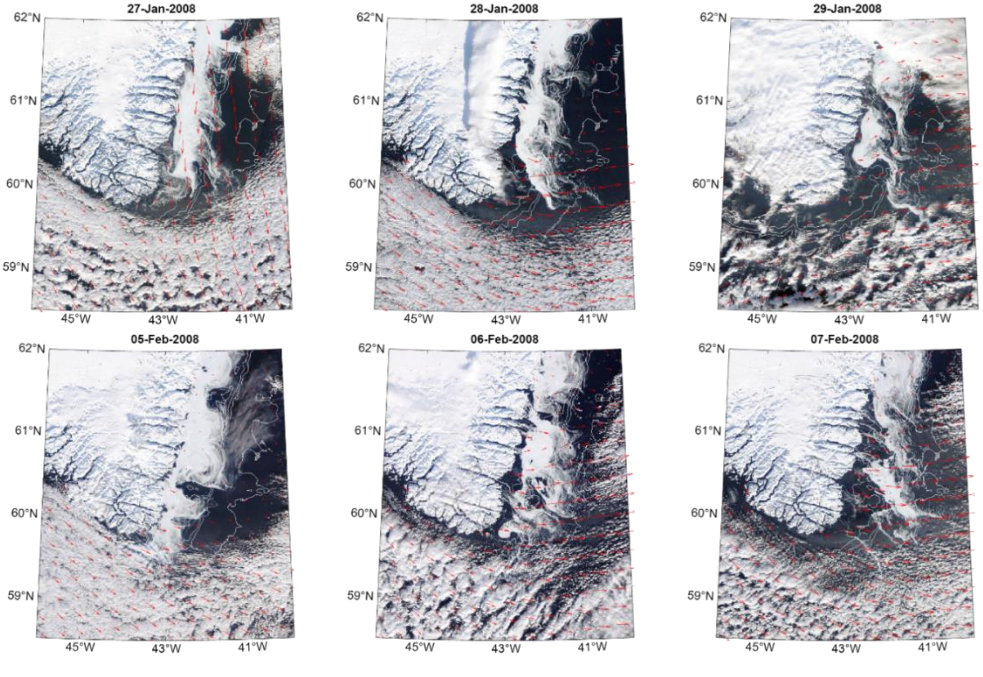

Figure 3.9: *MODIS imagery during the strong wind events taking place around 28 January and 6 February. Bathymetry is superimposed in white, isobaths are drawn for 5000, 2000, 1000, 500 and 200m deep. CARRA 10 m winds are shown in red.*

3.6 Summary and discussion

Using results from a high-resolution model, we show that strong westerly winds at Cape Farewell can impact the water column up to 100 m deep and lead to tilting of the front and an offshore extension of the fresh water layer, especially over Eirik Ridge. During these events, part of the surface waters is exported off the shelf, over Eirik Ridge and into the Irminger Sea, as visible in the particle deployment. Tip jets also impact sea-ice cover at Cape Farewell, but we find that they only lead to minimal sea-ice export at the shelfbreak. The following section discusses these results, in particular the importance of moderate versus extreme westerly winds in driving export, the contribution of sea-ice to total freshwater export, and potential future impacts on convection and overturning.

At the latitude of Cape Farewell the EGC in MITgcm has a yearly mean freshwater transport of 160 mSv in the upper 100 m (computed across section 1 in Figure 5a). This freshwater transport reaches 200 mSv during tip jets as the EGC is speeding up due to the enhanced wind forcing. On average, tip jet events lead to the export of 37.5 mSv of freshwater at the shelfbreak in the first 100 m, nearly one fifth of the upper EGC transport. Tip jets are associated with the strongest freshwater export at Cape Farewell, but moderate westerlies are much more frequent and can also drive offshore export at the very surface, as visible Figure 4c. On average, 15.9 mSv of freshwater was exported during moderate westerlies, amounting to a total of 78.4 km^3 of freshwater exported during moderate westerlies of the MITgcm year, against 38 km^3 during tip jet events. Contrarily to tip jets, moderate westerlies also take place in summer, when the shelf is particularly fresh. August was the third month with most freshwater export, with 11.8% of the total export, after December (15.6%) and January (19.1%). In total, 37.8% of the annual freshwater export across the shelfbreak took place from May to October. Such wind-driven freshwater export at Cape Farewell in summer could enhance re-stratification processes and impact the pre-conditioning for deep convection (Oltmans et al 2018). The particle deployment and salinity composites however showed that freshwater is brought the furthest offshore during the strongest wind events, which suggests that though moderate westerly winds can lead to export at the shelfbreak, tip jets are likely to be more important for export to deep convection regions.

In addition to liquid freshwater export, strong wind events also impact sea ice at Cape Farewell. Impact of strong wind events on sea-ice cover along the Greenland shelf elsewhere has previously been investigated by Oltmans et al (2014), who found that katabatic winds in the Ammassalik region lead to a strong decrease (29%) of ice cover in Sermilik Trough. Both in MITgcm and the satellite products of the CARRA reanalysis, tip jets are associated with an eastward shift and a decrease of sea ice concentration at Cape

Farewell, with sea ice remaining on the shelf, or disappearing as it reaches the shelfbreak. In MITgcm, sea ice export at the shelfbreak is not well correlated to wind events and is three orders of magnitude smaller than liquid freshwater export (Annual volume of freshwater exported, with a reference salinity of 34.9: 0.305 km^3 for sea-ice, against 207 km^3 for liquid freshwater in the first 100 m). This could be explained by the intermittent sea-ice cover at Cape Farewell: most of the tip jets and westerly events take place at times when there is not enough ice to lead to export. The MODIS imagery snapshots show that tip jets can lead to sea ice tongues crossing the shelfbreak, which we never see in either MITgcm or CARRA, even during the strongest events. MODIS shows that the sea ice brought offshore during these events is broken up and forms fine filaments, which could explain why it is not resolved in the other data sets, that have a lower resolution. However, even though the MODIS observations suggest an underestimation of sea-ice export in MITgcm, the filaments and broken up ice tongues that are not resolved in the model only represent a small amount of freshwater, and the actual ice export is still likely to be much smaller than the liquid export.

Deep convection in the Irminger Sea takes place in the central Irminger Gyre (De Jong et al 2016, Våge et al 2011) and south of Cape Farewell (de Jong et al 2012, Piron et al 2015, 2017). Particle tracking showed that a portion of surface waters exported across the shelfbreak during tip-jet events can reach these two regions, but such export is limited to the strongest events. Recent results also show convection up to 750 m at the edge of the EGC (Le Bras et al 2020). Le Bras showed that these lighter, shallower convective waters formed near Greenland enter the Deep Western Boundary Current more easily. The outward tilting of the EGC front, observed during tip jets, but also to a lesser extent during moderate westerlies, locally strengthens stratification where these waters are formed and may thereby affect the strength of near-boundary convection. When (shallow) convection does occur, the freshwater will be incorporated into the mixed layers, affecting the properties of the convectively formed water. This can also contribute to the lower salinities observed in mixed layers south of Cape Farewell compared to the central Irminger Sea, a signal which is subsequently transported to the central Irminger Sea at mid-depth (de Jong et al 2012). A smaller amount of freshwater is likely to enter the central Irminger Sea along the surface and will similarly affect stratification and properties of convective water there.

In this study, we identified the importance of tip jet events in driving freshwater from the shelf towards convection regions. There is a strong interannual variability in the number of tip jet events, which is linked to background synoptic conditions and in particular the NAO phase (Bakalian et al 2007, Våge et al 2009). Years with high NAO phase and numerous tip jet events have been linked to particularly deep convection in the Irminger Sea as well as particularly fresh vintages of convective water (van Aken et al 2011). Therefore, we conclude that current levels of freshwater export at Cape Farewell do not immediately inhibit convection, but can influence its strength and the properties of the convectively formed water masses. Whether this balance will be disrupted with increases in freshwater transport in the EGC linked to Greenland ice sheet melt and Arctic freshwater export is a subject for future studies.

Acknowledgments and Open Research

This project is financially supported by the Innovational Research Incentives Scheme of the Netherlands Organisation for Scientific Research (NWO) under grant agreement nos. 016.Vidi.189.130. RG is financially supported by the U.S. National Science Foundation under Grant OCE-2048496.

The MITgcm numerical solutions used in this study are available on SciServer (http://sciserver.org), developed by the Institute for Data Intensive Engineering and Science at Johns Hopkins University. Instructions for accessing the dataset can be found at: https://oceanspy.readthedocs.io/en/latest/datasets.html. The CARRA reanalysis data is available on the Copernicus Climate data store (https://cds.climate.copernicus.eu/). The MODIS data is available from the NASA worldview snapshots tool (https://wvs.earthdata.nasa.gov/). The NAO index is available from NOAA climate prediction center
(https://www.cpc.ncep.noaa.gov/products/precip/CWlink/pna/nao.shtml)

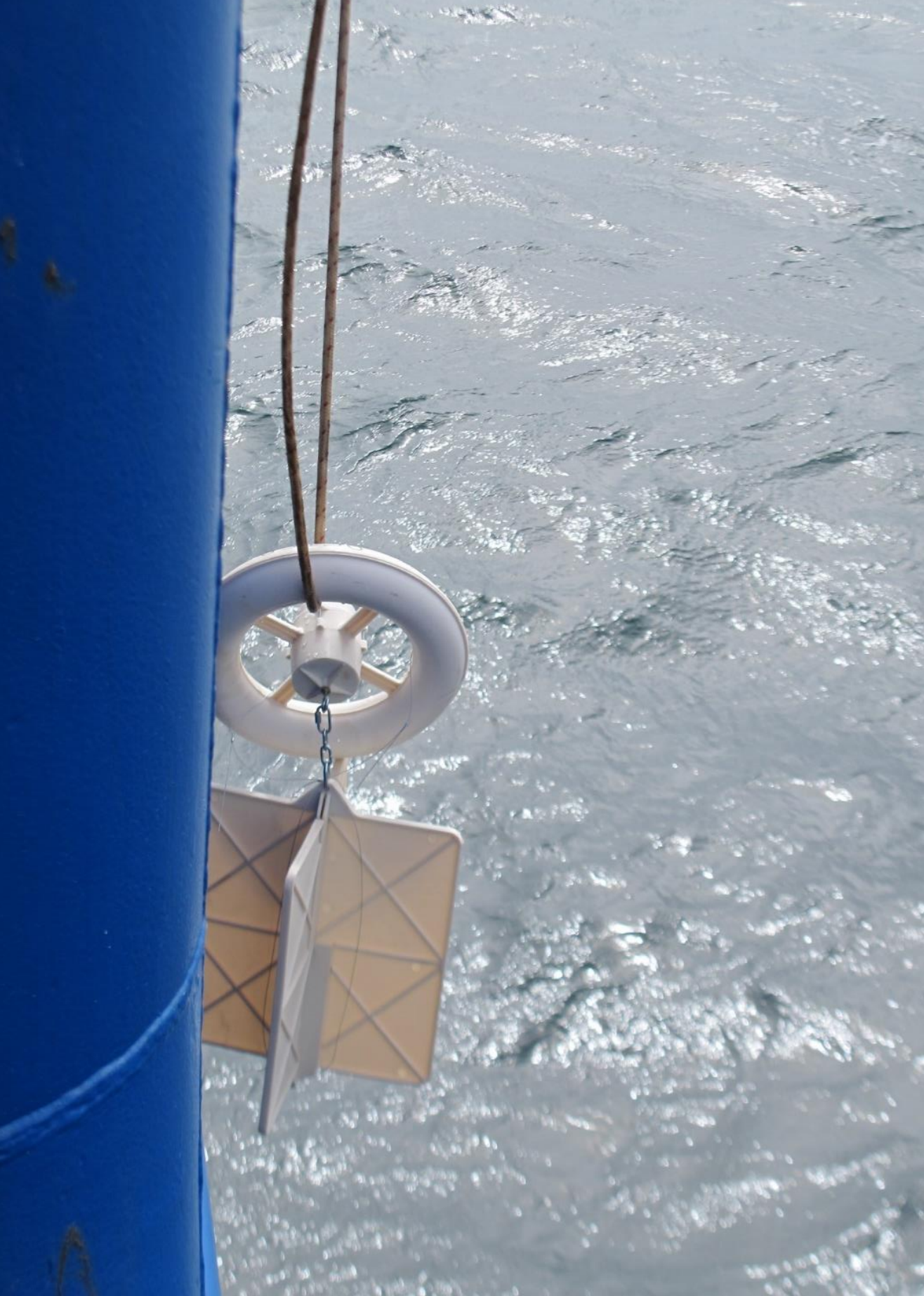

Chapter 4

Cross-shelf exchanges between the east Greenland shelf and interior seas

This chapter was published as:

Duyck, E., & De Jong, M. F. (2023). Cross-shelf exchanges between the east Greenland shelf and interior seas. Journal of Geophysical Research: Oceans, 128, e2023JC019905. https://doi.org/10.1029/2023JC019905

Illustration: Deployment of a CARTHE drifter in July 2020 at Cape Farewell: The CARTHE drifters were lowered to the water using a rope. Picture : Nora Fried.

Abstract

Increasing freshwater fluxes from the Greenland ice sheet and the Arctic to the Subpolar North Atlantic could cause a freshening of deep convection regions and affect the overturning circulation. However, freshwater pathways from the Greenland shelf to interior seas and deep convection regions are not fully understood. We investigate exchanges of liquid freshwater between the east Greenland shelf and neighboring seas using drifter data from five deployments carried out at different latitudes along the east Greenland shelf in 2019, 2020 and 2021, as well as satellite data and an atmospheric reanalysis. We compute Ekman transport from winds and geostrophic velocity from satellite altimetry at the shelfbreak and identify the Blosseville Basin and Cape Farewell as areas favorable to cross-shelf exchanges. We further investigate exchange processes in these regions using drifter data. In the Blosseville Basin, drifters are brought off-shelf towards the Iceland Sea and into the interior of the Basin. As they are advected downstream, they re-enter the shelf and are driven towards the coast. At Cape Farewell, the wind appears to be the main driver, although on one occasion we found evidence of an eddy turning drifters away from the shelf. The drifters brought off-shelf at Cape Farewell mostly continue around Eirik Ridge, where they re-enter the West Greenland Current. Overall, the identified export over the east Greenland shelf is limited, small scale and intermittent, thus unlikely to flux large amount of liquid freshwater into the interior, though exchange processes could enhance mixing in the near-shelf region.

4.1 Introduction

The Atlantic Meridional Overturning Circulation (AMOC) is a key element of the climate system, redistributing heat and freshwater across the oceans (Buckley & Marshall, 2016). Anthropogenic climate change is predicted to lead to a weakening of the overturning circulation in the coming century (Collins et al., 2019, Weijier et al 2020), which would have important consequences on global and regional climate (Jackson et al 2015, Zhang et al 2019).

Increasing upper ocean stratification in the Subpolar North Atlantic (SPNA) could lead to a weakening of deep convection and affect the AMOC. In particular, input of freshwater from the Arctic (Haine et al 2015) and Greenland (Bamber et al 2018, Shepherd et al 2020) is predicted to increase in the coming decades. If this additional freshwater enters interior seas of the SPNA, it could impact the stratification of deep convection regions (Aagaard & Carmack, 1989; Manabe & Stouffer, 1995; Bakker et al 2016, Weijer et al., 2019). However, model studies disagree on the timescale at which additional freshwater input could have a significant impact on the AMOC and whether it is already visible (Böning et al 2016, Yang et al 2016, Dukhovskoy et al 2019). There are still uncertainties on the exact pathways freshwater from Greenland and the Arctic would follow to enter the deep convection regions (Dukhovskoy et al 2016). While recent observations suggested that overturning east of Greenland dominates the total overturning in the SPNA (Lozier et al., 2019; Petit et al., 2020; Li et al., 2021), studies of the impact of additional freshwater input on deep convection and deep water formation mostly focused on the Labrador sea so far (e.g., Pennelly et al., 2019; Yang et al., 2016). In summer, shallow freshwater layers are seen over the deep convection region in the Irminger Sea (Sterl & de Jong, 2022). In winter, this layer is mixed down the water column by convective mixing, which reaches down to 400 m even in weak winters (de Jong et al. 2012). The re-formation of a new freshwater layer over a few months in spring (Sterl & de Jong 2022) suggests that it is fed by local sources. This restratification process in the Irminger Sea and the possibility of additional freshwater inhibiting convection in the Irminger and Nordic Seas, underline the need for a better understanding of freshwater pathways east of Greenland.

The East Greenland Current (EGC) transports fresh polar surface waters coming from the Arctic and from Greenland runoff (Rudels 2002) southwards over the shelf (Figure 1). The main branch of the EGC flows alongside the shelfbreak from Fram Strait to Cape Farewell (Sutherland and Pickart 2008, Havik et al 2017a). A fresher branch, referred to as East Greenland Coastal Current (EGCC) flows alongside the coast (Bacon et al 2014, Havik et al 2017a, Foukal et al 2020). The fresh surface waters in the EGCC and EGC are isolated from the warmer, more saline interior seas, by a strong hydrographic front at the shelfbreak. Over most of the east Greenland shelf, strong and consistent barrier winds driven by the steep topography of Greenland constrain the surface waters further towards the coast by driving onshore Ekman transport (Moore & Renfrew, 2005).

North of Denmark Strait, three permanent circulation features are known to contribute to export from the EGC into the Nordic Seas. The Jan Mayen Current is situated at the Jan Mayen fracture zone (Bourke et al 1992) and diverts shelf waters into the Greenland Sea. The East Icelandic Current branches off from the EGC at the latitude of Scoresby Sund into the southern Iceland sea (Jónsson, 2007, Casanova-Masjoan et al, 2020). The Jan Mayen and East Icelandic Current are estimated to only divert a small fraction of the total freshwater transport of the EGC towards the Nordic Seas (Macrander et al 2014, Havik et al 2017a). At the entrance of the Blosseville Basin, the EGC branches off and forms the separated EGC, that flows alongside the slope at the base of the Iceland shelf, diverting up to 37% of freshwater away from the shelfbreak (Våge et al 2013, Havik et al 2017b, De Steur et al 2017). Two hypotheses were proposed to explain the formation of this separated branch: Baroclinic instabilities at the northern end of Blosseville Basin, characterized by a sharp bend in the bathymetry, could lead to the shedding of eddies that coalesce on the other side of the basin, forming the separated branch (Våge et al 2013, Havik et al 2017a, Havik et al 2017b). Alternatively, the branch could be part of an anticyclonic gyre caused by negative wind stress curl over the Blosseville Basin (Harden et al 2016).

South of Denmark Strait, only limited export towards the Irminger Sea has been identified (Pennelly et al 2019, Duyck and De Jong 2021). Deep troughs along the shelf, notably the Kangerdlussuaq and Sermilik troughs, lead to exchanges between the shelfbreak and coastal current. Part of the shelfbreak EGC flows inside these troughs and either rejoins the shelfbreak current downstream or joins the EGCC (Sutherland and Pickart 2008, Sutherland and Cenedese 2009, Duyck and de Jong 2021). At Cape Farewell, northeasterly winds are less dominant than over the rest of the shelf and alternate with westerly winds. Strong westerly events, or Tip Jets (Moore 2003; Moore & Renfrew, 2005) could drive freshwater off the shelf at Cape Farewell (Duyck et al 2022), possibly impacting convection close to the shelfbreak or just south of Eirik Ridge (de Jong et al., 2012, Piron et al., 2016, 2017).

The study presented here investigates exchanges between the east Greenland shelf and neighboring seas, as well as processes responsible for these exchanges. It uses a new drifter dataset, as well as atmospheric reanalysis data and satellite observations. Section 2 describes the drifter deployments and the other datasets used. In section 3 we identify the main areas of cross-shelf exchange along the east Greenland shelf, and investigate processes that could lead to exchanges in the Blosseville Basin and at Cape Farewell. Section 4 discusses the importance of the identified exchange processes for freshwater export east of Greenland.

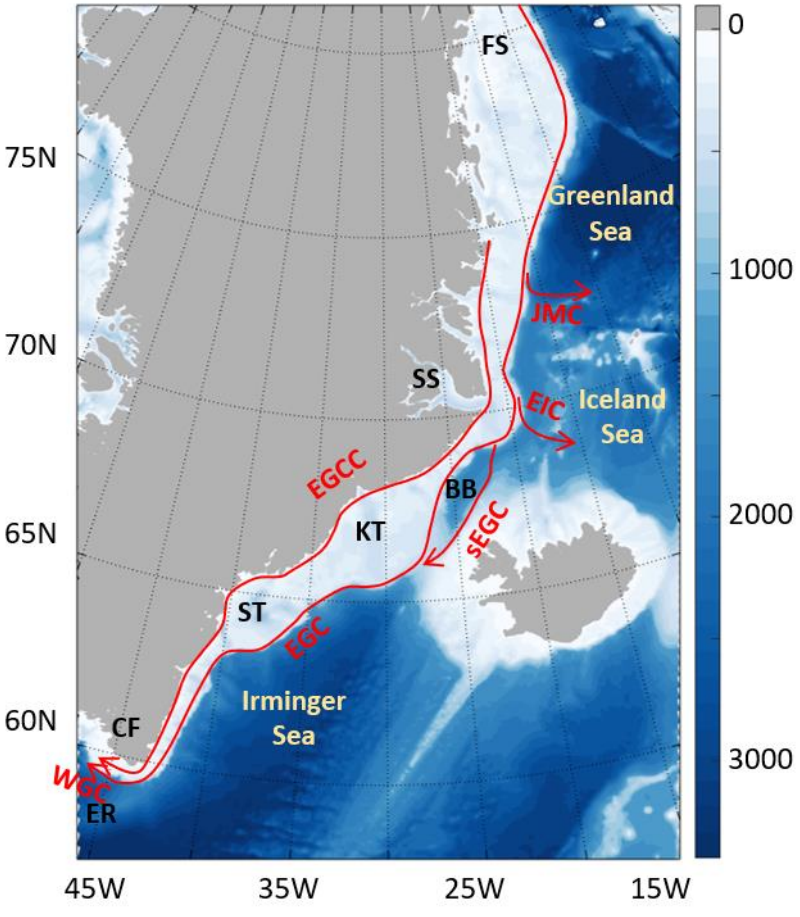

Figure 4.1: *Bathymetry and overview of the circulation over the East Greenland shelf. EGC: East Greenland Current; EGCC: East Greenland Coastal Current, sEGC: Separated East Greenland Current; JMC: Jan Mayen Current; EIC: East Icelandic Current; WGC: West Greenland Current. FS: Fram Strait. SS: Scoresby Sund. BB: Blosseville Basin. KT: Kangerdlussuaq Trough. ST: Sermilik Trough. DS: Denmark Strait. CF: Cape Farewell. ER: Eirik Ridge. Bathymetry is retrieved from the ETOPO2022 60 arc-seconds dataset (NOAA 2022)*

4.2 Materials and Methods

4.2.1 Drifter datasets

In this study, we use the final drifter dataset of the East Greenland Current Drifter Investigation of Freshwater Transport (EGC-DrIFT) project. As part of this project, 120 drifters were deployed at the east Greenland shelf, over 5 deployments, spread over 3 years, 2019, 2020 and 2021 (Figure 2). Each deployment consisted of two types of surface drifters: SVP and CARTHE drifters.

Surface Velocity Program (SVP) drifters are spherical buoys fitted with a holey sock drogue that anchors the drifter at 15m depth (Lumpkin et al 2017). We deployed SVP drifters fitted with a temperature sensor (named SVP-T in the following) and SVP drifters fitted with both temperature and conductivity sensors (SVP-S). The drifters transmitted measurements and GPS positions via Iridium at 3-hourly intervals for SVP-T drifters and 1-hourly interval for SVP-S drifters. CARTHE drifters (named after the Consortium for Advanced Research for the Transport of Hydrocarbon in the Environment, Novelli et al., 2017) are smaller drifters, made of a floating torus sitting low above water and a solid drogue that anchors them at 40cm. They transmit GPS position at 3-hourly interval. These two types of drifters, anchored at different depth, were deployed in pairs to describe the behavior of different water layers.

The EGC-DrIFT dataset was processed as follows: We first removed duplicate positions, erroneous positions (null or out of bounds coordinates) as well as repeated message dates. We then used a speed criterion to detect spikes in GPS positions. We removed temperature and conductivity values outside of range (Conductivity below 1 S.m-1 or above 50 S.m-1, and sea surface temperature below -2°C or over 20 degrees). We removed remaining spikes in temperature and conductivity manually. Hydrographic properties, such as absolute salinity and density were derived from measurements using the TEOS-10 toolbox (Mc Dougall and Barker, 2011), and drifter velocities were computed and filtered with a 25-hour centered Butterworth filter to remove tidal and inertial motions (as in Koszalca and LaCasce 2011). We then interpolated the drifter trajectories on a 3h timestep, from August 2019 to November 2022, where data gaps are shorter than 12h. We evaluated the presence of a drogue on SVP drifters using the GPS time to first fix (for SVP-T drifters) or a combination of this parameter and the submergence parameter (SVP-S). Both parameters exhibit drastic changes when the drifter drogue is lost as the buoy is not dragged underwater as frequently (Lumpkin et al 2013). The trajectory of undrogued drifters is more directly impacted by wind slippage and Stokes drift (Poulain et al 2009), so it is essential to know when drifters lose their drogues to analyze their behavior. In the following, only drogued SVP drifters are considered, unless specified otherwise.

In the following paragraphs, we describe the drifter deployments and provide a short description of the trajectories. The five deployments are summarized in Table 1, and the

resulting trajectories are shown in Figure 2. The different regions mentioned are shown Figure 1.

The first deployment took place on 14 August 2019, just upstream of Sermilik Trough. Fifteen CARTHE drifters, seven SVP-T and eight SVP-S drifters were deployed along two lines at the shelfbreak. Five of the CARTHE drifters were exported off the shelf east of Greenland, most of them at Cape Farewell, while all SVP drifters continued on the west Greenland shelf after rounding Cape Farewell. This first deployment and its results were described in Duyck and De Jong (2021).

The second deployment took place in Fram Strait, from 2 to 13 September 2019. Fifteen CARTHE, eight SVP-T and seven SVP-S drifters were deployed along one line at 78.8°N. Deployment positions were adjusted to avoid an area of the shelf where sea ice was encountered. Unfortunately, many of these drifters were steered into sea ice shortly after deployment. This resulted in more than half of the drifters ceasing to work within the first two weeks. Of the drifters that continued working, two SVP and two CARTHE drifters exited the shelf at the latitude of Fram Strait, and a third SVP drifter was exported towards the Greenland Sea at the latitude of Jan Mayen.

The third deployment took place on 20 July 2020 at Cape Farewell, with fifteen CARTHEs, seven SVP-T and eight SVP-S drifters deployed across the shelfbreak at 60°N. The drifters deployed the most onshore remained on the shelf, while the others exited the shelf, and re-entered it west of Greenland. Part of them entered an eddy off Eirik Ridge. Eventually all SVP and CARTHE drifters were transported west of Greenland.

The fourth deployment took place just south of Denmark Strait on 27 July 2021, with five CARTHE, two SVP-T and three SVP-S drifters. The CARTHE drifters stopped working within the first month and a half, and none of them reached Cape Farewell. All the SVP drifters rounded Cape Farewell, and one was exported into the Labrador Sea just west of Cape Farewell instead of continuing into the West Greenland Current (WGC).

The fifth deployment took place near Scoresby Sund on 3 and 4 August 2021, along two lines at 69.65 and 69.95°N. Ten CARTHE, six SVP-T and four SVP-S drifters were deployed. Similarly as for the Denmark Strait deployment, most CARTHEs did not survive past the first month. Both the CARTHE and SVP drifters showed important cross-shelf exchanges between Scoresby Sund and the southern Blosseville Basin, but all the SVP drifters re-entered the shelf and rounded Cape Farewell into the WGC. Two CARTHE drifters were exported into the Iceland Sea and did not re-enter the shelf.

Overall, the majority of the drifters deployed at the east Greenland shelfbreak remained on the shelf or in the shelfbreak current on the eastern side of Greenland. Most SVP drifters were driven further towards the coast as they were advected downstream. After rounding Cape Farewell, some were exported into the Labrador Sea. The trajectories from CARTHE drifters are similar, but CARTHEs tended to remain at the shelfbreak and

were more frequently exported east of Greenland than SVP drifters. Both CARTHE and SVP drifter trajectories indicate exchanges at the shelfbreak, with drifters exiting and re-entering the shelf instead of being exported into interior seas. With the EGC-DrIFT dataset, we added 15000 drogued drifter days in the area, and improved coverage especially close to the coast alongside the southern east and west Greenland shelf, as well as between Kangerdlussuaq Trough and Scoresby Sund, where there was little drifter data before (Figure S1). The life duration of each drifter depended on the type of drifter and the deployment area, ranging from a few hours to more than two years. A summary of all drifters deployed, their life duration and drogue off date can be found in Figure S2 and Table S1.

	DEPLOYMENT DATE	CARTHE	SVP-T	SVP-S
SERMILIK	August 2019	15	7	8
FRAM STRAIT	September 2019	15	8	7
CAPE FAREWELL	July 2020	15	7	8
DENMARK STRAIT	August 2021	5	2	3
SCORESBY SUND	August 2021	10	6	4

Table 4.1: *Summary of drifter deployments as part of the EGC-Drift project*

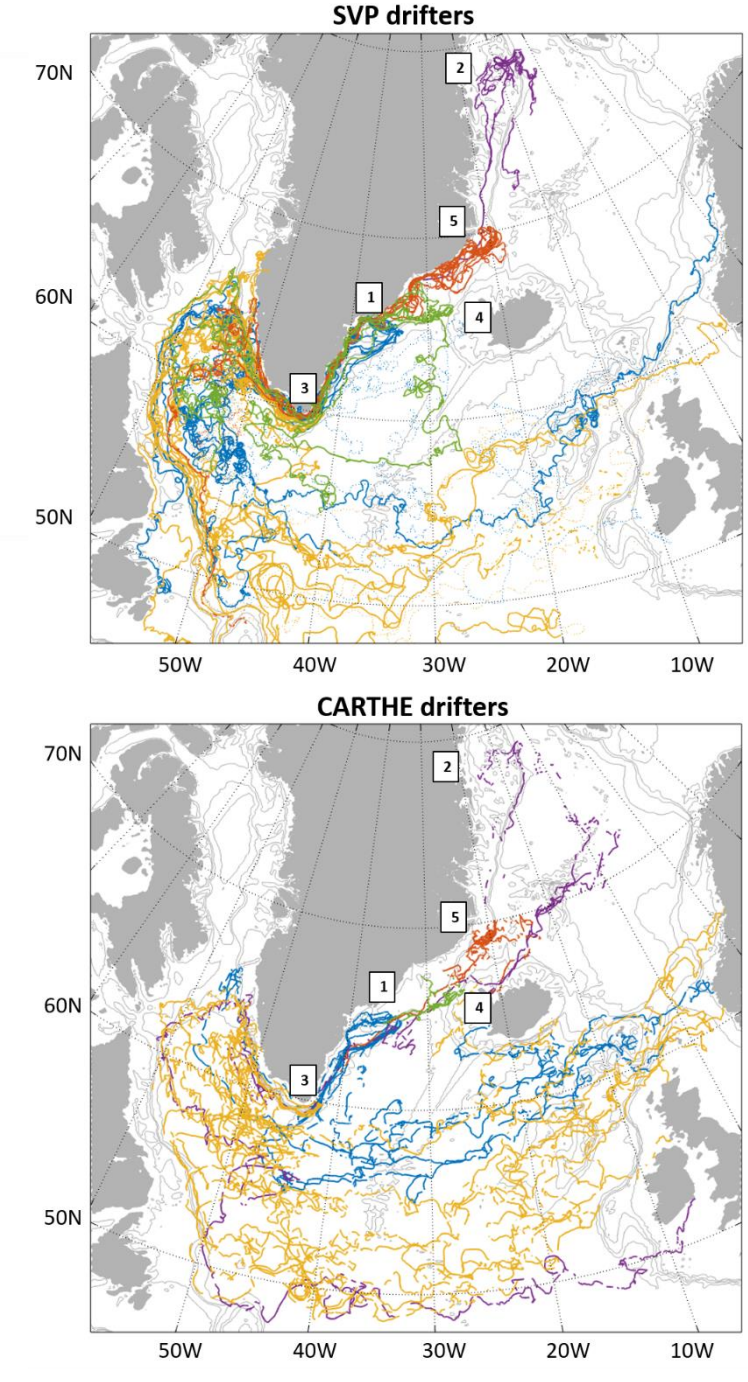

Figure 4.2: *Trajectories of SVP (up) and CARTHE (down) drifters per deployment. 1: Sermilik (blue), 2: Fram Strait (purple), 3: Cape Farewell (yellow), 4: Denmark Strait (green), 5: Scoresby Sund (red). Bathymetric contours are shown at 2000, 1000, 500 and 200m.*

Additionally, we used drifter trajectories from the Global Drifter Program 6-hour interpolated dataset (GDP, Lumpkin and Centurioni, 2019, Centurioni et al 2019), from July 1993 to July 2022. There are only sparse data north of Denmark Strait in the GDP and EGC-DrIFT datasets, therefore we also included SVP drifters from the International Arctic Buoy Program dataset (IABP, Rigor et al 2002). There are caveats with using drifters from this dataset as most of them were deployed on sea-ice and no information on drogue status is available. To detect when drifters are on ice, we used a temperature threshold of -1.8 °C following the IABP recommendation. We only use parts of trajectories identified as being in water in the following. We included the IABP drifters in the study because they add crucial information in areas where data are scarce, while keeping in mind that some of the IABP drifters may be undrogued. Figure S3 shows the mean circulation computed with and without the IABP dataset. The IABP drifter data were processed to remove spikes in the positions and measurements in the same way as the EGC-DrIFT dataset, and were interpolated on a 6-hourly timestep from January 1993 to November 2022.

4.2.2 Other datasets

To complement results from drifters, we used sea level anomaly, geostrophic velocities and eddy kinetic energy derived from the Copernicus Marine Service global satellite altimetry product in delayed time SEALEVEL_GLO_PHY_L4_MY_008_047. This merged satellite altimetry product has a 0.25° resolution and is available from 1993 to 2021. It merges data from all available altimeter missions. Only a minority of satellites collect data up to 81°N, most of them only collecting data up to 66°N. Grid cells with ice coverage > 15% are set to NaN, and we did not consider areas covered with ice more than 50% of the time, which excludes the inshore Greenland shelf north of 76°N.

We retrieved satellite sea surface temperature (SST) from the GHRSST Level 4 MUR Global Foundation SST Analysis (JPL MUR MEaSUREs Project, 2015), a data blend of microwave, infrared, ice fraction and in situ measurements, with a very high resolution (1 km) in cloudless conditions (Chin et al., 2017). We used MUR data from 1st August to 30th September 2021 and verified that MUR data along drifter tracks correlates well with drifter temperature measurements (mean correlation of 0.95).

We retrieved the wind speed and wind angle at 10m from the CARRA (Copernicus Climate Data Store Arctic Regional Reanalysis on single levels, Schyberg et al 2020) atmospheric reanalysis. We computed the zonal and meridional wind velocities from these variables. We selected CARRA data from 1998 to 2022 with a 6-h temporal resolution. The reanalysis has a 2.5 km spatial resolution. We identified Tip Jets and strong northeasterly wind events in the dataset using the method described in Duyck and De Jong 2022. We identified Tip Jets as westerly winds (mean wind direction towards the 45° to 135° quadrant with respect to north) with a mean speed over 17 m.s^{-1}, that persist for at least 12h. For moderate westerlies, the threshold was lowered to 8 m.s^{-1}. Strong and moderate north-easterlies were defined with the same threshold, and mean wind direction towards the 180° to 270° quadrant with respect to north.

4.2.3 Computations of transports and export across the east Greenland shelfbreak

The east Greenland shelf is on average 200 to 400m deep, with some deeper troughs cutting across the shelf, that can reach 1000m depth. A strong bathymetric slope delimitates the continental shelf and deep ocean, with the ocean floor falling from 400 to 2000m deep over a few kilometers. In the following, we use the 600m isobath as a boundary for the shelf to identify cross shelf fluxes and refer to that boundary as "shelfbreak". This isobath was retrieved from Fram Strait to Cape Farewell from the ETOPO2022 60 arc-seconds dataset, and smoothed with a 50km window. We divided the shelfbreak into 31 100km-long sections and computed the number of shelfbreak crossings by drogued SVP drifters within these sections. Sections of the shelfbreak where more offshore than inshore crossings occur indicate areas of possible freshwater export. However, drifters are sometimes exported at one section and re-imported in the following section. Thus, these numbers are indicative of exchange areas rather than a quantitative estimate of export.

We computed Ekman transport at the shelfbreak to estimate potential wind-driven export in different areas of the shelf. Ekman transport was computed for each time step from wind stress as per Equation 1 and 2, interpolated on the shelfbreak and rotated according to the local shelf angle to obtain Ekman transport across the shelfbreak (T_{ek_sh}, Equation 3).

$$\begin{cases} \tau_x = \rho_{air} C_d u \sqrt{u^2 + v^2} \\ \tau_y = \rho_{air} C_d v \sqrt{u^2 + v^2} \end{cases} , \quad (1)$$

with τ_x, τ_y the meridional and zonal wind stress, u and v the zonal and meridional wind components at 10m, ρ_{air}=1.2 kg.m^{-3} the air density, and C_d the wind drag defined non-linearly according to Trenberth et al 1990.

$$\begin{cases} T_{x\_ek} = \frac{\tau_y}{f\,\rho} \\ T_{y\_ek} = \frac{-\tau_x}{f\,\rho} \end{cases} , \quad (2)$$

$$T_{ek\_sh} = \cos(\theta_{sh})\, T_{y\_ek} - \sin(\theta_{sh})\, T_{x\_ek} , \quad (3)$$

with T_{x_ek} and T_{y_ek} the zonal and meridional Ekman transports, f the Coriolis parameter at 70°N retrieved from TEOS 10 GSW oceanographic toolbox (Mc Dougall and Barker 2011), ρ=1027 kg.m^{-3} the water density, and θ_{sh} the local angle of the shelfbreak, computed anticlockwise from the x axis, so that in the rotated frame, axes are along shelf southwards, and across shelf offshore.

We similarly computed geostrophic velocities across the shelfbreak at each time step to identify areas most favorable to export. Geostrophic velocities from satellite altimetry (u_g and v_g) were interpolated at the shelfbreak and rotated to obtain geostrophic velocity across the shelfbreak (v_{g_sh}, Equation 4).

$$v_{g\_sh} = \cos(\theta_{sh})\, v_g - \sin(\theta_{sh})\, u_g \quad (4)$$

4.3 Results

4.3.1 Overview of the East Greenland circulation and possible exchange areas

The EGC-DrIFT dataset provides new insight close to the southeast Greenland coast and in areas with scarce drifter density, such as the Blosseville Basin, but the data are concentrated in specific time periods, mostly in summer. In the following, we use data from the EGC-DrIFT, GDP and IABP datasets, as well as geostrophic velocities from dynamic topography and surface winds from the CARRA reanalysis to identify potential regions of enhanced export at the east Greenland shelfbreak.

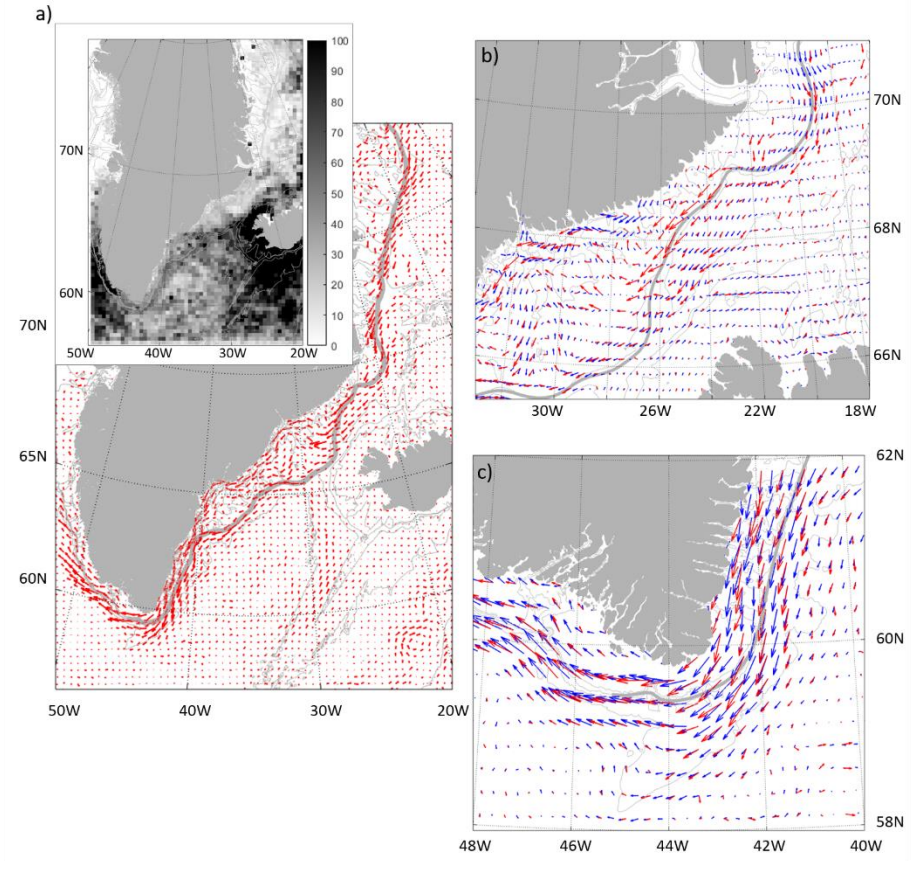

Figure 4.3: *Mean circulation from drifters and altimetry-derived geostrophic velocities A. Number of drifter day per bins and mean surface circulation computed using the EGC-DrIFT, IABP and GDP drifter datasets; B. Mean surface circulation from drifters (red) and mean geostrophic velocity*

(blue) upstream of Denmark Strait; C. Same at Cape Farewell. To obtain the circulation map, we compute mean drifter velocities in 30x30 km bins using the jlab 2dstats function (Lilly et al 2021). Only bins with more than 5 drifter days are shown. Bathymetry in grey at -2000, -1000, -500, -200 m. The thick gray line represents the shelfbreak.

The data coverage and mean circulation inferred from the three drifter datasets are shown Figure 3A. South of Denmark Strait, the drifter-derived circulation agrees well with geostrophic velocities derived from dynamic topography (figure 3C). In the Denmark Strait area (Figure 3B), the available drifter data mostly originate from our 2021 deployment (Figure S1). This concentration in time results in some differences between the two. North of Scoresby Sund, the drifter data density is very sparse. Only the shelfbreak EGC is well sampled there.

Over most of the shelfbreak, the geostrophic velocities are strongly directed along the shelf. At the Blosseville Basin and Cape Farewell, both the drifter-derived and geostrophic mean circulation show shelf waters being driven off-shelf, the first one as shelf waters flow through Blosseville Basin, the second one as they are driven over Eirik Ridge. On the contrary, deep troughs like the Sermilik and Kangerdlussuaq troughs, contribute to constraining freshwater on the shelf by driving part of the shelfbreak current towards the coast. Data coverage is too sparse to investigate exchanges upstream of Scoresby Sund.

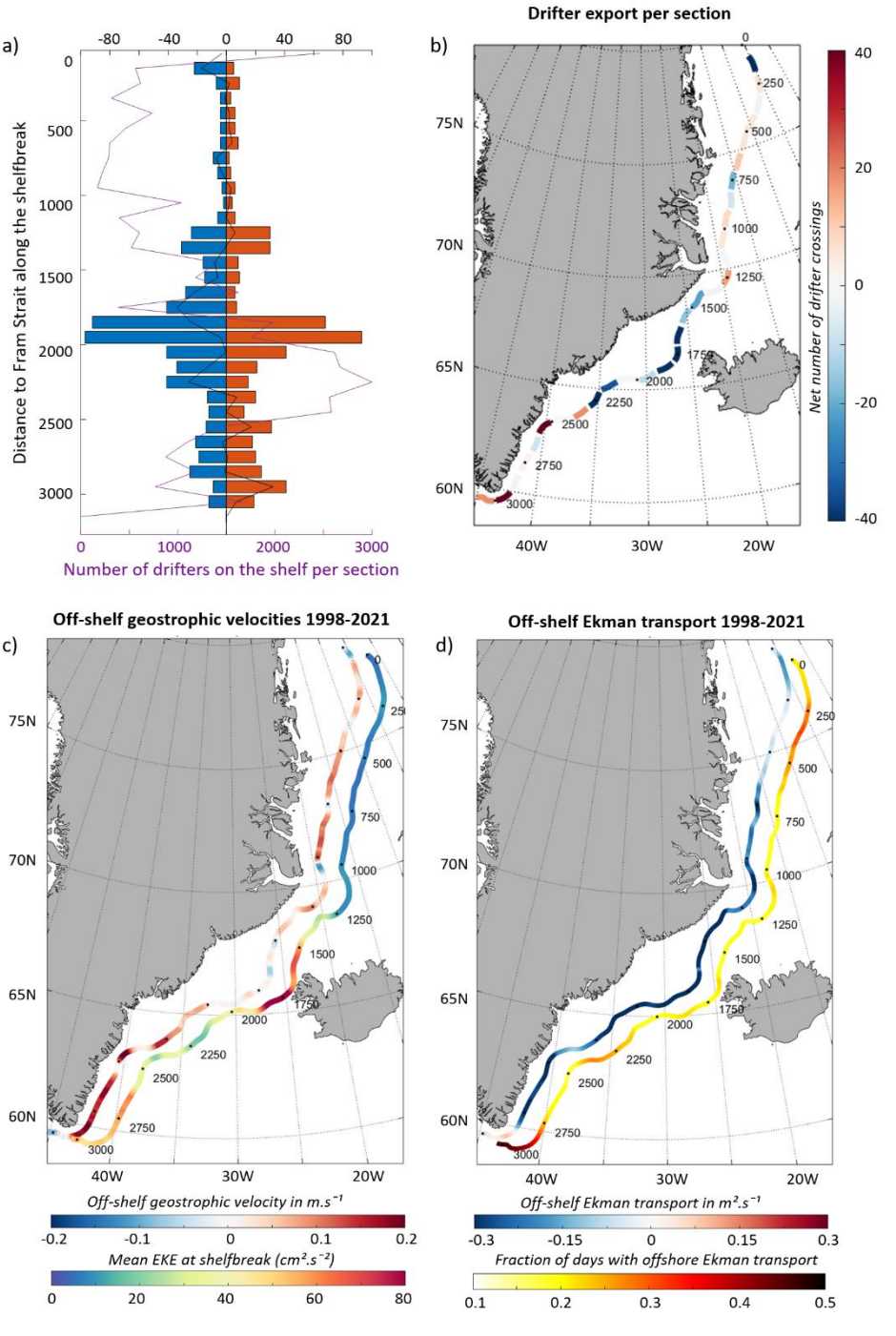
a)
Distance to Fram Strait along the shelfbreak
Number of drifters on the shelf per section
b)
Drifter export per section
Net number of drifter crossings
c)
Off-shelf geostrophic velocities 1998-2021
Off-shelf geostrophic velocity in m.s⁻¹
Mean EKE at shelfbreak (cm².s⁻²)
d)
Off-shelf Ekman transport 1998-2021
Off-shelf Ekman transport in m².s⁻¹
Fraction of days with offshore Ekman transport

4

Figure 4.4: *A. Number of drifter crossings per section of the shelfbreak. The purple line shows the number of drifter days on the shelf per section, and the black line shows the net number of offshore crossings (offshore-inshore). B. Net number of offshore crossings (off-shore crossings – onshore crossings) per shelfbreak section. C. Mean geostrophic transport across the shelfbreak (positive is offshore) and mean eddy kinetic energy at the shelfbreak, 1998-2021. The mean eddy kinetic energy is not shown at the geographic location of the shelf, but next to it, to allow for comparisons with the mean geostrophic transport; D. Mean Ekman transport across the shelfbreak and fraction of days with offshore Ekman transport, 1998-2021.Similarly as for C., the fraction of days is shown next to the mean Ekman transport rather than at the geographic location of the shelf.*

The computation of drifter crossings at the shelfbreak shows four areas that display more drifter export than import, which indicates possible export of fresh shelf waters towards the interior (Figures 4A and B): At 75°N, north of Scoresby Sund, south of Sermilik Trough, and at Cape Farewell. As noted before, the scarcity of data north of Scoresby Sund limits our insight into possible export in the northern part of the east Greenland shelf. The export region just south of Sermilik Trough corresponds to a bend in the shelf. The strongest net export is observed at Cape Farewell. At some of the sections we observe a lot of exchanges, but no net export of drifters. It is unknown what this means in terms of freshwater exchange.

The mean across-shelf geostrophic velocity is oriented offshore over most of the shelfbreak, except for a few areas that correspond to bends in the topography (figure 4C). The section of the shelfbreak with the strongest mean offshore geostrophic velocity is the southeast shelf, from downstream of Sermilik Trough to Cape Farewell. Eddy kinetic energy derived from satellite altimetry indicate the Denmark Strait sill as the most energetic area, followed by the shelfbreak region from just upstream to just west of Cape Farewell. Eddies in these areas could contribute to freshwater exchanges with interior seas.

Between 74°N and 60°N the wind is predominantly north-easterly and along-shelf. This drives inshore Ekman transport (Fig. 4D). A few regions stand out where winds are more often favorable to export. At Cape Farewell, north-easterlies alternate with localized westerly winds, including Tip Jets. Winds are favorable for export about 50% of the time. Two other regions show weaker mean on-shelf transport than the rest of the shelf: Between 74°N and 76°N, the dominant northerly winds are not along-shelf, which leads to a lesser onshore transport than over the rest of the shelf. At Sermilik Trough, the weaker inshore Ekman transport could be associated to wind variability and to the sharp bend of the shelfbreak.

In the following, we investigate the local circulation and processes driving exchanges in the Blosseville Basin, and Cape Farewell regions, two areas highlighted as potential enhanced export regions.

4.3.2 Exchange processes in the Blosseville Basin

One of the areas identified as favorable to cross-shelf exchanges and potential freshwater export in the previous section is the Blosseville Basin and Denmark Strait region, where drifters were brought on and off the shelf. This is consistent with existing studies, that identified a bifurcation of the EGC just upstream of Blosseville Basin (Vage et al 2013) and described eddies at the shelfbreak and in the basin (Havik et al 2017b).

Exchanges between the shelf and the interior in this region are illustrated by the drifters deployed at Scoresby Sund and Denmark Strait in summer 2021. The drifters that were deployed at Scoresby Sund separated into four groups with distinct behaviors after they were deployed (figure 5A).

1) A first group, consisting of five SVP (in blue) and five CARTHE drifters (in blue, dashed line) deployed inshore of the shelfbreak, were apparently deployed in a warm and fresh eddy (Fig. 5C & D). The drifters remained in the eddy between 15 and 25 days and exited the eddy as it reached Blosseville Basin at 67.5°N. After leaving the eddy, one of the CARTHE drifters crossed to the Iceland side of the Blosseville Basin. The SVP drifters were pushed back on the shelf and two SVP drifters ran aground on the Greenland coast while the rest were advected downstream along the coast while continuing to show eddying behaviour. They entered the core of the EGCC as they approached Kangerdlussuaq trough (Figure 5E).

2) A second group, consisting of one SVP (in red) and three CARTHE drifters (red, dashed line) deployed at the northern line, initially followed the shelfbreak without entering the eddy. The three CARTHE drifters exited the Greenland shelf just south of Scoresby Sund, were advected across the Blosseville Basin and back on the shelf at Denmark strait. The SVP drifter followed the shelfbreak to ~68.5°N, turned towards Iceland, followed the east side of the Blosseville Basin south to Denmark Strait and re-entered the east Greenland shelf at ~67°N. That drifter also measured rapid sea surface temperature changes, cooling down as it crossed from the shelfbreak into the Blosseville Basin, and cooling further as it re-entered the shelf downstream.

3) A third group, consisting of two SVP (in yellow) and two CARTHE drifters (yellow, dashed line), deployed offshore of the shelfbreak at the southern line, exited the shelfbreak at Scoresby Sund (figure 5A). The two SVP drifters were exported off-shelf at the latitude of Scoresby Sund, were advected south into the Blosseville Basin, and reentered the shelf close to the Denmark Strait sill. The two CARTHE drifters remained off the Greenland shelf after being exported.

4) The remaining two SVP drifters (in purple) were driven towards the coast shortly after deployment and were advected downstream over the shelf before entering the EGCC as they approached Kangerdlussuaq Trough.

The drifters deployed at Denmark Strait can similarly be categorized in three groups (figure 5B): 1) A first group, consisting of the 3 SVP (in blue) and 3 CARTHE drifters (blue, dashed line) deployed most offshore, first headed northwards into the strait. They then

headed back southwards, entered the shelf, drifted towards the coast and entered the EGCC at Sermilik Trough. 2) A second group, consisting of one SVP (in yellow) and the 2 CARTHE drifters (yellow, dashed line) deployed most inshore, were immediately advected southwards along the shelfbreak. The SVP drifter was driven into the EGCC at the level of Sermilik Trough. 3) A third group, consisting of the remaining two SVP (in red) and one CARTHE drifter (red, dashed line), was steered into the Kangerdlussuaq Trough towards the coast where they entered the EGCC.

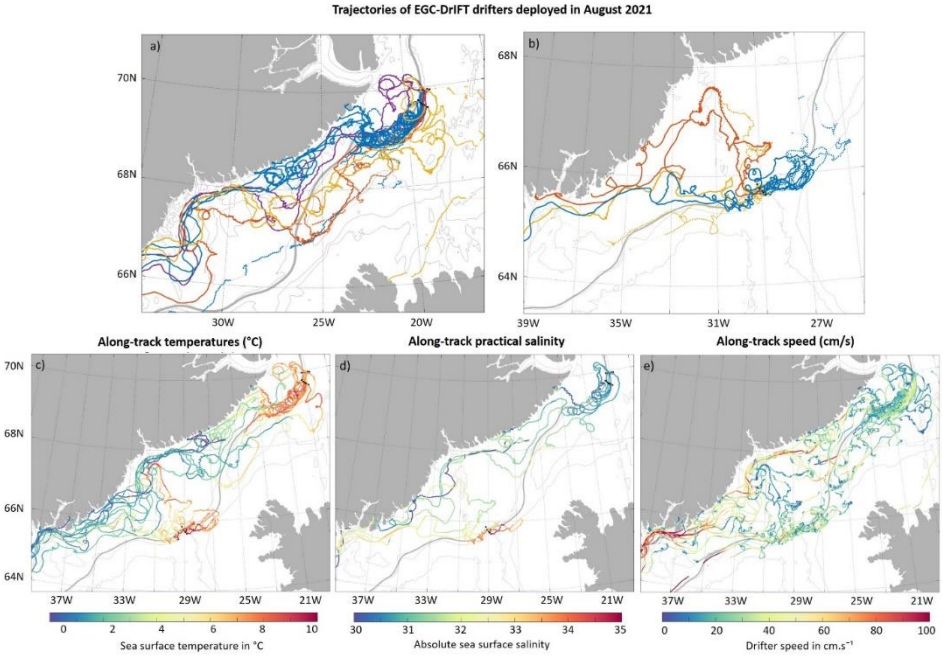

Figure 4.5: *Trajectories and properties of drifters deployed at Scoresby Sund and Denmark Strait. A. Trajectories from drifters deployed at Scoresby Sund. See text for explanation of colors. B. Same for drifters deployed at Denmark Strait. C. Temperatures along trajectories as measured by SVP drifters. D. Salinity along trajectories as measured by SVP-B drifters. E. Velocities from SVP and CARTHE drifters. Bathymetry in grey at -2000, -1000, -500 and 200m. The thick gray line represents the shelfbreak.*

The drifter tracks show exchanges in the Blosseville Basin area. SVP drifters exported at the Blosseville Basin all re-entered the shelf as they reached Denmark Strait and were driven into the EGCC at Kangerdlussuaq Trough. A few CARTHE drifters did not join the EGCC, but they all stopped transmitting within the first two weeks after deployment. We now further investigate the conditions in the Blosseville Basin that led to the exchange.

From mid-June to early September 2021, the winds over Scoresby Sund, the shelf, and the Blosseville Basin, were mostly south-westerly, which is unusual, as winds in the regions are normally predominantly north-easterly, including in the summer (Figure 6C).

This resulted in an anticyclonic circulation in the basin and a cyclonic circulation over the shelf (Figure 6A). This circulation was strongest in the first part of August, at the time of deployment. From mid-August, strong north-easterly winds started dominating again (Figure 6D) and the anticyclonic circulation in the Blosseville Basin disappeared. This caused the geostrophic velocities to be intensified at the coast (Figure 6B), concurrently with an acceleration of the drifters (Figure 5E). The change in wind conditions and circulation was reflected in sea surface temperature.

Figure 7 shows satellite sea surface temperature over the same period, together with drifter trajectories. The along-track temperature measured by SVP drifters is close to the satellite sea surface temperature. We observe a rapid cooling (by 4°C) of the shelf waters and the Blosseville Basin between the end of August and early September, concurrently with the strengthening of northeasterly winds and the associated change in dynamic topography. The colder waters first appear at the shelf, maybe coming from upstream, and then extend towards the Iceland Sea and into the Blosseville Basin. South of the Blosseville Basin, the sea surface temperature and drifter trajectories shows the impact of the deep Kangerdlussaq Trough on exchanges between the shelf and warmer waters at the sheflbreak, with warmer interior waters entering the trough and drifters being steered around it.

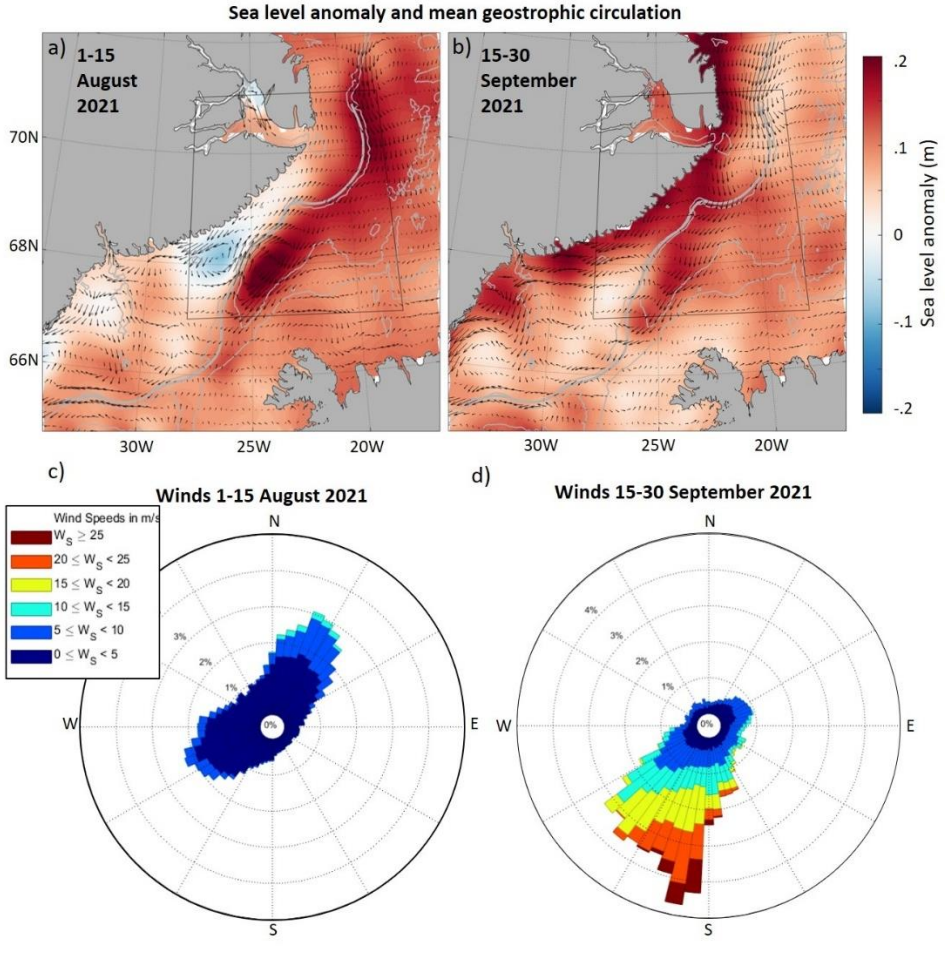

Figure 4.6: *A. Mean sea level anomaly and mean geostrophic velocities from 1-15 August 2021 (left) and 15-30 September 2021 (right). Bathymetry in grey at -2000, -1000, -500, -200m. The thick gray line represents the shelfbreak; B. Wind polar plot for winds in the area delimited in 6A and 6B, for the same time periods. The wind angle corresponds to the direction winds flow towards*

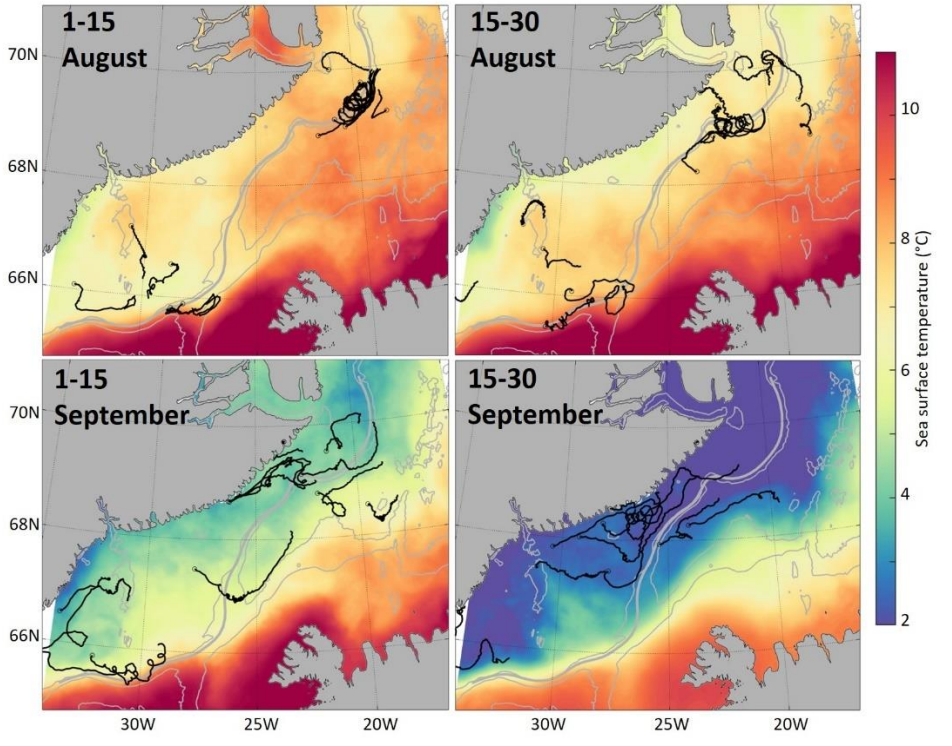

Figure 4.7. *Mean sea surface temperature from MUR per 15 days and drifter trajectories during the corresponding time period. Bathymetry in grey at -2000, -1000, -500, -200m. The thick gray line corresponds to the shelfbreak.*

4.3.3 Cape Farewell

Cape Farewell is another area identified as favorable to cross shelf exchanges and potential freshwater export. In that region, strong westerly wind events (Tip Jets) could contribute to local off-shelf freshwater export (Duyck et al 2022; Duyck and de Jong 2021). Moreover, both geostrophic velocities and the combined drifter dataset suggest that the EGC moves away from the shelfbreak as it is steered around Eirik Ridge (Figure 3C).

This is illustrated by the drifters deployed at Cape Farewell in July 2020 (Figure 8A). After deployment, the drifters separated in three groups. 1) The first group consists of the nine SVP (in blue) and 13 CARTHE drifters (blue, dashed line) deployed most offshore. They meandered closer and further from the shelfbreak while travelling around Cape Farewell. They arrived at 46°W seven days after deployment. 2) A second group, consisting of five SVP drifters (in red) were driven off-shelf over Eirik Ridge, where they appear to have been trapped in an eddy. The eddy moved west along the shelfbreak and the SVPs entered the WGC at different points of the shelfbreak. It took these drifters 15

days longer to arrive at 46°W. CARTHEs deployed together with the SVP drifters from this second group did not enter the eddy and are in group one. 3) The inshore group, consisting of two CARTHEs (in yellow, dashed line) and one SVP (yellow) remained on the shelf, were advected towards the WGC as they arrived west of Greenland, and headed back towards the coast. This is similar to trajectories of drifters originating from the EGCC described by Duyck and de Jong 2021.

Temperature and salinity along the tracks show a sharp transition in water properties between drifters deployed at the shelfbreak and off-shelf (Figure 8C and D). As they enter the eddy, drifters from the second group measure much warmer (from 4 to 7°) and saline (33.5 to 34.9) waters, similar to the offshore group.

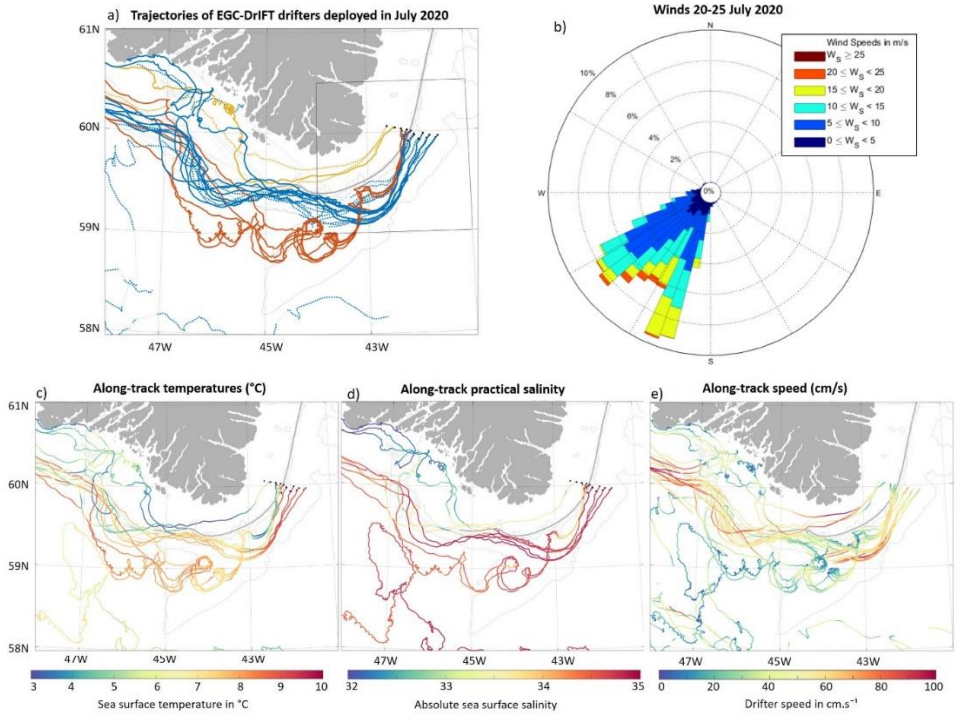

Figure 4.8: *Trajectories and properties of drifters deployed at Cape Farewell in 2020.* ***A.*** *Trajectories of SVP and CARTHE drifters colored as described in the text. Faded colors correspond to CARTHEs.* ***B.*** *Wind polar plot showing the direction winds flow towards, for the area shown in black in A. from 25th to 30th July 2020, in the week after deployment.* ***C.*** *Along track temperatures,* ***D.*** *Along track salinity.* ***E.*** *Along track speed. Bathymetry in grey at -2000, -1000, -500, -200m. The thick gray line represents the shelfbreak.*

The deployment at Cape Farewell in 2020 took place at a time when winds were northeasterly (figure 8B) and therefore not favorable to export. Drifters crossing the shelfbreak east of Cape Farewell suggest that even as winds could be an important driver

of export at Cape Farewell, they are not the only one. The eddy sampled by the drifters is an indication that eddy activity could play a role in mixing shelf waters into interior waters. This cannot be explored further with this data.

We can further investigate the role played by winds at Cape Farewell. Using the combined (EGC-Drift, GDP, IABP) drifter dataset, we look at drifter advection during specific wind events identified in the CARRA reanalysis. We identify strong northeasterlies and Tip Jets (defined in section 2.2) using time series of spatially averaged wind direction and speed at Cape Farewell (see box figure 9A) from 1998 to 2022. We select trajectories from drifters from 1 day before to 1 day after the peak of these Tip Jet and strong north-easterly events. Figure 9A shows these composites for drifters from the GDP (blue), the IABP (red) and EGC-DrIFT (green) datasets. The pale colors indicate undrogued drifters, which are more sensitive to wind. We find two times more drifters in the area during strong northeasterlies than during Tip Jets, due to seasonal differences in occurrences of these wind events and drifter coverage. The effect of the wind is most clearly visible off the shelf, outside of the influence of the strong EGC. During northeasterlies, tracks are directly along the shelf. During Tip Jets, tracks are directed to the east. In both cases, undrogued drifters from the GDP dataset show a stronger response to the wind direction.

We extend the analysis to moderate westerlies and northeasterlies (defined in section 2.2), that have also been shown to be of importance by Duyck et al 2022. We compute the mean circulation from drifters during these two types of events. During northeasterlies (blue), we find a slightly stronger EGC. During westerlies (red), we see stronger steering towards the shelf edge upstream of Eirik Ridge and offshelf at Eirik Ridge (Figure 9B).

4

At Cape Farewell winds, eddies, but also the topographically steered mean circulation contribute to enhancing the potential for surface waters from the shelf mixing with interior waters. We however observe only limited freshwater export as most of the drifters that arrive at Cape Farewell round the Cape and continue into the WGC, even if they were driven off-shelf east of Greenland.

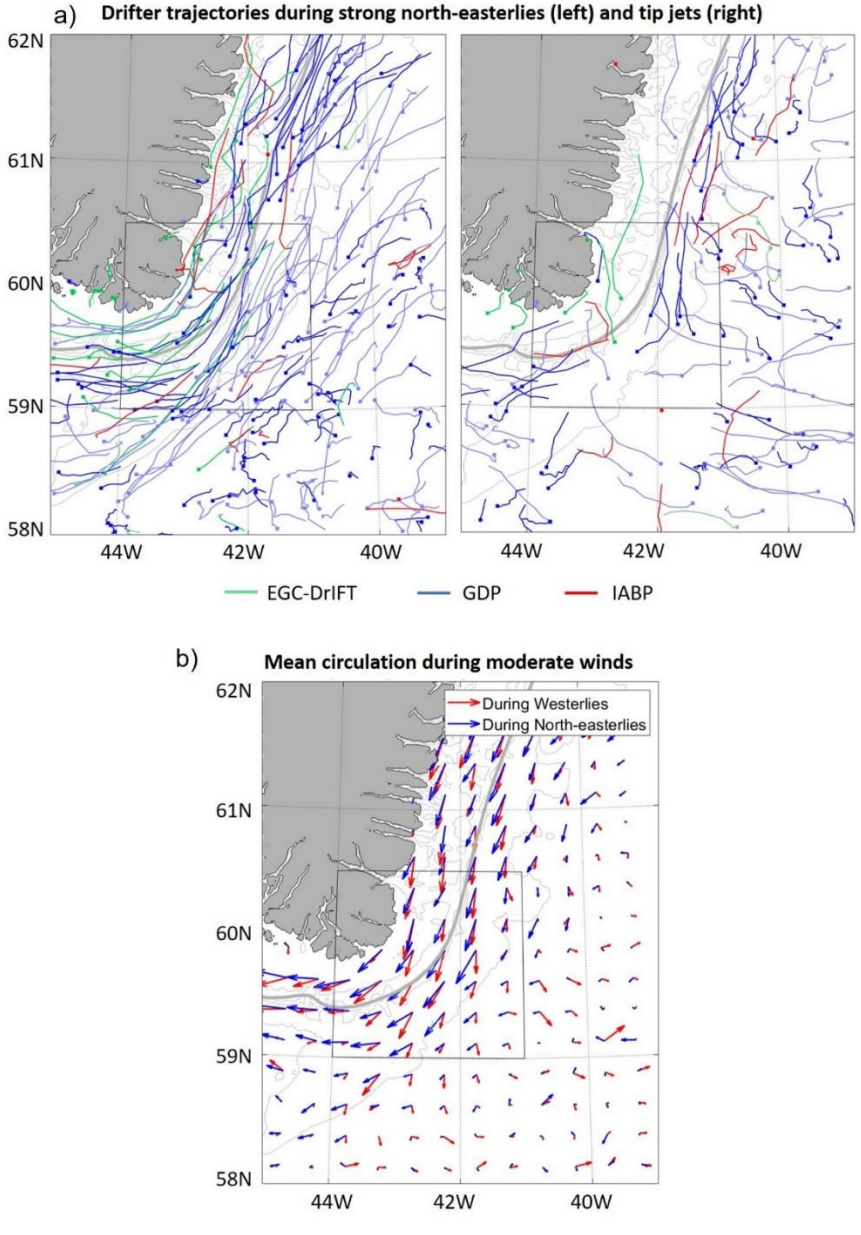

Figure 4.9: *Impact of wind events on drifters at Cape Farewell.* ***A.*** *Trajectories of drifters from 1 day before to 1 day after peak Tip Jet (left) and strong north-easterlies events. The direction of trajectories is represented by a large dot at the end of the segment.* ***B.*** *Binned circulation of drifters from the combined dataset during westerly and north-easterly events. Bathymetry in grey at -2000, -1000, -500, -200m. The thick gray line represents the shelfbreak.*

4.4 Discussion and conclusions

The data presented here highlight two areas of exchange, the Blosseville Basin and Cape Farewell, and point towards winds and eddies as exchange processes. Over most of the rest of the shelf, northeasterly winds and deep troughs constrain the flow to the EGC and EGCC. Scarce drifter coverage north of 71°N hinders investigation on the northern part of the shelf. The export of fresh surface waters from the northern Greenland shelf into the Nordic Seas could be of particular importance to the formation of the dense waters that form the overflow waters in the AMOC lower limb (Chafik and Rossby 2019, Huang et al 2020). Observations along the shelf (Dickson et al 2007, Havik et al 2017a) suggest that some of the fresh surface waters are exported away from the shelf between Fram Strait and Denmark Strait, while other studies suggest only limited export (Dukhovskoy et al 2019). Dodd et al 2009 argue that a majority of the export is due to sea ice. Using CARRA, we show that winds over the northern part of the shelf are less constraining than in other areas, which could allow for enhanced export, in particular of sea ice. Further studies are necessary to quantify liquid and solid freshwater export of the Greenland shelf north of 71°N.

At Scoresby Sund, the EGC-DrIFT drifters were initially in an eddy, until they reached Blosseville Basin. Part of them were then advected on the shelf while the rest crossed the basin (Figure 5A). The mean circulation derived from all drifters shows the shelfbreak EGC and separated EGC flowing on both sides of the basin (Figure 3B). During the EGC-DrIFT deployment, winds were predominantly southwesterly, causing an anticyclonic circulation in the Blosseville Basin. By September, the winds were northeasterly and the anticyclone disappeared. This change was associated with inflow of colder waters, which extended towards Iceland. This is consistent with Havik et al 2018 who argued that upwelling favorable winds (that lead to offshore Ekman transport) are associated with an extension of lighter waters over the Greenland slope in the Blosseville Basin area. There are two hypotheses for the formation of the separated EGC (Våge et al, 2013). It could result from the shedding of eddies just upstream of Blosseville Basin that coalesce at the base of the Iceland shelf (Havik et al 2017b, De Steur et al 2017). Alternatively, it could result from negative wind stress curl over the basin creating an anticyclone, of which the shelfbreak EGC is the return branch (Harden et al 2016). These hypotheses are not mutually exclusive and our results offer support for both.

At Cape Farewell, we show that surface water can be brought offshore due to wind, eddy, and topography driven processes. Westerly winds at Cape Farewell have a strong impact on local circulation (Figure 9B) and facilitate export as Duyck et al 2022 suggested using a high-resolution model. The mean circulation in that area is slightly offshore of the shelfbreak as it is steered by Eirik Ridge (figure 3C). Additionally, eddies could contribute to export or mixing. Nearly all SVP drifters that left the east Greenland shelf at Cape Farewell re-entered it on the western side of Greenland. However, this does not preclude export of freshwater as mixing and loss of freshwater may occur along the way. A quantitative measure of export along the east Greenland shelf cannot be determined as this would require high quality salinity fields in the Greenland shelf region. Current

salinity satellite products are not accurate at high latitude, near land or near ice (Vinogradova et al 2019). Salinity data from Argo are sparce and limited to regions deeper than 2km. An estimate derived from changes in salinity, or freshwater storage, in the region is difficult because of the large uncertainties on precipitation and evaporation. Our analysis suggests that export of liquid freshwater between Scoresby Sund and Cape Farewell is likely to be small.

Export off the west Greenland shelf is known to be larger. There it is driven both by eddies and winds (Hátún et al 2007, Chanut et al 2008, Schulze Chretien and Frajka Williams 2018). In the EGC-DrIFT dataset, 13 of the 34 SVP drifters that arrived west of Greenland were exported in the Labrador Sea, five of which were originally in the EGCC (Figure 2). This indicates exchange between the coastal current and the shelfbreak current as they round Cape Farewell, as also shown by Lin et al 2018. Previous studies showed that most of the freshwater exported in the Labrador Sea originated from the East Greenland Current, instead of glaciers from southeast Greenland (Luo et al 2016) or from the Canadian Arctic Archipelago (Wang et al 2018). Exchanges between the coast and shelfbreak at Cape Farewell influence the freshwater distribution over the west Greenland shelf and are therefore important for freshwater export west of Greenland.

On a longer timescale, if additional freshwater is exported into the Labrador Sea, it will influence other regions of the subpolar north Atlantic. A freshening of the Labrador Sea would indirectly impact the Irminger sea. However, a freshwater anomaly at the surface of the Labrador Sea must be advected to the Irminger Sea quickly to remain at the surface, as freshwater is mixing down and diluted over a layer of several hundred meters thick through fall and winter (Dukhovskoy et al 2019), after which it will affect intermediate levels of the Irminger Sea hydrography (Lavender 2005, de Jong et al. 2012). The EGC-DrIFT deployments (Figure 2), as well as GDP data, suggest there is no short and fast route from the west Greenland shelf to the central Irminger Sea. The freshwater anomaly that formed off the Labrador shelf in 2012 (Holliday et al. 2020) travelled around the subpolar gyre, was further strengthened at the surface by precipitation, and was seen to arrive in the eastern Irminger Sea in 2016 (de Jong et al. 2020, Bilo et al 2022). In general, the seasonal appearance of a fresh layer suggests more regular and nearby sources. We did not find evidence of a clear advective pathway from the east Greenland shelf in this study.

Exchanges between the southeast Greenland shelf and interior seas are driven by winds, eddies and topographic steering. These processes are small scale, intermittent and highly localized. It is likely the eddies and topographic effect enhance mixing of freshwater into the water column in the near shelf region, but it seems less likely that these will export large volumes of freshwater into the interior. Wind events, if sustained long or often enough, may export larger amounts and would be found in a shallow layer (Duyck et al., 2022). However, strong freshwater years (Oltmanns et al., 2018, Bilo et al., 2019, Sterl & de Jong, 2022) were preceded by low Tip Jet winters. Nor did precipitation fully explain the interannual variability in freshwater stratification (Sterl & de Jong, 2022). Further study into the interannual variability of local wind, ice and precipitation driven

freshwater fluxes will be needed to explain the large changes in freshwater stratification seen in some summers.

Acknowledgments and Open Research

The EGC-DrIFT project is financially supported by the Innovational Research Incentives Scheme of the Netherlands Organisation for Scientific Research (NWO) under grant agreement nos. 016.Vidi.189.130.

The EGC-DrIFT dataset is available from Duyck and De Jong 2023. The IABP dataset can be retrieved from the IABP website (https://iabp.apl.uw.edu/, Rigor et al 2002), and the GDP dataset is available from Lumpkin and Centurioni 2019.

This research made use of the EU Copernicus Marine Service Information altimetry product (Copernicus Marine 2022), the MUR satellite sea surface temperature dataset (JPL MUR MEaSUREs Project. 2015), the CARRA atmospheric reanalysis reanalysis from the Copernicus Climate Data Store (Schyberg et al 2020) and the ETOPO2022 bathymetry (NOAA, 2022)

Supplementary material

This supportive information provides additional figures relative to the combined drifter dataset, that includes the EGC-DrIFT, GDP and IABP datasets

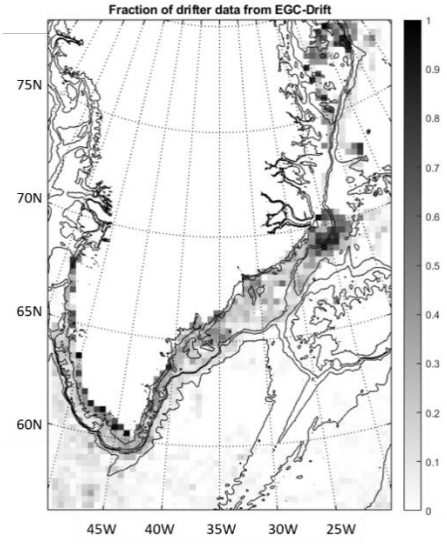

Figure S4.1. *Fraction of drifter days in each bin that is provided by EGC-DrIFT drifters. The new dataset provides new data in previously poorly covered areas close to Scoresby Sund, Fram Strait, and close to the Greenland south-east and south-west coast.*

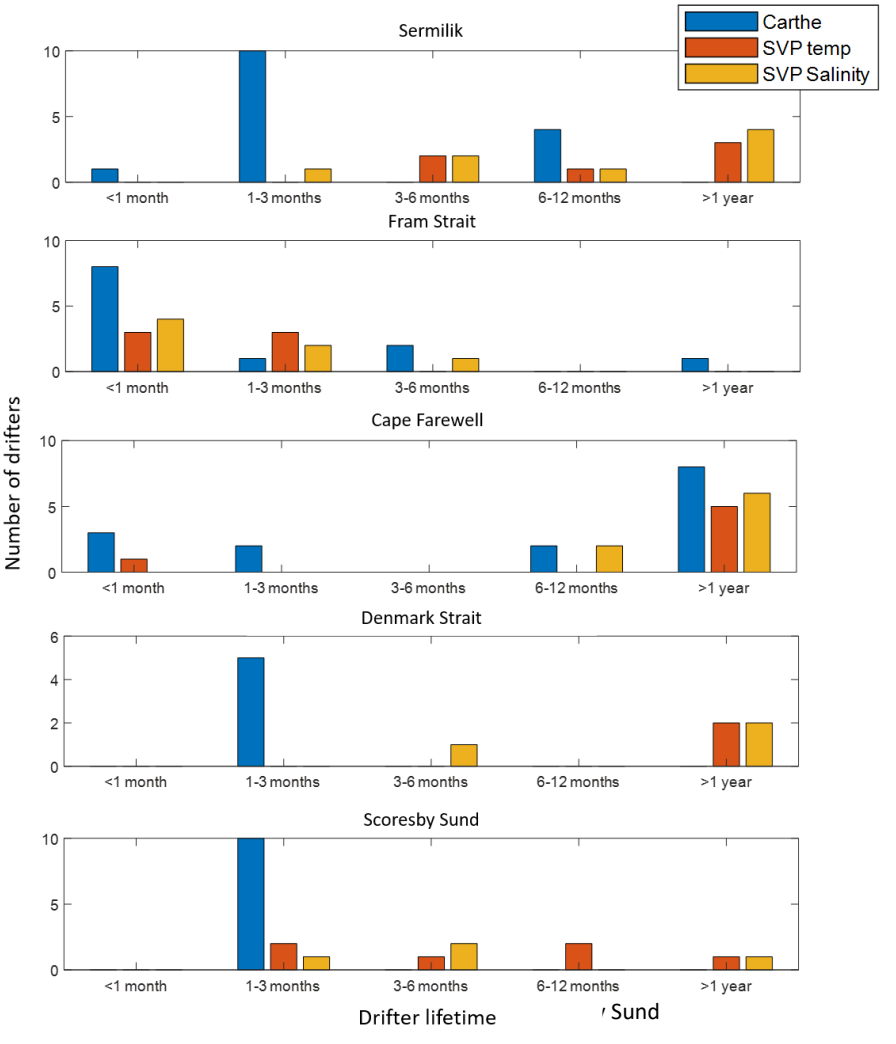

Figure S4.2. *Histograms showing how long drifters transmitted depending on the type of drifter and where they were deployed. CARTHE drifters are in blue, SVP-T drifters in red and SVP-S drifters in yellow*

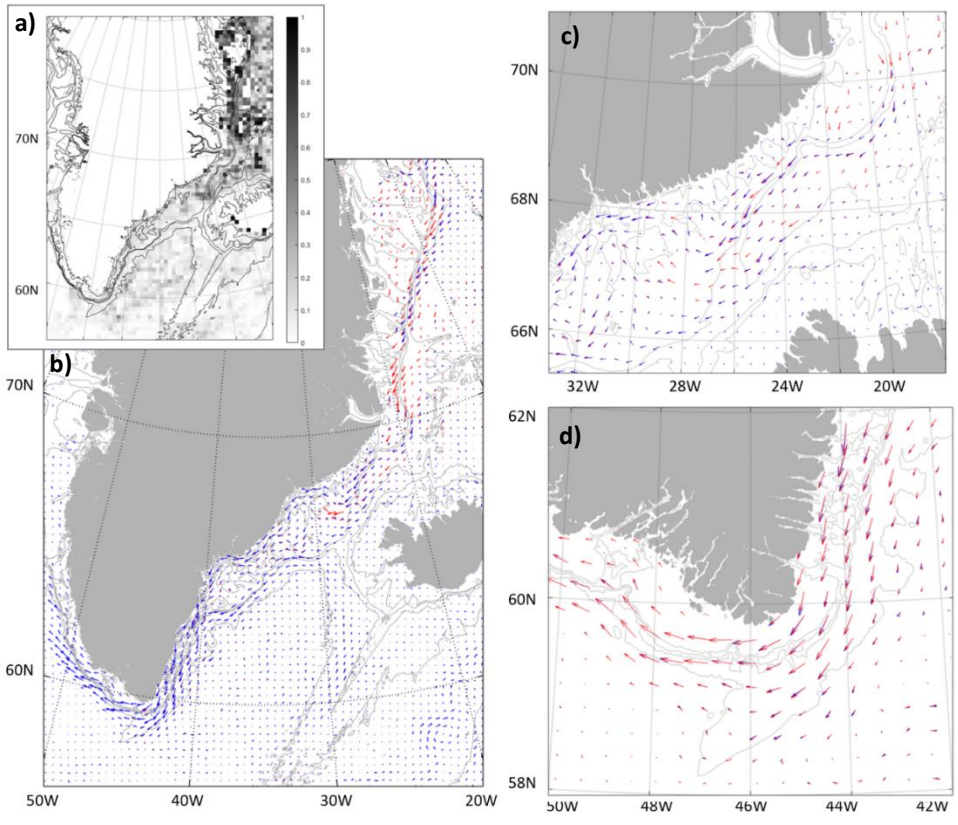

***Figure S4.3**. A. Fraction of drifter days in each bin that is provided by the IABP drifter dataset; B. Mean surface circulation computed from the EGC-DrIFT, IABP and GDP datasets (red), and from the EGC-DrIFT and GDP datasets only (blue). C. Same at Denmark Strait. D. Same at Cape Farewell. To obtain the circulation maps, we compute mean drifter velocities in 30x30 km bins using the jlab 2dstats function (Lilly et al 2021). Only bins with more than 5 drifter days are shown. Bathymetry in grey at -2000, -1000, -500, -200 m. IABP drifters provide information in areas with very scarce coverage of drifter data such as north of Denmark Strait, and do not create artifacts due to their unknown drogue status in areas with existing dense coverage.*

Drifter ID	Deployment area	Drifter type	Deployment time	Deployment longitude	Deployment latitude	Drifter death date	Drogue off date	Drifter life (days)
0-2671530	Sermilik	CARTHE	14-Aug-2019 07:15:00	-33.8095	64.7989	06-Jul-2020 12:59:51	X	327.2
0-2677305	Sermilik	CARTHE	14-Aug-2019 08:05:00	-33.9452	64.8570	17-Sep-2019 10:37:43	X	34.1
0-2677308	Sermilik	CARTHE	14-Aug-2019 09:00:00	-34.0717	64.9147	03-Sep-2019 20:56:07	X	20.5
0-2677309	Sermilik	CARTHE	14-Aug-2019 09:30:00	-34.2078	64.9705	01-Oct-2019 09:17:31	24-Sep-2019 09:10:06	48.0
0-2677313	Sermilik	CARTHE	14-Aug-2019 10:30:00	-34.3337	65.0242	06-Jul-2020 14:20:06	X	327.2
0-2677318	Sermilik	CARTHE	14-Aug-2019 11:20:00	-34.4770	65.0845	04-Oct-2019 20:11:23	18-Sep-2019 11:12:39	51.4
0-2677319	Sermilik	CARTHE	14-Aug-2019 12:15:00	-34.6128	65.1408	05-Jul-2020 09:02:28	06-Jun-2020 21:01:08	325.9
0-2677332	Sermilik	CARTHE	14-Aug-2019 12:45:00	-34.7498	65.1962	20-Sep-2019 13:22:13	X	37.0
0-2677647	Sermilik	CARTHE	14-Aug-2019 13:30:00	-34.8862	65.2525	27-Sep-2019 06:15:31	X	43.7
0-2677651	Sermilik	CARTHE	14-Aug-2019 14:05:00	-35.0030	65.3081	17-Sep-2019 20:19:24	X	34.3
0-2677691	Sermilik	CARTHE	14-Aug-2019 20:00:00	-33.4988	64.9483	06-Jul-2020 14:08:55	X	326.8
0-2677692	Sermilik	CARTHE	14-Aug-2019 21:00:00	-33.6375	65.0033	18-Sep-2019 11:06:57	17-Sep-2019 16:58:39	34.6
0-2677694	Sermilik	CARTHE	14-Aug-2019 21:45:00	-33.7725	65.0622	14-Oct-2019 06:45:34	17-Sep-2019 15:57:56	60.4
0-2677696	Sermilik	CARTHE	14-Aug-2019 22:45:00	-33.9520	65.1388	18-Sep-2019 06:48:17	X	34.3
0-2677706	Sermilik	CARTHE	14-Aug-2019 23:45:00	-34.0860	65.1975	29-Sep-2019 02:55:35	29-Sep-2019 00:47:54	45.1
0-2677830	Fram Strait	CARTHE	02-Sep-2019 23:00:00	-1.5731	78.4960	15-Sep-2019 21:23:37	X	12.9
0-2679032	Fram Strait	CARTHE	04-Sep-2019 14:20:00	-4.0842	78.7955	08-Sep-2019 15:24:14	X	4.0
0-2679470	Fram Strait	CARTHE	03-Sep-2019 15:15:00	-4.5007	78.8333	06-Sep-2019 15:39:29	X	3.0
0-2679528	Fram Strait	CARTHE	06-Sep-2019 00:50:00	-10.9997	78.8333	11-Dec-2019 07:45:36	X	96.3
0-2679547	Fram Strait	CARTHE	03-Sep-2019 05:55:00	-3.5049	78.8318	17-Sep-2019 20:22:28	X	14.6
0-2679713	Fram Strait	CARTHE	06-Sep-2019 02:13:00	-11.5005	78.8329	09-Sep-2019 22:17:06	X	3.8
0-2679714	Fram Strait	CARTHE	12-Sep-2019 22:42:00	-3.6627	78.8003	07-Nov-2021 14:29:27	X	786.7
0-2679716	Fram Strait	CARTHE	09-Sep-2019 14:00:00	-10.9948	78.6217	12-Sep-2019 11:55:13	X	2.9
0-2679720	Fram Strait	CARTHE	09-Sep-2019 14:40:00	-10.6590	78.6102	13-Sep-2019 15:50:29	X	4.0
0-2679723	Fram Strait	CARTHE	13-Sep-2019 14:58:00	-2.7467	78.7982	11-Mar-2020 04:00:10	X	179.5
0-2679725	Fram Strait	CARTHE	03-Sep-2019 00:30:00	-2.5060	78.8247	22-Oct-2019 21:54:07	X	49.9
0-2679865	Fram Strait	CARTHE	13-Sep-2019 15:32:00	-2.4496	78.8065	26-Sep-2019 18:26:48	X	13.1
300234067053940	Sermilik	SVP-I-XDGS	14-Aug-2019 08:05:00	-33.9452	64.8570	08-Mar-2022 12:01:07	15-Dec-2020 12:04:12	937.2
300234067055920	Sermilik	SVP-I-XDGS	14-Aug-2019 09:30:00	-34.2078	64.9705	24-Sep-2021 06:00:39	10-Jun-2020 15:00:59	771.9
300234067056930	Sermilik	SVP-I-XDGS	14-Aug-2019 12:45:00	-34.7498	65.1962	23-Feb-2020 23:00:39	X	193.4
300234067059920	Sermilik	SVP-I-XDGS	14-Aug-2019 11:20:00	-34.4770	65.0845	28-Sep-2020 03:04:11	X	410.7
300234067943750	Sermilik	SVP-I-XDGS	14-Aug-2019 21:00:00	-33.6375	65.0033	31-Dec-2019 04:00:39	X	138.3
300234067948730	Sermilik	SVP-I-XDGS	14-Aug-2019 22:45:00	-33.9520	65.1388	15-Jan-2020 00:06:35	26-Sep-2019 06:00:40	153.1
300234067949780	Fram Strait	SVP-I-XDGS	13-Sep-2019 15:32:00	-2.4496	78.8065	03-Nov-2019 07:00:44	X	50.6
300234067055970	Fram Strait	SVP-I-XDGS	12-Sep-2019 23:55:00	-3.2425	78.8254	05-Dec-2019 01:04:11	X	83.0
300234067945770	Fram Strait	SVP-I-XDGS	05-Sep-2019 22:50:00	-10.9997	78.8333	16-Nov-2019 18:00:40	X	71.8
300234067059930	Fram Strait	SVP-I-XDGS	03-Sep-2019 03:55:00	-3.5049	78.8318	02-Oct-2019 17:00:39	X	29.5
300234067057580	Fram Strait	SVP-I-XDGS	02-Sep-2019 23:00:00	-1.5731	78.4960	10-Sep-2019 14:00:38	X	7.6

300234067052580	Fram Strait	SVP-I-XDGS	12-Sep-2019 20:00:00	-4.0671	78.8194	14-Sep-2019 01:00:56	X	1.2
300234068602110	Sermilik	SVP-BSC	14-Aug-2019 07:15:00	-33.8095	64.7989	18-Mar-2020 09:00:44	09-Mar-2020 23:58:00	217.1
300234068607550	Sermilik	SVP-BSC	14-Aug-2019 21:45:00	-33.7725	65.0622	07-Sep-2022 21:00:48	24-Feb-2020 17:59:00	1120.0
300234068608590	Sermilik	SVP-BSC	14-Aug-2019 09:00:00	-34.0717	64.9147	07-Jan-2020 15:00:47	X	146.3
300234068609910	Sermilik	SVP-BSC	14-Aug-2019 23:45:00	-34.0860	65.1975	08-Mar-2022 03:00:00	12-Jan-2020 02:58:00	936.1
300234068703270	Sermilik	SVP-BSC	14-Aug-2019 10:30:00	-34.3337	65.0242	24-Oct-2020 00:00:45	05-Mar-2020 17:58:00	436.6
300234068704240	Sermilik	SVP-BSC	14-Aug-2019 20:00:00	-33.4988	64.9483	19-Sep-2019 03:00:50	X	35.3
300234068705260	Sermilik	SVP-BSC	14-Aug-2019 12:15:00	-34.6128	65.1408	08-Mar-2022 12:00:51	21-Mar-2020 05:58:00	937.0
300234068809380	Sermilik	SVP-BSC	14-Aug-2019 13:30:00	-34.8862	65.2525	15-Jan-2020 12:00:47	X	153.9
300234068602310	Fram Strait	SVP-BSC	06-Sep-2019 00:13:00	-11.5005	78.8329	15-Sep-2019 18:01:46	X	9.7
300234068609530	Fram Strait	SVP-BSC	13-Sep-2019 14:58:00	-2.7467	78.7982	05-Jan-2020 06:01:15	19-Sep-2019 23:58:00	113.6
300234068708270	Fram Strait	SVP-BSC	04-Sep-2019 12:20:00	-4.0842	78.7955	12-Sep-2019 21:00:45	X	8.4
300234068604400	Fram Strait	SVP-BSC	09-Sep-2019 12:40:00	-10.6590	78.6102	03-Oct-2019 12:00:42	X	24.0
300234068803170	Fram Strait	SVP-BSC	03-Sep-2019 00:30:00	-3.5057	78.8247	04-Sep-2019 21:01:41	X	1.9
300234068501770	Fram Strait	SVP-BSC	12-Sep-2019 20:42:00	-3.6627	78.8003	22-Oct-2019 03:00:49	X	39.3
300234068603290	Fram Strait	SVP-BSC	03-Sep-2019 22:45:00	-4.0102	78.8323	06-Oct-2019 18:01:59	X	32.8
0-2692878	Cape Farewell	CARTHE	20-Jul-2020 11:18:00	60.0655	-42.5979	15-Sep-2020 02:42:55	X	56.6
0-2693174	Cape Farewell	CARTHE	20-Jul-2020 12:40:00	60.0492	-42.4291	05-Jan-2022 12:50:42	X	534.0
0-2693184	Cape Farewell	CARTHE	20-Jul-2020 13:08:00	60.0369	-42.3329	14-Feb-2022 15:55:43	X	574.1
0-2693511	Cape Farewell	CARTHE	20-Jul-2020 13:09:00	60.0369	-42.3329	29-Jan-2021 21:25:55	X	193.3
0-2695574	Cape Farewell	CARTHE	20-Jul-2020 14:10:00	60.0239	-42.2059	14-Feb-2022 14:16:23	X	574.0
0-2695254	Cape Farewell	CARTHE	20-Jul-2020 14:10:00	60.0239	-42.2059	21-Oct-2021 02:13:54	X	457.5
0-2693512	Cape Farewell	CARTHE	20-Jul-2020 14:38:00	60.0141	-42.1153	06-Dec-2021 05:14:19	X	503.6
0-2696828	Cape Farewell	CARTHE	20-Jul-2020 14:39:00	60.0141	-42.1153	01-Jun-2021 15:24:30	X	316.0
0-2697093	Cape Farewell	CARTHE	20-Jul-2020 16:05:00	60.0039	-42.0273	24-Jul-2020 00:13:24	X	3.3
0-2697094	Cape Farewell	CARTHE	20-Jul-2020 16:06:00	60.0039	-42.0273	08-Aug-2020 18:09:37	X	19.1
0-2697095	Cape Farewell	CARTHE	20-Jul-2020 17:40:00	59.9898	-41.8824	24-Oct-2021 12:20:52	X	460.8
0-2697101	Cape Farewell	CARTHE	20-Jul-2020 17:40:00	59.9898	-41.8824	25-Jul-2020 03:20:04	X	4.4
0-2698117	Cape Farewell	CARTHE	20-Jul-2020 19:37:00	59.9738	-41.7421	01-Oct-2020 13:37:16	X	72.8
0-2697420	Cape Farewell	CARTHE	20-Jul-2020 19:37:00	59.9738	-41.7421	14-Feb-2022 13:45:00	X	573.8
0-2698125	Cape Farewell	CARTHE	20-Jul-2020 20:23:00	59.9588	-41.5928	13-Sep-2021 19:41:42	X	420.0
300534060383600	Cape Farewell	SVP-I-XDGS	20-Jul-2020 13:10:00	60.0369	-42.3329	11-Jan-2022 04:08:40	18-Dec-2020 15:01:10	539.6
300534060383610	Cape Farewell	SVP-I-XDGS	20-Jul-2020 10:16:00	60.0239	-42.2059	18-Aug-2020 17:00:40	X	29.3
300534060384610	Cape Farewell	SVP-I-XDGS	20-Jul-2020 14:38:00	60.0141	-42.1153	07-Jun-2022 12:01:31	X	686.9
300534060385600	Cape Farewell	SVP-I-XDGS	20-Jul-2020 16:05:00	60.0039	-42.0273	07-Jun-2022 12:01:18	X	686.8
300534060385620	Cape Farewell	SVP-I-XDGS	20-Jul-2020 17:35:00	59.9898	-41.8824	07-Jun-2022 12:00:41	23-Feb-2022 12:04:16	686.8
300534060386630	Cape Farewell	SVP-I-XDGS	20-Jul-2020 19:36:00	59.9738	-41.7421	07-Jun-2022 12:00:40	X	686.7
300234067779190	Cape Farewell	SVP-BSC	20-Jul-2020 12:41:00	60.0492	-42.4291	25-Mar-2021 15:03:24	20-Dec-2020 00:59:00	248.1
300234067770220	Cape Farewell	SVP-BSC	20-Jul-2020 13:09:00	60.0369	-42.3329	07-Jun-2022 13:00:53	19-Mar-2021 15:59:00	687.0

300234067676100	Cape Farewell	SVP-BSC	20-Jul-2020 14:12:00	60.0239	-42.2059	19-Jul-2021 02:00:00	01-Dec-2020 17:00:00	363.5
300234067676130	Cape Farewell	SVP-BSC	20-Jul-2020 14:37:00	60.0141	-42.1153	02-Mar-2021 00:06:31	X	224.4
300234067672160	Cape Farewell	SVP-BSC	20-Jul-2020 16:04:00	60.0039	-42.0273	07-Sep-2022 23:00:52	26-Nov-2020 11:59:00	779.3
300534060125630	Cape Farewell	SVP-BSC	20-Jul-2020 17:35:00	59.9898	-41.8824	07-Jun-2022 13:01:00	05-Nov-2020 15:00:00	686.8
300534060129610	Cape Farewell	SVP-BSC	20-Jul-2020 19:38:00	59.9738	-41.7421	08-Mar-2022 14:00:00	30-Dec-2020 13:00:00	595.8
300534060128630	Cape Farewell	SVP-BSC	20-Jul-2020 20:22:00	59.9588	-41.5928	07-Sep-2022 23:01:02	19-Oct-2020 01:48:00	779.1
0-2698135	Scoresby Sund	CARTHE	03-Aug-2021 19:32:39	69.9501	-19.1492	05-Sep-2021 06:42:48	X	32.5
0-2693173	Scoresby Sund	CARTHE	03-Aug-2021 20:02:00	69.9508	-18.9500	13-Sep-2021 21:39:22	X	41.1
0-2687500	Scoresby Sund	CARTHE	03-Aug-2021 20:26:00	69.9493	-18.7991	05-Sep-2021 00:37:36	X	32.2
0-2690765	Scoresby Sund	CARTHE	03-Aug-2021 20:50:00	69.9494	-18.6483	13-Sep-2021 06:33:13	X	40.4
0-2697827	Scoresby Sund	CARTHE	03-Aug-2021 21:25:00	69.9479	-18.4488	05-Sep-2021 09:47:52	X	32.5
300534060380650	Scoresby Sund	SVP-I-XDGS	03-Aug-2021 19:31:57	69.9499	-19.1515	06-Dec-2021 10:01:32	X	124.6
300234068731430	Scoresby Sund	SVP-BSC	03-Aug-2021 20:01:00	69.9508	-18.9521	06-Dec-2021 07:01:33	X	124.5
300534060384620	Scoresby Sund	SVP-I-XDGS	03-Aug-2021 20:25:00	69.9494	-18.8011	05-Sep-2021 15:00:43	X	32.8
300534060126650	Scoresby Sund	SVP-BSC	03-Aug-2021 20:50:00	69.9494	-18.6509	07-Sep-2022 23:01:05	09-Dec-2021 12:59:00	400.1
300534060382560	Scoresby Sund	SVP-I-XDGS	03-Aug-2021 21:20:00	69.9495	-18.4532	20-Apr-2022 21:00:46	X	260.0
0-2684286	Scoresby Sund	CARTHE	04-Aug-2021 00:20:00	69.7188	-19.1475	05-Sep-2021 09:39:19	05-Sep-2021 00:38:18	32.4
0-2697317	Scoresby Sund	CARTHE	04-Aug-2021 00:43:00	69.6909	-19.0303	18-Oct-2021 00:47:01	X	75.0
0-2692714	Scoresby Sund	CARTHE	04-Aug-2021 01:08:00	69.6605	-18.9038	08-Sep-2021 00:39:17	01-Sep-2021 18:52:38	35.0
0-2694782	Scoresby Sund	CARTHE	04-Aug-2021 01:37:00	69.6261	-18.7531	05-Sep-2021 12:39:52	05-Sep-2021 12:39:52	32.5
0-2696946	Scoresby Sund	CARTHE	04-Aug-2021 02:35:00	69.6697	-18.8304	18-Oct-2021 03:48:16	17-Oct-2021 00:55:18	75.1
300534060383620	Scoresby Sund	SVP-I-XDGS	04-Aug-2021 00:20:00	69.7191	-19.1485	22-Feb-2022 20:04:10	X	202.8
300234067209310	Scoresby Sund	SVP-BSC	04-Aug-2021 00:42:00	69.6912	-19.0315	29-Jan-2022 17:01:22	17-Sep-2021 02:59:00	178.7
300534060386530	Scoresby Sund	SVP-I-XDGS	04-Aug-2021 01:08:00	69.6607	-18.9044	25-Oct-2021 03:04:02	X	82.1
300234068631580	Scoresby Sund	SVP-BSC	04-Aug-2021 01:36:00	69.6264	-18.7543	28-Oct-2021 03:00:49	X	85.1
300534060380600	Scoresby Sund	SVP-I-XDGS	04-Aug-2021 02:10:00	69.6698	-18.8303	07-Sep-2022 18:01:49	X	399.7
0-2692051	Denmark Strait	CARTHE	27-Jul-2021 02:41:19	65.8460	-29.1731	10-Sep-2021 22:01:57	02-Sep-2021 12:49:37	45.8
0-2692986	Denmark Strait	CARTHE	27-Jul-2021 03:09:00	65.8071	-29.0637	05-Sep-2021 01:41:52	X	39.9
0-2697099	Denmark Strait	CARTHE	27-Jul-2021 03:35:00	65.7561	-28.9766	05-Sep-2021 13:44:55	X	40.4
0-2697100	Denmark Strait	CARTHE	27-Jul-2021 03:59:00	65.7052	-28.8979	04-Sep-2021 22:37:35	X	39.8
0-2698119	Denmark Strait	CARTHE	27-Jul-2021 04:26:00	65.6517	-28.8022	27-Aug-2021 16:34:16	X	31.5
300234067674320	Denmark Strait	SVP-BSC	27-Jul-2021 02:38:00	65.8448	-29.1762	07-Sep-2022 23:01:31	21-Mar-2022 04:59:00	407.8
300534060385590	Denmark Strait	SVP-I-XDGS	27-Jul-2021 03:07:55	65.8084	-29.0656	07-Sep-2022 18:00:41	08-Dec-2021 10:00:41	407.6
300534060122920	Denmark Strait	SVP-BSC	27-Jul-2021 03:33:00	65.7569	-28.9782	19-Dec-2021 12:03:04	03-Oct-2021 23:59:00	145.4
300534060389600	Denmark Strait	SVP-I-XDGS	27-Jul-2021 03:58:00	65.7058	-28.8989	07-Sep-2022 18:01:22	16-Jun-2022 12:02:49	407.6
300534060228340	Denmark Strait	SVP-BSC	27-Jul-2021 04:25:00	65.6520	-28.8031	07-Sep-2022 23:01:02	09-Jan-2022 11:59:00	407.8

Table S4.1 *Metadata of EGC-DrIFT drifters. SVP-I-XDGS are SVP-T drifters, SVP-BSC are SVP-S drifters.*


WARNING
Hydrography
Oceanography


Hydrography
Oceanography
Ensta Bretagne

Chapter 5

Impact of model resolution on the representation of exchanges between the east Greenland shelf and interior seas of the Subpolar North Atlantic

Illustration : Deployment of SVP drifters in July 2020 at Cape Farewell: The SVP drifters were thrown in the water with their drogue folded in cardboard that would later disintegrate for the drogue to unfold. Picture : Nora Fried.

Abstract

Climate models predict a weakening of the AMOC under climate change in the 21st century, however there is a large inter-model spread in the speed and magnitude of the predicted weakening. Moreover, additional uncertainties such as future increasing input of meltwater from Greenland to the Subpolar North Atlantic, could result in further weakening of the AMOC. In this study we use the HadGEM3-GC3.1 fully coupled climate model at 1°, 0.25° and 0.12° to investigate the impact of model resolution on exchanges between the east Greenland shelf and interior seas of the Subpolar North Atlantic, the properties of the upper layer of the interior seas, and deep convection. Increasing resolutions allow for a better representation of the circulation over the shelf, but it is not clear whether they provide more realistic export from the shelf to interior seas. The 0.25° model exports too much fresh shelf waters and sea ice to the Nordic seas, leading to too fresh Nordic seas and a too large sea ice extent. In the 0.12° model, the Subpolar North Atlantic is too salty, and fresh waters are too constrained towards the coast south of Denmark Strait, preventing any export of relatively fresh waters towards the Irminger Sea. In the three resolutions, most of the export of liquid freshwater and sea ice takes place in the northern part of the shelf towards the Nordic Seas. We show that a decline in sea ice export during the 25 model years examined here happened concurrently with increasing salinities in the Nordic Seas for all resolutions. We suggest that sea ice export could potentially have a strong influence on the Nordic Seas, which would require both further observational studies and studies with a wider range of climate models.

5.1. Introduction

The Atlantic Meridional Overturning Circulation (AMOC) redistributes heat and freshwater from the tropics to the poles and is therefore a key element of the climate system (Buckley and Marshall 2016). The AMOC is expected to weaken in the coming century as a response to anthropogenic climate change (Weijer et al 2020, Fox-Kemper et al 2021), which could have major impacts on local and global climate (Jackson et al 2015, Zhang et al 2019, Collins et al 2019). There is a large inter-model spread in the speed and magnitude of the predicted weakening (Weijer et al 2020, Fox-Kemper et al 2021), and better constraining the future evolution of the AMOC is critical to improving climate projections (Bellomo et al 2021).

The representation and evolution of the AMOC in CMIP (Coupled Model Intercomparison Projects) models has been investigated in numerous studies. A few studies focused specifically on the impact of model resolution on the representation of the AMOC in CMIP6 and showed that the AMOC is generally stronger and shows more weakening as a response to climate change in higher (0.25 to 0.1 degrees) resolution models (Hirschi et al 2020, Roberts et al 2020, Jackson et al 2020). These differences could be related to the impact of resolution on processes that are important for the AMOC. For instance, higher resolution models tend to have a warmer and saltier subpolar gyre (Jackson et al 2020, Menary et al 2015) and more limited sea ice area and volume (Docquier et al 2019), which could influence where and how much deep convection takes place. Though higher resolution models allow for a marked improvement of simulated mean circulation in the Subpolar North Atlantic (SPNA) (Marzocchi et al 2015), it is not clear whether this also leads to more realistic predictions of the evolution of the AMOC (Jackson et al 2020?). Moreover, biases remain in high-resolution models and both coarse and high-resolution coupled climate models generally convect too deeply and over a too large area (Heuzé et al 2021).

One of the possible drivers of a weakening of the AMOC as a response to climate change is the increase in freshwater input to the SPNA from the Greenland ice sheet (Bamber et al 2012) or the Arctic (Haine et al 2015). Along with the warming of the SPNA and the intensification of precipitation, this additional input of freshwater would lead to a reduction of the density of the upper layer. This increase in the surface stratification of the SPNA could inhibit deep convection and the formation of deep waters. However, the pathways for freshwater from Greenland and the Arctic to deep convection regions are not straightforward. These waters first enter the Greenland shelf and need to be stirred into the interior seas to affect deep convection in the subpolar north Atlantic (Frajka Williams et al 2016, Dukhovskoy et al 2016).

Fresh Polar Surface Water (Rudels et al 2002) from the Arctic is advected along the east Greenland shelf by the East Greenland Current (EGC) and its coastal branch, the East Greenland Coastal Current (EGCC, Bacon et al 2002, Sutherland and Pickart 2008, Havik et al 2017a). As the EGC and EGCC flow from Fram Strait to Cape Farewell, additional fresh waters from Greenland enters the EGCC (Bacon et al 2002, Sutherland and Pickart 2009). The relatively cold and fresh waters advected over the shelf are isolated from

warmer and saltier waters of the interior seas by a strong hydrographic front at the shelfbreak, and only limited exchanges take place between the two. North of Denmark Strait, the Jan Mayen Current (Bourke et al 1992), the East Icelandic Current (Macrander et al 2014) and the separated EGC (Vage et al 2013) divert waters from the EGC towards the Greenland Sea and Nordic Seas. Over the shelf, exchanges between the EGC and EGCC also take place, especially at the deep Kangerdlussuaq and Sermilik troughs that divert part of the EGC towards the coast (Sutherland and Pickart 2008, Duyck and De Jong 2021). At Cape Farewell, the EGC and EGCC become the West Greenland current (WGC) and West Greenland coastal current (WGCC), and exchanges take place between the coastal and shelfbreak cores (Lin et al 2018, Pacini et al 2020, Duyck and De Jong 2021). West of Greenland, these two current cores flow side by side before entering Baffin Bay and the Labrador Current. Both eddies (Lilly et al 2003, Hatún et al 2007) and winds (Schulze Chrétien and Frajka Williams 2019) export part of the fresh shelf waters into the Labrador Sea. This circulation is summarized Figure 1A.

It is unclear how much exchanges take place between the shelf and the interior seas, and whether and when additional input of freshwater could impact deep convection in these regions (Böning et al 2016, Yang et al 2016). Moreover, while most studies of exchanges between the shelf and interior seas have focused on the Labrador Sea and a possible weakening of deep convection in that region, recent observations showed that the eastern SPNA dominates the mean and variability of the subpolar overturning, shedding a new light on the role of the Irminger and Nordic Seas (Lozier et al 2019, Li et al 2021). Though freshwater export is expected to be much more limited on the eastern than western side of Greenland, these new results highlight the importance of a better understanding of possible pathways for Arctic and Greenland waters into the Irminger Sea and Nordic Seas. Modelling studies that released tracers to track Greenland meltwater showed that meltwater generally follows the boundary currents over the shelf, and that part of it is stirred into the Labrador Sea (Dukhovskoy et al 2016, Gillard et al 2016, Dukhovskoy et al 2019). The Irminger and Nordic Seas are mostly only affected after the meltwater recirculated via the subpolar gyre or Labrador Sea. Waters from the Arctic are likely to follow a similar path, except in the north-east of Greenland, because contrarily to Greenland meltwater, they are already present in the EGC in that area. These studies also highlight difference between model resolutions, with high resolution models leading to more intense stirring of shelf waters into the Labrador Sea (Dukhovskoy et al 2016). Simulating these pathways represents a challenge for models because of the high-resolution that is necessary to represent cross-shelf exchanges (Martin et al 2023, Swingedouw et al 2022).

In this study we use the HadGEM3-GC3.1 (hereafter HadGEM3) fully coupled climate model at 1 degree, 0.25 degree and 0.12 degree resolution, to investigate the impact of model resolution on the representation of shelf-interior exchanges. Section 2 describes the model data, as well as other datasets we used to compare model results to observations. In section 3, we describe salinity, sea ice concentration, deep convection, the mean circulation and wind regimes over the shelf in the different resolutions of HadGEM3, and compare it to an ocean reanalysis. Section 4 presents freshwater and sea

ice exchanges along the east Greenland shelf, the differences between the different resolutions, and what drives variability in freshwater export. In section 5, we discuss the importance of resolution for a realistic representation of shelf-interior exchanges and possible implications.

5.2. Methods

5.2.1 HadGEM3-GC3.1 in three resolutions

To investigate the representation of freshwater pathways in climate models and the importance of resolution, we use results from the third Hadley Centre Global Environmental Model, run in the Global Coupled configuration 3.1 (HadGEM3-GC3.1 at three different resolutions. The HadGEM3-GC3.1 fully coupled climate model is developed by the UK Met Office. It constitutes the UK contribution to the 6th generation of the Coupled Model Intercomparison Project (CMIP6).

The components of the coupled model are the Unified Model for the atmosphere (GA7.1, Walters et al 2019), JULES for land surface processes (GL7.0, Walters et al 2019), Nucleus for European Modeling of the Ocean (NEMO) for the ocean (GO6.0, Storkey et al 2018), CICE for the sea ice (GS1.8, Ridley et al 2018), coupled with the OASIS3-MCT coupler (Valcke et al., 2015). More details about the configuration of the model can be found in Williams et al 2017.

The low-resolution version (HadGEM3-GC3.1-LL, LL in the following, Kuhlbrodt et al 2018) has an atmospheric resolution of 135km and an ocean resolution of 1 degree. The medium-resolution version (HadGEM3-GC3.1-MM, MM in the following, Menary et al 2018), has an atmospheric resolution of 60km and an ocean resolution of 0.25 degrees. The high-resolution version (HadGEM3-GC3.1-HH, HH in the following, Roberts et al 2019) has an atmospheric resolution of 25 km and an ocean resolution of 0.12 degrees. In the study region, between 55 and 80°N and -65 and 15°E, this corresponds to between 35 and 70km (55km in the mean) for LL, 9 to 18km (mean 14km) for MM and 3.5 to 6km (mean 5km) for HH. Table 1 summarizes these properties. Details on the resolution hierarchy of HadGEM3-GC3.1 can be found in Williams et al 2018. For all resolutions, HadGEM3 has 75 ocean levels.

Validations of HadGEM3-GC3.1 in its MM and LL configurations can be found in Menary et al 2018 and Kuhlbrodt et al 2018. Jackson 2020 and Menary et al 2020 showed that the MM and LL version of HadGem3 have a good representation of the time mean and variability of overturning at the OSNAP section. The overturning stream function in the LL and MM resolutions is close to the inter-model mean (Weijier et al 2020). Roberts et al 2019 showed that increasing ocean resolution allowed for a reduction in model bias, with the HH model performing best in representing the AMOC streamfunction (Roberts et al 2020).

	ATMOSPHERE	OCEAN
LL	N96 135km	ORCA1, 1deg ~55km in study region
MM	N216 60km	ORCA025, 0.25deg, ~14km in study region
HH	N512 25km	ORCA12, 0.12deg, ~5km in study region

***Table 5.1**: Characteristics of the HadGem3-GC3.1 model at different resolutions*

We use results from the hist-1950 experiment for the 3 resolutions and use data from 1990-2014, for consistency with observational products. The hist-1950 experiment is part of the CMIP6 HighResMIP experimental design and uses the time varying external forcings from 1950-2014 described in Haarsmaa et al 2016 (aerosols, solar, ozone concentration, greenhouse gas emissions). HighResMIP is a specific CMIP6 protocol that focuses on allowing comparisons between different resolutions of climate models. It is composed of the hist-1950 with historical forcings, control-1950, with mean forcing, and highres future, with projected forcings until 2050. The spinup and run time of the model are shorter than for other CMIP6 protocols, to allow the use of very high-resolution models (Haarsmaa et al 2016, Roberts et al 2019).

We use one ensemble member per model resolution, r1i1p1f1. We use these variables at monthly frequency: zonal and meridional winds “uas” and “vas”, the ocean salinity “so”, zonal and meridional velocity “uo” and “vo”, sea ice zonal and meridional velocity “siu” and “siv”, sea ice volume per cell, or effective thickness “sivol”, sea ice concentration “siconc”, precipitations “pr” and evaporation “evap”. In the LL and MM model the sea ice concentration variable is on the same grid as the winds, in the HH model it is on the same grid as ocean variables. We also use zonal and meridional winds at a 3 hour frequency. The bathymetry is computed for each resolution using “thkcello”.

5.2.2- Ocean and atmospheric reanalyses

To estimate whether simulations at different resolutions are realistic in the SPNA, we compare results to an ocean and sea-ice reanalysis, the CMEMS GLORYS12V1 reanalysis (Lellouche et al 2021) and an atmospheric reanalysis, the ECMWF ERA5 reanalysis on single levels (Hersbach et al 2020).

The GLORYS12V1 (hereafter GLORYS) reanalysis is a global ocean reanalysis, with a 1/12° horizontal resolution (4.5km at subpolar latitudes) and 50 vertical levels. The atmosphere is forced by ERA-5 and the ocean and sea ice model are based on the ORCA12 implementation of NEMO. We retrieve the salinity, zonal and meridional ocean velocities, mixed layer depth and sea ice cover from GLORYS for the period 1993-2014. GLORYS assimilates global ocean data based on a reduced order Kalman filter, and it was shown to compare well with independent observations in the SPNA, such as the Irminger Current moorings (Fried et al 2022) the LOCO moorings (Sterl and De Jong 2022).

The ERA5 reanalysis is an atmospheric reanalysis with a horizontal resolution of 1/4°, (15km zonally and 30km meridionally at subpolar latitudes). We retrieve the 10m zonal and meridional speeds both at a monthly and 3-hourly intervals for 1990-2014.

5.2.3- Computation of transports across the boundary

We investigate exchanges between the east Greenland shelf and interior seas in the three resolutions of HadGEM3. To do so, we define a boundary between these two regions, that corresponds to the offshore limit of the shelfbreak EGC in MM (Figure 1B). We divide that boundary in two regions, north and south of Denmark Strait. Starting from Fram Strait, the northern part of the boundary ranges from 0 to 1750km, and the southern part of the boundary from 1750 to 3100km (Figure 1B). We compute the Ekman transport, volume transport, freshwater transport and sea ice transport across that boundary.

We compute zonal and meridional Ekman transport (T_{x_ek} and T_{y_ek}) from wind stress (τ_x and τ_y), calculated from the monthly zonal and meridional velocities (Equation 1 and 2). We interpolate, rotate and integrate Ekman transport along the boundary, to obtain Ekman transport across the boundary (Tek , Equation 3).

$$\begin{cases} \tau_x = \rho_{air} C_d u \sqrt{u^2 + v^2} \\ \tau_y = \rho_{air} C_d v \sqrt{u^2 + v^2} \end{cases} , \quad (1)$$

with u and v the zonal and meridional wind components at 10m, ρ_{air}= 1.2 kg.m^{-3} the air density, and C_d the wind drag defined non-linearly according to Trenberth et al 1990.

$$\begin{cases} T_{x\_ek} = \frac{\tau_y}{f\,\rho} \\ T_{y\_ek} = \frac{-\tau_x}{f\,\rho} \end{cases} , \quad (2)$$

$$\mathrm{T_{ek}} = \int_0^{\max(dist_b)} \cos(\theta(x)) * T_{\mathrm{y_{ek}}}(x) - \sin(\theta(x)) * \mathrm{T_{x_{ek}}}(x)\,\mathrm{dx} \quad , \quad (3)$$

with T_{x_ek} and T_{y_ek} the zonal and meridional Ekman transports, f = 1e-4s^{-1} the Coriolis parameter, ρ=1027 kg.m^{-3} the water density, $dist_b$ the distance along the boundary in km, and θ the local angle of the boundary. The angle is computed anticlockwise from the x axis, and the rotated axes are oriented southwards along the boundary and offshore across the boundary.

For all three resolutions, the fresh shelf waters are mostly found over the first 200m of the shelf, throughout the year (Figure 3C). Moreover, the salinity variability in the interior seas also predominantly takes place in the first 200m. Therefore, and because of data processing limitations in the case of HH, we compute volume and freshwater transport at the boundary only over the first 200m. We first interpolate the zonal and meridional velocity (v_b, u_b) as well as salinity (S_b) at the boundary. We then rotate velocities according to the local boundary angle θ. To obtain the volume transport across the

boundary T_{b_vol}, we integrate the velocity over the length of the boundary ($dist_b$), and over the first 200m (Equation 3). To obtain the freshwater transport across the boundary T_{b_FW}, we use the mean salinity in the central Irminger Sea as a reference salinity S_{ref} (Equation 4). This allows to compensate for model bias in salinity between the three different model simulations and focusses on investigating the export of freshwater defined as fresher than the hydrographic front between the shelf and the interior Irminger Sea. We therefore use reference salinities (S_{ref} of 34.7 for LL, 34.9 for MM, 35 for HH). We will discuss the differences in salinity between the model versions in more detail later. How much freshwater is computed at the boundary is dependent on the choice of the boundary and reference salinity but is a good indication of where freshwater is brought off shelf and how this varies in time.

Volume transport:

$$T_{b\_vol} = \int_0^{\max(dist_b)} \int_0^{200} (\cos(\theta(x)) * v_b(x,z) - \sin(\theta(x)) * u_b(x,z) dx dz, \quad (3)$$

Freshwater transport:

$$T_{b\_FW} = \int_0^{\max(dist_b)} \int_0^{200} (\cos(\theta(x)) * v_b(x,z) - \sin(\theta(x)) * u_b(x,z) * \left(\frac{S_{Ref} - S_{sh}(x,z)}{S_{Ref}}\right) dx dz, \quad (4)$$

The sea ice transport across the boundary T_{b_ice} is computed from the sea ice zonal and meridional velocity interpolated at the boundary (u_b and v_b), and the sea ice volume ($SIvol_b$), all interpolated at the boundary (Equation 5). Sea ice volume is given in meters and corresponds to the height of sea-ice if it was homogeneous over the cell.

$$T_{b\_ice} = \int_0^{\max(dist_b)} (\cos(\theta(x)) * v_b(x) - \sin(\theta(x)) * u_b(x)) * SIvol_b(x)\, dx, \quad (5)$$

In addition, we also compare salinity variability within four regions, defined Figure 1B: The North-East shelf, South-East shelf, Nordic Seas and Irminger Sea. To compute the mean salinity in the first 200m over each region, we weight the salinity in each cell that is part of the region by the area and thickness of the cell, computed from “thkcello” and “areacello”.

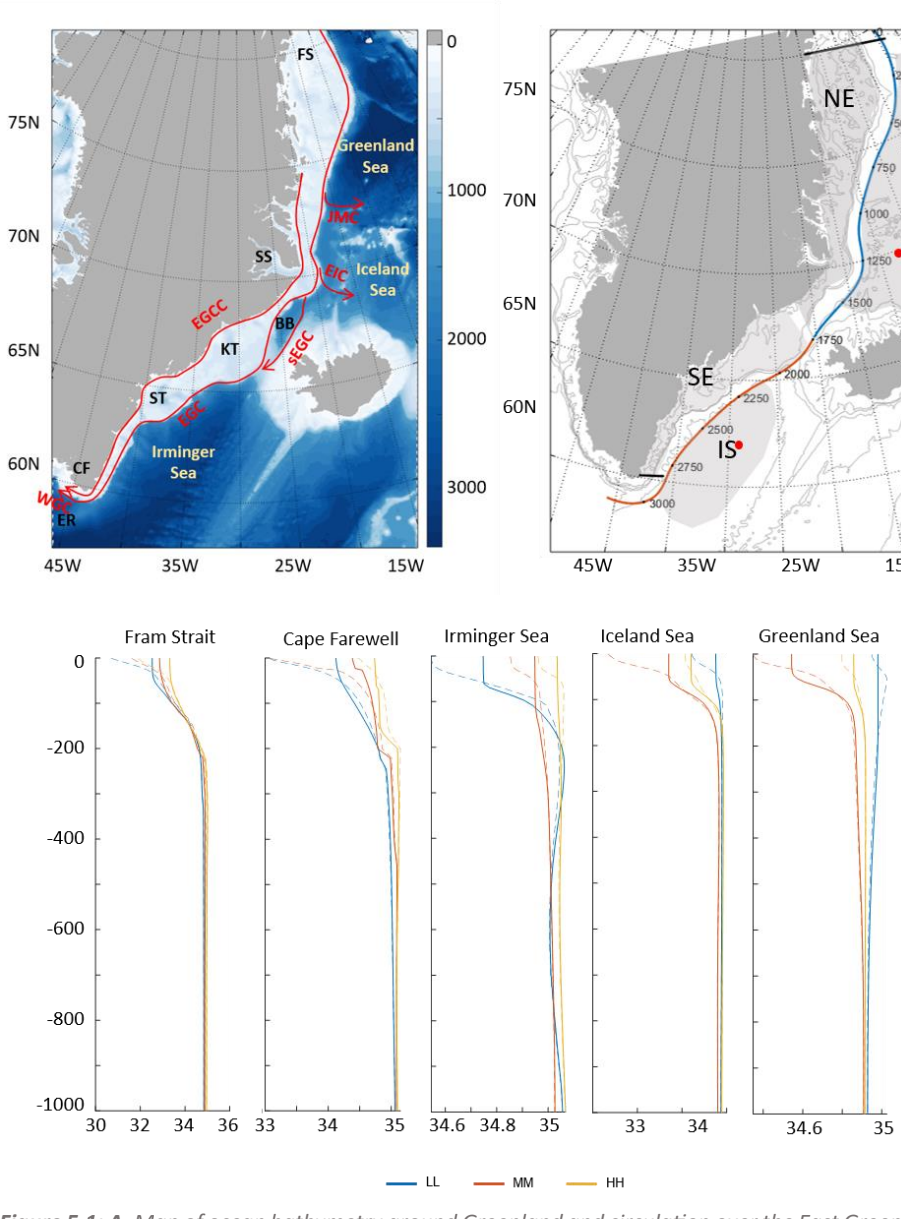

Figure 5.1: A. *Map of ocean bathymetry around Greenland and circulation over the East Greenland shelf. From Duyck and De Jong 2023. EGC: East Greenland Current; EGCC: East Greenland Coastal Current, sEGC: Separated East Greenland Current; JMC: Jan Mayen Current; EIC: East Icelandic Current; WGC: West Greenland Current. FS: Fram Strait. SS: Scoresby Sund. BB: Blosseville Basin. KT: Kangerdlussuaq Trough. ST: Sermilik Trough. DS: Denmark Strait. CF: Cape Farewell. ER: Eirik* Ridge. ***B.*** *Map of ocean bathymetry around Greenland, with delimitations and boundaries used*

further in the study. The blue and red line denote the north and south boundary between the shelf area and interior seas, while the shaded areas indicate the Nordic Seas (Green), Irminger Sea (Yellow), North-East shelf (Blue) and South-East shelf (Red) regions. The two black lines indicate the Fram Strait and Cape Farewell sections used to compute figure 1B. ***C.*** *Freshwater transport across the Fram Strait and Cape Farewell sections, in the model at three resolutions.* ***D.*** *Salinity profiles in the first 1000m in the Greenland Sea, Iceland Sea and Irminger Sea as indicated by red dots Figure 1B. Full lines are winter profiles and dashed lines summer profiles.*

5.3. Representation of the upper layer of the SPNA in HadGEM3 at three resolutions

5.3.1- Mean circulation

The circulation over the Greenland shelf is small scale and unlikely to be well resolved in coarse resolution model, while a good representation of shelf circulation is essential to realistically represent exchanges between the shelf and the interior seas. The mean circulation in the upper layer of the Subpolar North Atlantic in GLORYS and HadGEM3 at three resolutions is shown in the third column of Figure 2.

The mean circulation in the GLORYS reanalysis (Figure 2C) highlights the narrow character of the boundary currents on the Greenland shelf, and the importance of topography. East of Greenland, the EGC flows along the shelf edge from Fram Strait to Cape Farewell, while the EGCC is found at the coast from Sermilik Trough southwards. Off the northeast shelf, the Jan Mayen Current, the East Icelandic Current, and the separated EGC divert shelf waters towards the Nordic Seas. On the southeast shelf, the deep Sermilik and Kangerdlussuaq fjords divert part of the EGC towards the coast. At Cape Farewell, the EGC extends over Eirik Ridge, bringing shelf waters off-shelf. The mean velocity of the EGC and EGCC, about 0.5 $m.s^{-1}$, is of similar magnitude than observed at mooring sections (e.g Le Bras et al 2018), and consistent with observations from drifter data (Duyck and De Jong 2021).

The low-resolution LL model is not able to adequately represent these narrow boundary currents (Figure 2F). The EGC is represented as a slow, wide flow, with a mean speed that does not go over $0.15m.s^{-1}$. Details of the circulation over the shelf are not represented, nor the Jan Mayen Current. A weak flow branches off the shelf just north of Iceland, that could be identified with the East Icelandic Current. Increasing the resolution from 1° to 0.25° improves the circulation significantly. In the medium-resolution model, the shelfbreak EGC is well defined, and its velocity is comparable to GLORYS (Figure 2I). Though, bifurcations of the EGC towards the coast upstream of the deep Sermilik and Kangerdlussuaq troughs are visible, there is no distinction between the shelfbreak EGC and the EGCC. The two are merged into one wide current. Off the northern part of the shelf, the JMC and EIC can be identified, but they are wider and weaker than in GLORYS. Additionally, there is a current off the southeast shelf (possibly the Irminger Current) that is not present in GLORYS. Increasing resolution further to 0.12° allows the model to resolve the narrow currents to a close approximation of what is seen in GLORYS (Figure

2L). The EGCC is clearly visible as are the East Icelandic Current and Jan Mayen Current. The strength of the currents appears to be overestimated when compared to GLORYS (Figure 2C), especially around southern Greenland and on the northeast shelfbreak around 75°N.

5.3.2 Mean salinity, sea ice concentration and mixed layer depth

The circulation is strongly improved by each increase in resolution shown here. We then compare the salinity, sea ice cover and mixed layer depths in GLORYS and HadGEM3 at three resolutions. An adequate representation of both salinity and sea-ice is important to correctly represent convective mixing in ocean models. Through additional freshwater at the surface, salinity can strongly increase stratification and thereby inhibit convection, while sea ice can both affect the location of (thermally driven) convection as it isolates the ocean from atmospheric heat fluxes, and create additional strong heat loss on the sea-ice edge as cold air suddenly reached open water (Våge et al 2018). The first two columns of Figure 2 show the mean salinity in the first 200m, mean sea ice coverage (black contours) and mean mixed layer depth (white contours) in GLORYS and the three resolutions of HadGEM3, for the summer months (first column) and the winter months (second column).

In the GLORYS reanalysis, the seasonal cycle of the EGC salinity is clearly visible down to Sermilik Trough, with lower salinities in summer compared to winter (Figure 2A-B). South of Sermilik Trough, salinities below 33 are only found in the EGCC. The JMC and EIC are seen to bring the freshwater offshore into the Greenland and Iceland Seas, especially in summer. The Labrador Sea has much lower upper ocean salinities than the rest of the Subpolar Gyre likely due to eddy shedding off the west Greenland coast (Lilly et al 2003, Chanut et al 2008). The Irminger Sea has a high interior salinity, with some fresher waters from the Labrador Sea extending into the Irminger gyre. Sea-ice in GLORYS extends over the western Greenland Sea in winter, but is confined to the (inner) shelf on southeast Greenland. In the Labrador Sea, most of the ice is found on the western side, where cold Canadian wind meet fresh water from Davis Strait and Baffin Bay.

In the low-resolution model, a seasonal cycle in salinity is represented but the band of low salinity wrapping around southern Greenland is too wide (Figure 2D-E). The wide offshore flow north of Iceland visible in the circulation map transport fresh shelf waters into the Nordic Seas. The Labrador Sea is fresher than observed, and lower salinity waters also enter the Irminger Gyre. The sea-ice is somewhat underrepresented over the Greenland Sea, but the offshore branch north of Iceland brings sea ice into the Iceland Sea. Sea ice is overrepresented along the southern shelf and in the Labrador Sea. In the medium-resolution model, the salinity front between the shelf and interior seas is better represented (Figures 2G-H). The Greenland and Iceland Seas are much fresher than GLORYS, apparently the result of strong export of freshwater in the JMC and EIC. This is especially true in summer, due to the lower shelf salinities. The Labrador Sea and

Irminger Sea are more saline in MM than in GLORYS and LL. Sea-ice is strongly overrepresented in the Greenland and Iceland Seas, possibly linked to the low salinities. In the high-resolution model, the salinity is too high throughout the domain shown here (Figure 2J-K). The EGCC and EGC are too saline, and the fresher waters are constrained at the coast, especially in the southern part of the shelf. The JMC and EIC are still exporting freshwater offshore, but less than in the MM model. The Labrador Sea and Irminger Sea are too saline compared to GLORYS and low salinity waters are too constrained at the coast.

In general, the higher resolution models show a more saline western SPNA than the lower resolution model. In the southern part of the shelf, the low-resolution model is not able to well represent the sharp front between the shelf and interior seas, which may contribute to the Irminger and Labrador Seas being much fresher in LL than in the two other resolutions and inhibit winter deep convection in the subpolar gyre (Figure 1C). In MM, the export of fresh shelf waters to the Nordic Seas via the JMC and EIC is stronger than in GLORYS, which leads to a too fresh upper layer, and may contribute to the too extensive sea ice cover. The strong stratification of the upper layer and sea ice cover prevents deep convection in the Nordic Seas (Figure 1D-E and Figure 2F-G). The HH model shows deep convection both in the Nordic Seas and the subpolar gyre. However, other issues occur at that resolution, as waters over the shelf are much saltier in GLORYS, and too constrained at the coast, likely preventing exchanges of fresh waters with interior seas. For all these models and in all areas, the mean winter mixed layer depth is much too deep, as for CMIP models more generally (Heuzé et al 2021).

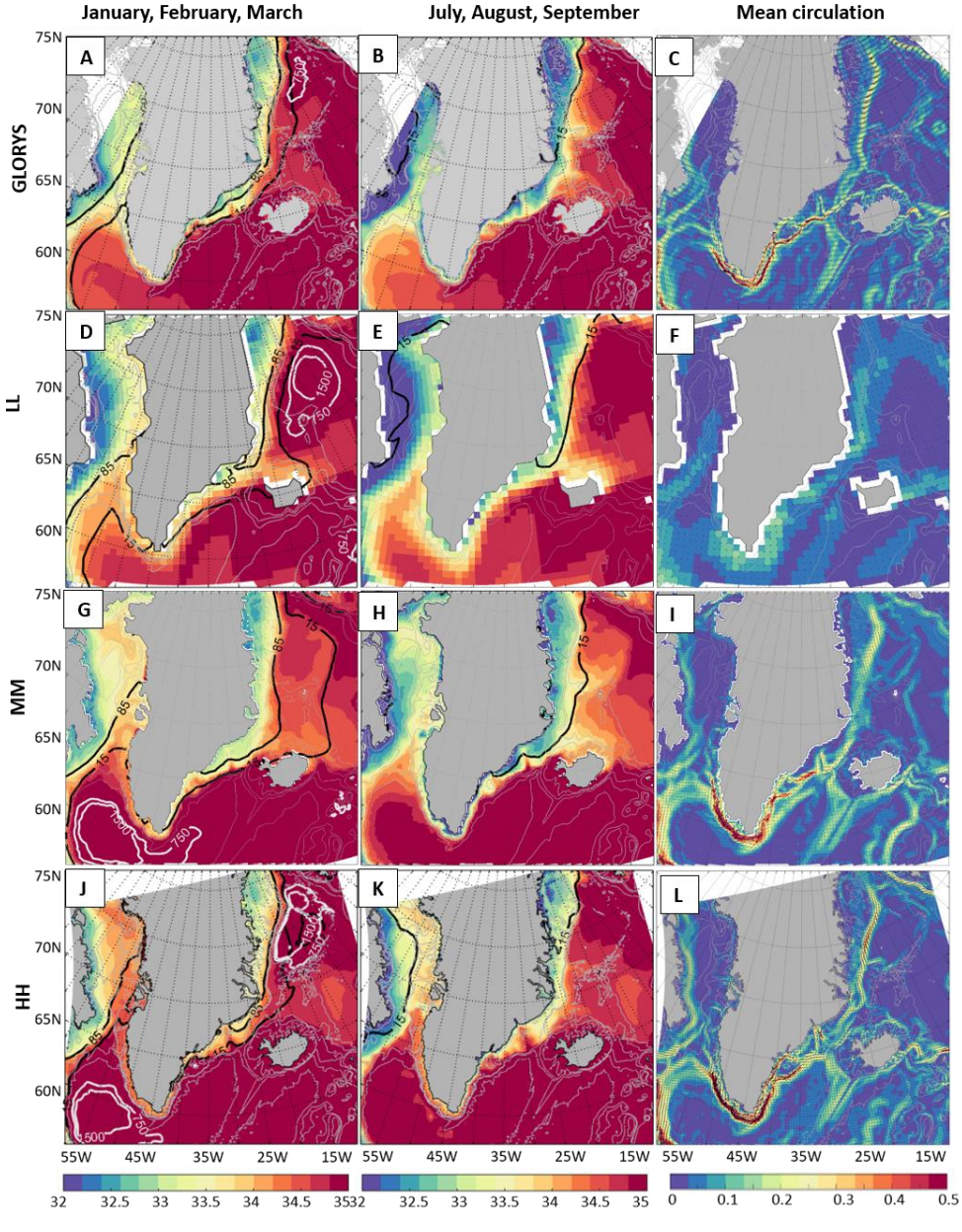

***Figure 5.2**: **A, D, G, J.** Mean salinity in the first 200m, sea ice concentration at 15 and 85 %, and mixed layer depth at 750 and 1500m during winter (January, February, March) for GLORYS and HadGEM3 LL, MM and HH. **B, E, H, K**. Same for summer (July, August, September). **C,F,I,L.** Mean circulation at 200m in GLORYS and HadGEM3 LL, MM and HH.*

5.3.3 Mean winds

The wind fields around Greenland (Figure 3) are particularly important to both the shelf circulation and convection. The negative wind stress curl over the Irminger Sea contributes to the cyclonic Irminger gyre, which brings dense waters upwards and preconditions the water column for convection (De Jong et al 2012). Strong Tip Jets at Cape Farewell creates large (as much as 800 $W.m^{-2}$) ocean heat fluxes driving convection in the gyres (Pickart et al 2003). These same Tip Jets can be conducive to freshwater export from the southeast Greenland shelf (Duyck et al. 2022). At Fram Strait, northerly winds, in particular cyclones, are important for the flow of sea ice from the Arctic Ocean to the EGC (Brümmer et al 2001, Smedsrud et al 2011, Wei et al 2018). Over much of the rest of the east Greenland shelf, the topography of Greenland drives strong and consistent north-easterly winds that act to constrain waters towards the coast (Moore and Renfrew 2005, Harden et al 2011).

Mean winds from the ERA5 product shows strong North-Easterly winds over the shelf from 60 to 71°N and weaker north-easterly winds from 71 to 75°N (Figure 3A). At Cape Farewell, the mean wind field shows north-westerly winds, due to north-easterly and westerly winds alternating in the region. The polar wind distribution shown in the top left corner of Figure 3A and computed from ERA5 3h winds in the Cape Farewell region (black box) shows that 37% of winds are westerlies, 32% north-easterlies, and 1 % of these are stronger than 17m/s, the threshold for gale force winds, used by Duyck et al 2022 to define Tip Jets.

Since the scales in the atmospheric circulation are much larger than in the ocean, the differences between the three models are less stark. The pattern leading to negative wind stress curl over the Irminger Sea is seen in all three models, as are the barrier winds along the eastern shelf. Winds over the eastern shelf are closest to ERA5 in the MM model, apart from the Cape Farewell area (Figure 3C). The LL model shows too strong mean winds north of Denmark Strait and too weak close to Cape Farewell (Figure 3B). In the HH model, the mean winds over the eastern shelf are overall stronger than in ERA5 but show a very similar pattern (Figure 3D).

The variability of the winds over the shelf is well represented in all models. In particular, all resolutions of HadGEM3 represent both westerly winds and north-easterly winds in the Cape Farewell region, including stronger manifestations of these wind events (Figure 3, polar wind distribution plots). In LL, the winds are slightly less bidirectional than in ERA, and generally weaker: only 0.6 % of westerly and north-easterly wind events reach $17m.s^{-1}$. In MM, the two wind patterns are clearer than in LL, and occur a similar percentage of time. Westerly wind events above $17m.s^{-1}$ take place 1% of the time, and 2% for north-easterly winds. In HH, westerly winds occur more often than north-easterly winds (40% against 27%), and strong wind events are found more often than in ERA5 and MM (respectively 3 and 2% of the time for westerlies and north-easterlies).

Overall, the good representation of wind patterns at all resolutions is encouraging for the representation of the influence of wind on either driving or limiting exchanges at the east Greenland shelf.

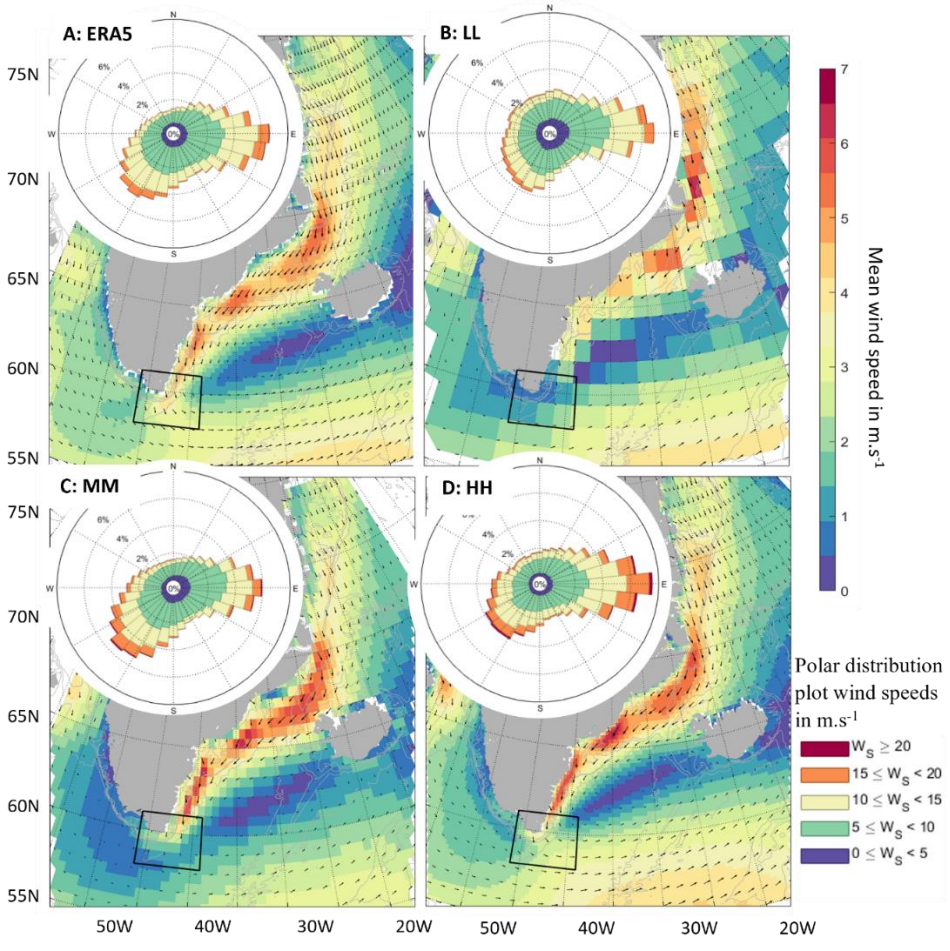

Figure 5.3: A. *Mean winds computed from monthly ERA5 wind fields, and polar wind distribution plot for 3-hour winds averaged over the Cape Farewell region. The polar wind distribution plot is a histogram of the occurrence frequency of winds in a given direction, with colors indicating the strength of these winds as described in the legend in the bottom right.* ***B.*** *Same with LL model.* ***C.*** *Same for MM model.* ***D.*** *Same for HH model.*

5.4 Exchanges between the east Greenland shelf and interior seas

5.4.1 Export of liquid freshwater and sea ice from the shelf to the interior basins

The maps in Figure 2 showed large differences in salinity off the east Greenland shelf between the three resolutions of HADGEM3. Here, we show the results from the calculation of export across the boundary that separates the shelf from the interior basins, as described in the methods and illustrated Figure 1B. In the following, we discuss the mean liquid volume transport (Figure 4A), liquid freshwater transport (Figure 4B) and sea ice transport (Figure 4C) across the boundary for each model resolution.

In the low-resolution model, volume transport across the boundary is weak everywhere and does not show a lot of geographical differences along the boundary, which is consistent with the broad and slow flow along the shelfbreak (Figure 2F). This is contrary to the MM and HH models, that show intensified transport in distinct areas. From north to south: Near Fram Strait, a region of onshore transport is visible in both models, likely corresponding to the recirculation of the West Spitsbergen Current (Marnela et al 2013). In the MM model, offshore transport takes place over a wide region between 78 and 72 °N, while the HH model only shows a narrow band of increased offshore transport corresponding to the Jan Mayen Current. Offshore transport due to the EIC is clearly visible both for MM and HH and is of a similar magnitude than the transport observed further north. Both models show increased offshore transport upstream of Denmark Strait, and on-shelf transport just downstream of Denmark Strait. Over the south-eastern shelf they show off-shelf transport, that peaks at Cape Farewell. The computation of Ekman transport shows that in all three models winds tend to constrain surface waters towards the shelf over most of the boundary. The exception is Cape Farewell, where the wind regime is more favorable to export (Duyck et al 2022). The small differences between the Ekman transport in the three models suggest that differences in the mean transport between the models are not related to different representations of winds along the shelf but are primarily ocean driven.

The freshwater transport across the boundary is similar to the volume transport but its magnitude is modulated by the salinity of the waters. Figure 4B shows both freshwater transport across the boundary, and the mean salinity at the boundary. For each resolution, we used the mean salinity in the central Irminger Sea as reference salinity to account for salinity biases in each model. In the LL model, only weak freshwater transport is observed across the boundary compared to the two other model resolutions, which is consistent with the weak volume transport. The exception are increases in freshwater transport upstream of Denmark Strait and at Cape Farewell. In the MM and HH models, the signature of the JMC, EIC and separated EGC are visible as peaks in freshwater export over the northern part of the shelf. The freshwater export is strongest in the MM model, due to the shelf being fresher at that resolution. Freshwater transport across the boundary south-east of Greenland is very limited in MM and HH and the peak in freshwater export at Cape Farewell observed in LL is absent, despite off-

shelf volume transport in that area (Figure 4A). This is likely due to fresh waters being constrained close to the coast over the south-east shelf in both the MM and HH model.

Sea ice transport across the boundary mostly takes place in the northern part of the shelf, which is due to the sharp decrease in sea ice concentration at Denmark Strait (Figure 4C). In the LL resolution, sea ice export takes place over most of the north-east shelf. In the MM resolution, we find peaks of sea ice export at the latitude of the JMC, the EIC and just upstream of Denmark Strait. In the HH model, the export of sea ice is much lower than in MM and LL, due to the much lower sea-ice concentration in the area.

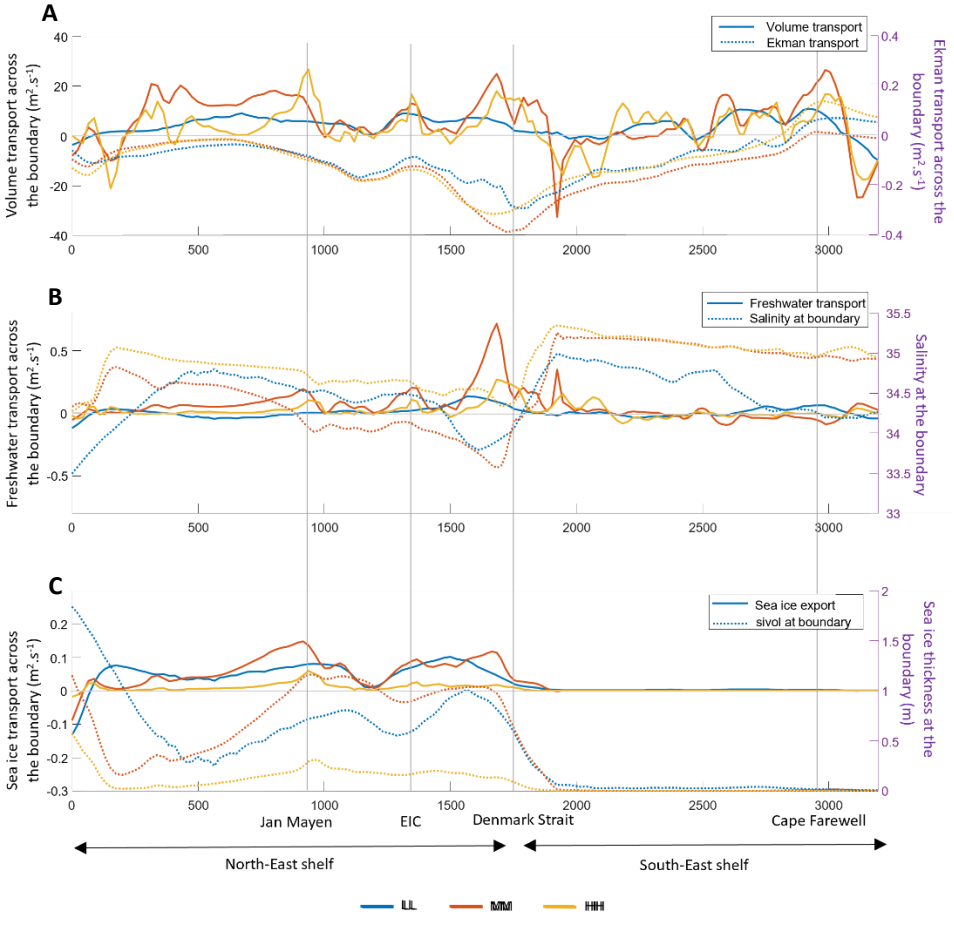

Figure 5.4: A. *Mean volume transport across the boundary in the first 200m (full line) and mean Ekman transport across the boundary (dashed line).* ***B.*** *Mean freshwater transport across the boundary in the first 200m (full line) and mean salinity at the boundary in the first 200m (dashed line).* ***C.*** *Mean sea ice transport across the boundary (full line) and mean sea ice effective thickness at the boundary. For each parameter, the results are shown for the three resolution: LL in blue, MM in red and HH in yellow. The lines show the position of topographic features along the boundary.*

Most of the sea ice and freshwater export across the boundary takes place north of Denmark Strait (Table 2), even when accounting for the longer boundary north of Iceland (1750km from Fram Strait to Denmark Strait, 1400 km from Denmark Strait to Cape Farewell). The stronger freshwater transport north of Denmark Strait is due to stronger volume transport via the JMC, EIC and separated EGC, and to the fresher northern shelf. The stronger sea ice transport is due to the scarce amount of sea ice south of Denmark Strait. The MM model shows the strongest offshore transports north of Denmark Strait (Table 2). Offshore volume transport in MM is twice as strong as in LL and HH. Offshore freshwater transport in MM is 14 times stronger than in LL and three times stronger than in HH. This suggests that the enhanced freshwater export towards the Nordic Seas in MM is both due to more export of shelf waters towards the interior seas, and to a fresher northern shelf compared to the mean salinity of the Irminger Sea.

	LL (Sref=34.7)	*MM (Sref=34.9)*	*HH (Sref=35)*
Volume (Sv)			
North-East	8.00	15.4	7.20
South-East	4.49	5.10	3.18
Freshwater (mSv)			
North-East	12.3	173	50.3
South-East	3.49	11.4	12.9
Ice (mSv)			
North-East	89.2	107	21.5
South-East	3.61	3.73	0.46

Table 2 Mean volume, freshwater and sea ice transport across the north-east and south-east boundary, integrated over these segments and over the first 200m.

5.4.2 Variability of export and impact on interior seas

We now take a closer look at the interannual and seasonal variability in freshwater and sea ice export in the northern and southern regions. Figure 5 shows the evolution of freshwater transport, sea ice transport, surface freshwater fluxes and salinity in the interior seas and at the shelf, north (Figure 5A) and south (Figure 5B) of Denmark Strait.

The Nordic Seas are most saline in the LL model and freshest in the MM model. All three models show an increasing trend in the salinity of the upper layer over the 25-year record. There is a strong seasonality, with the summer freshening reaching depths of 30m (LL) to 75m (MM). This summer freshening is strongest in the MM model. By the end of the record, the summer freshening is not as strong, which is visible in all models, but most especially in the LL model. In the following, we investigate whether the changes

in salinity of the upper layer of the Nordic Seas are related to freshwater and sea-ice export from the shelf, are driven by surface freshwater fluxes (precipitation and evaporation), or whether they need to be explained by another process, such as changes in salt import related to the inflow of Atlantic water.

Over the whole record, the MM (LL) model is both the freshest (saltiest) model in the Nordic Seas and the one with strongest (weakest) freshwater transport. This suggests an influence of fresh shelf waters on the Nordic Sea. It is less clear whether the variability in liquid freshwater transport throughout the record leads to changes in the salinity of the Nordic Seas. The interannual variability in freshwater transport across the boundary shows a correlation with the salinity in the upper layer of the Nordic Seas, strongest in the higher resolution models (Figure 6A, correlation coefficients: LL: 0.5, MM: 0.62, HH: 0.68, significant at 95%). However, there is no trend in freshwater export towards the Nordic Seas in any of the models that could explain the increasing salinity of the Nordic Seas. There is also no correlation between the salinity in the Nordic Seas and salinities over the northern part of the shelf. In LL, the first 200m of the shelf freshen between the beginning and the end of the record, in MM the salinity is stable during that period, while it first increases, and then decreases in HH (Figure 5A). This suggests that even though there is a connection between the shelf and the Nordic seas, variations in salinity at the shelf did not have a strong impact on the mean salinity in the Nordic Seas over the 25 years of these model records. This does not preclude that large salinity anomalies over the shelf could have a larger effect on the salinity of the Nordic Seas in these models.

The sea ice transport into the Nordic Seas strongly decreases in all three models, consistently with the diminishing sea ice concentration over the shelf. This reduction in sea-ice is the consequence of the increased CO2 forcing in the historical period. While the decline in sea-ice is visible for all model resolutions, there is a slower decrease in the MM model, which still shows a strong seasonality in sea ice export by the end of the record (Figure 5A). A reduction in sea ice input and subsequent sea ice melt in the interior basin in summer could be one of the drivers of the increased salinity and reduced summer freshening in the upper layer of the basin. This is supported by strong correlations between sea ice transport and upper layer salinities in the Nordic seas (Figure 6B, LL: 0.82, MM:0.76, HH:0.78, significant at 95%).

Upper layer salinity in the basin may also vary due to changes in net precipitation. Both precipitation and evaporation into the Nordic seas increased nearly equally during the record, in all models. This leads to no net trend in the net input of freshwater from surface freshwater fluxes to the Nordic Seas. The interannual variability of freshwater input from precipitation is not correlated with the salinity in the Nordic seas (Figure 6C). Precipitation may however play a role in the mean state of each model: MM is freshest in the Nordic seas and has most net freshwater input from precipitation in that area. The reverse is true for LL, that is the saltiest in the Nordic Seas. This suggests that P-E, like freshwater export, may play a role in the mean salinity of the Nordic Seas upper layer, but not in its variability.

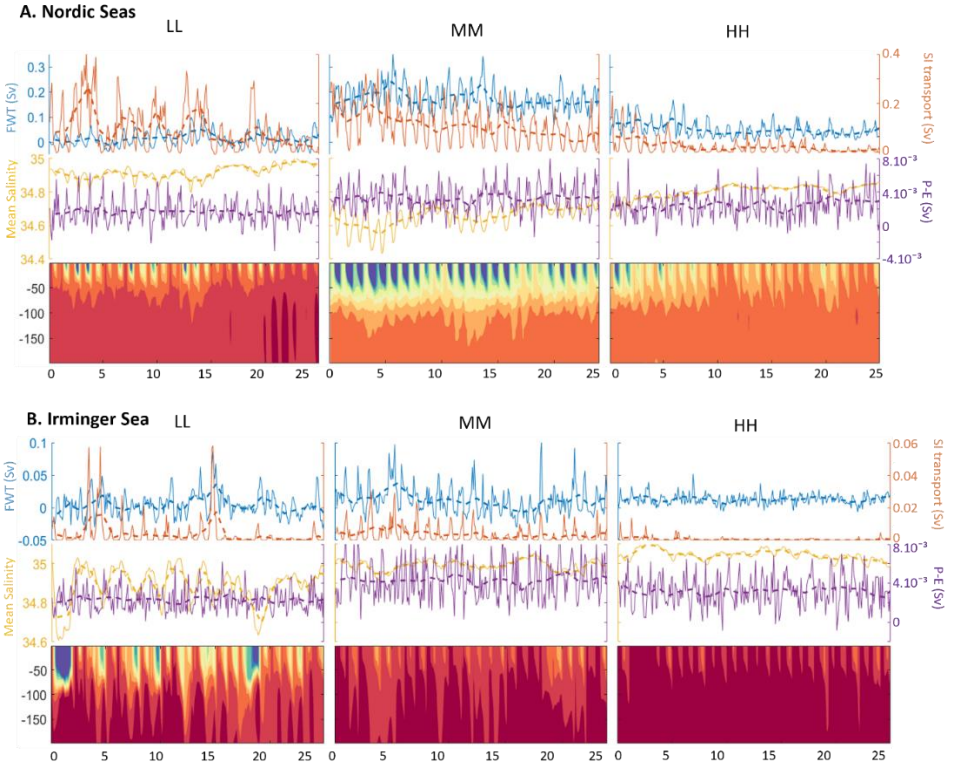

Figure 5.5: A. *Evolution of freshwater transport (blue) and sea ice transport (red) at north-east boundary, precipitation – evaporation (purple) and mean salinity in the first 200m (yellow) in the Nordic Seas, evolution of salinity in the first 200m, in the Nordic Seas.* ***B.*** *Same for the south-east boundary and the Irminger Sea. The Nordic Seas and Irminger Seas are as defined Figure 1A. Dashed lines are yearly means.*

5

No trend comparable to the one in the Nordic Seas is visible in the Irminger Sea. There is however a strong interannual variability in the salinity of the upper layer, that dominates the seasonal variability. The upper layer of the Irminger Sea is freshest in the LL model, with a strong freshening of the first 100m in some summers (Figure 5B). This seasonality is also present in the MM and HH models but much more limited.

Freshwater transport across the south-east boundary towards the Irminger Sea shows no trend. In the HH model, freshwater export is very weak, which is due to fresh shelf waters being too far inshore and the EGC being too saline (Figure 2J-K). We find a weak correlation for interannual variability between changes in freshwater transport and salinity in the Irminger Sea for the MM model and no correlation for the LL and HH models (Figure 6D). Moreover, while for the Nordic Seas, the models with highest (lowest) mean freshwater export were also the freshest (saltiest), this relation does not

hold for the Irminger Sea, which suggests that freshwater export from the southern shelf plays no significant role in the salinity of the Irminger Sea.

There is only sparse ice cover over the southern part of the shelf, even in winter, which leads to very little sea-ice export towards the Irminger Sea. We can still observe some seasonality, interannual variability and a decreasing trend in sea ice transport, but years with strong sea ice transport are not associated with summer freshening as they are for the Nordic Seas (Figure 6E).

Similarly as for the Nordic Seas, both precipitation and evaporation into the Irminger Sea increased throughout the record, leading to no trend in net freshwater input from the atmosphere. However, while in the Nordic Seas, the freshest model was also the model with most surface freshwater fluxes, in the Irminger Sea, the LL model is both fresher than MM and HH and has less freshwater input from the atmosphere (Figure 6F).

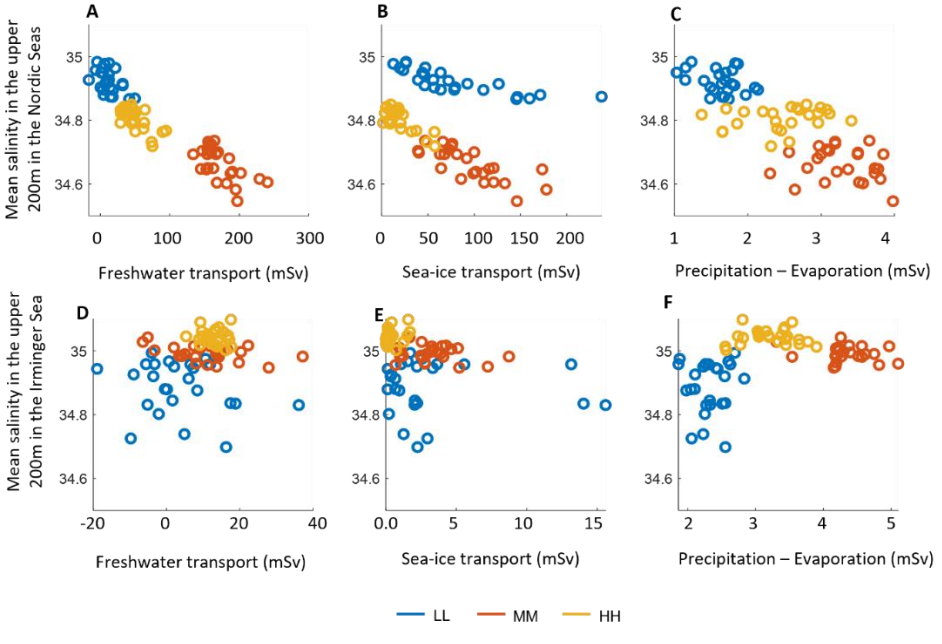

Figure 5.6 *Correlation between the evolution of salinity in the upper 200m of the Nordic Seas (A-C) and Irminger Sea (D-F), freshwater transport and sea ice transport across the North-East or South-East boundary, and precipitations.*

5.5 Summary and discussion

This study investigated exchanges between the east Greenland shelf and the Irminger and Nordic Seas in three different resolutions of the HadGEM3 global coupled climate model. We analysed the differences in circulation and water properties in the upper 200m and computed freshwater and sea ice export from the shelf towards the interior. In the following we summarize the differences between the three resolutions, discuss the most important drivers of transport variability, and some possible implications for future projections of freshwater input to the SPNA and the overturning circulation.

The LL model represents the EGC as a broad and weak flow, leading to weak transport towards the Nordic Seas, which could explain why this region is the saltiest at that resolution. The Labrador and Irminger Sea are the freshest in the LL model and both the upper layer stratification and the sea ice cover prevent deep convection in these areas. This could, among others, be due to the poor representation of the shelf circulation and the fresher shelf waters extending too far off the shelfbreak. In the MM model, the Nordic Seas are fresher than in the other resolutions. One likely cause is the too strong freshwater and sea ice flux from the east Greenland shelf to the Nordic Seas, that is stronger in MM than in LL and HH (Table 2, Figure 6 A-B). The resulting strong stratification in the Nordic Seas, combined with the too extensive winter sea ice, prevents deep convection in the region. MM shows only limited freshwater export from the shelf south of Denmark Strait towards the Irminger Sea. The HH model represents the mean circulation best, with well-defined boundary currents, a distinct coastal current, and a more realistic EIC and JMC. The Nordic Seas are more saline in HH than in the MM model, sea ice is not as extensive, and deep convection takes place both in the Nordic Seas and in the Labrador Sea. However, south of Denmark Strait fresh shelf waters are constrained too close to the coast compared to observations (Le Bras et al 2018, Sutherland and Pickart 2008), which makes it unlikely for that model to realistically represent freshwater export towards the Irminger Sea.

Coupled climate models with a coarse resolution (>= 1°) cannot accurately represent the narrow boundary currents over the Greenland shelf, which is well illustrated by the LL model from this study. Increasing the resolution to 0.25° allows for a better representation of boundary currents, but these models are eddy-permitting rather than eddy resolving at high latitudes, which does not allow for a proper representation of shelf-interior sea exchanges. In the 0.25° MM model investigated here, we find unrealistically high freshwater fluxes from the north-east shelf towards the Nordic Seas, that seem to contribute to the absence of deep convection in that region. As more coupled climate models are developed at this resolution, it would be useful to investigate whether this behaviour is found in other 0.25° coupled models. The HH model does seem to do better in the Nordic Seas and the Labrador Sea, however it still shows too deep convection in these areas, as is the case for most CMIP6 models (Heuzé et al 2021). Furthermore, the HH model is too saline overall in the SPNA, and over the east Greenland shelf the fresh waters are only found near the coast (what would correspond to the EGCC), limiting possible export towards the interior seas. The HH model, with a

resolution of 0.12° may still not be enough to fully resolve processes likely to bring fresh shelf waters towards the interior (Swingedouw et al 2022, Martin et al 2023).

Higher resolution models tend to show a stronger mean overturning circulation, and a stronger weakening in future projections (Hirschi et al 2020, Jackson et al 2020, Roberts et al 2020). In particular, Roberts et al 2020 showed that HadGEM3 HH has a stronger AMOC than the MM version in the historical period, and that the two have a similar rate of weakening until 2050, that is itself stronger than the weakening in LL. Jackson et al 2020 suggested that the higher reduction in overturning strength in the MM model compared to LL could be due to the MM model only convecting in the Subpolar Gyre, causing the overturning strength to be more impacted by the reduction of deep water formation in that area. The HH model however convects in both the Nordic Seas and the Subpolar Gyre, regions, and shows a similar weakening rate than MM, so there must be other causes contributing to the variations in AMOC weakening rate at different resolutions.

In the three resolutions of Hadgem3 investigated here, most of the exchanges east of Greenland take place north of Denmark strait, towards the Nordic seas, which is consistent with observations (Dickson et al 2007). In MM and HH, sea ice and freshwater export have a similar magnitude, but the export of sea ice rapidly decreases towards the end of the record, likely due to the decrease in sea ice cover at the shelf. This decrease in sea-ice export is concurrent with increasing salinities in the upper 200m of the Nordic Seas, and could have contributed to this increase, though variability in upper layer salinity might also have other sources, such as inflowing Atlantic waters (Glessmer et al 2014). On the contrary, we found no relation between the salinity at the shelf and in the Nordic seas during the 25 years of the record. In LL the increase in salinity in the Nordic Seas was concurrent with a freshening of the shelf. In the MM and HH models, which show the most exchanges from the shelf to the Nordic Seas, there is no strong variability in salinity over the shelf. It is therefore unclear whether a large salinity anomaly over the shelf caused by the accelerated melt of Greenland or a release of the Beaufort Gyre (Lin et al 2023) could lead to a freshening of the Nordic Seas in these models.

Sea-ice is more easily fluxed off-shelf than surface shelf waters and could represent an important part of the freshwater flux from the shelf to the Nordic Seas (Dodd et al 2009, Duyck et al 2022). In the future, more liquid freshwater and less sea ice is predicted to enter the shelf via Fram Strait (Haine et al 2015, Wang et al 2022). If sea ice is indeed more easily exported to the Nordic Seas than liquid freshwater, a freshening of the shelf happening concurrently with a reduction of sea ice cover might not lead to increasing fluxes to the Nordic seas in the short term. Moreover, the retreating sea ice cover could affect the location and intensity of deep water formation in the Nordic Seas by modifying air-sea heat fluxes (Moore et al 2015, Moore et al 2022). In this study, we found that both sea ice cover and sea ice export towards the Nordic Seas varied depending on resolution, with the medium resolution model showing both too much ice export and too much ice cover in the Nordic Seas. Studies with a wider range of models would be necessary to verify whether this behavior is also found in other medium resolution

models, and what is the impact of the representation of sea ice in the Nordic Seas on AMOC projections.

Acknowledgements and Open Research

The EGC-DrIFT project is financially supported by the Innovational Research Incentives Scheme of the Netherlands Organisation for Scientific Research (NWO) under grant agreement nos. 016.Vidi.189.130.

The HadGEM3 fields used throughout the study are available from the Earth System Grid Federation (ESGF) node (https://esgf-index1.ceda.ac.uk/). We also make use of the EU Copernicus Marine Service GLORYS ocean reanalysis (Copernicus Marine Service 2023) and the ERA5 hourly and monthly datasets from the Copernicus Climate Change Service (Hersbach et al 2023a, Herbach et al 2023b). We used bathymetry from the ETOPO2022 product (NOAA 2022)

Chapter 6

Conclusions and research outlook

Illustration: SVP and Carthe drifters floating behind the Pelagia after deployment at Cape Farewell in 2020. Picture : Fleur Wellen.

The work carried out in this thesis has provided new observational insights of the surface circulation over the east Greenland shelf, and exchanges between the shelf and neighboring seas. The drifters deployed as part of the EGC-DrIFT project contributed novel observational data in previously poorly covered areas such as the coastal part of the east Greenland shelf and the Blosseville Basin and Denmark strait region. In addition to this new drifter dataset, I used existing drifter data, ocean and atmospheric reanalyses, satellite data, a high-resolution regional model, and results from a coupled climate model, to understand what drives exchange processes at the shelf, and discuss implications for the future of deep convection east of Greenland.

In the following, I present what I learned from this work, and sketch future research outlooks.

6.1 Conclusions

The EGC and EGCC have two distinct velocity cores but they interact as they flow downstream, steered by the complex topography of the east Greenland shelf. This is most notably the case at Kangerdlussuaq Trough, Sermilik Trough and Cape Farewell.

For all five drifter deployments conducted as part of EGC-DrIFT, most drifters were deployed in the shelfbreak core of the East Greenland Current. However, as they were advected downstream, drifters, and in particular the SVP drifters, were brought closer to the coast, and most entered the coastal current before reaching Cape Farewell.

The deep Sermilik (Chapter 2) and Kangerdlussuaq (Chapter 4) troughs both drive bifurcations of the shelfbreak current into the trough. Part of the shelfbreak current then joins the EGCC, and part re-enters the EGC past the trough. Exchanges also take place between the two current cores as they round Cape Farewell. In Chapter 2, drifters in the EGCC on the eastern side of Greenland were found to be equally likely to enter the WGC than the WGCC west of Greenland. Such exchanges between waters from the shelfbreak and the fresher coastal core at Cape Farewell could influence how much freshwater is exported into the Labrador Sea west of Greenland (Chapter 4).

Only minimal advective export of shelf waters towards the Irminger and Nordic Seas was observed. However, small scale and intermittent exchanges driven by wind and eddies were identified in a few locations, that could lead to mixing of fresh shelf waters with waters from the interior seas.

Only limited export of surface drifters was observed on the eastern side of Greenland, which suggests that large leakages of freshwater is unlikely. Most of the drifters deployed at the east Greenland shelfbreak followed the EGC and EGCC until Cape Farewell and entered the west Greenland shelf. This is in contrast with the western side of Greenland, where more than 1/3 of the EGC-DrIFT drifters that entered the west Greenland shelf were exported into the Labrador Sea.

Two caveats should be mentioned here: Only limited drifter data is available north of Iceland, which likely is one of the reasons for the Jan Mayen Current and East Icelandic Current not appearing as export pathways from our drifter dataset. Most of the drifter data was collected during summer months, including when adding drifters from other datasets. Exchange mechanisms are likely different in winter.

Chapter 4 identified areas of enhanced exchanges at the shelfbreak, that can be driven by winds, eddies, or the topography-driven mean circulation. Westerly wind events at Cape Farewell can drive fresh shelf waters off-shelf. This was first observed by the export of five CARTHE drifters from the south-east Greenland shelf to the Irminger Sea (Chapter 2), and confirmed with a high resolution model of the region (Chapter 3). Using the model winds and salinity fields as well as a particle release, I showed that Tip Jet events, strong winter westerly wind events, can drive shelf waters towards the Irminger Sea, but also that weaker westerly events can contribute to some extension of fresh waters off-shelf. The use of additional drifter data showed that drifters are indeed brought offshore during such events (Chapter 4).

Though liquid freshwater export is limited east of Greenland, sea ice can potentially play an important role in driving freshwater off-shelf.

Sea ice reacts differently to wind forcing than surface waters. At Cape Farewell, winter Tip Jet events were associated with the steering of sea ice towards the Irminger Sea (Chapter 3). There is only limited sea-ice cover over the south-east Greenland shelf and sea ice export could be most important from the northeastern shelf to the Nordic Seas. The model study of Chapter 5, that used the HadGEM3 coupled models at low, medium and high resolution, suggested that decline in sea ice export might be a significant driver of upper salinity changes in the Nordic Seas. As less ice and more liquid freshwater is exported through Fram Strait, it is necessary to understand the distinct processes that lead to their export to estimate how much fresh shelf water will enter the Nordic Seas in the coming decades.

Mechanisms that drive or inhibit export at the east Greenland shelfbreak are small scale, and some are intermittent. They are unlikely to be well represented in the current generation of global coupled climate models.

On the eastern side of Greenland, fresh polar waters from the Arctic and Greenland runoff first enter the Greenland shelf and are transported southwards by the East Greenland Current. The EGC is a narrow boundary current, that cannot be well represented in 1 degree resolution models (Chapter 5). In these models, the EGC is too wide, too slow, and the front between shelf and interior waters is not sharp enough. However, even though increasing the resolution to 0.25° or 0.12° allowed a better representation of the shelf circulation and the hydrographic front at the shelfbreak in HadGEM3 models, these resolutions might not be sufficient to realistically resolve

exchanges at the shelfbreak. Moreover, other biases prevented a realistic simulation of freshwater export in the medium and high-resolution model: In the 0.25° model, exchanges between the shelf and the Nordic Seas are too strong, contributing to unrealistically fresh Nordic Seas. In the 0.12° model, fresh and cold waters are constrained to close to the coast over the south-eastern shelf compared to observations. This and would prevent freshwater export to the Irminger Sea, even where and when cross-shelf exchanges take place.

6.2 Research outlook

The impact of sea ice export from the east Greenland shelf into the Nordic seas should be further investigated with observational datasets

As summarized in the previous section, chapters 3 and 5 showed that sea ice could be a notable driver of freshwater export, especially north of Denmark Strait. A better understanding of sea-ice versus liquid freshwater fluxes to that region is important because of current and future reduction of sea ice export via Fram Strait and of sea ice cover over the East Greenland shelf. Future research could focus on investigating sea ice export at the shelfbreak, how much sea ice from the Arctic reaches and melts in the Nordic seas, and what is its impact on convection in that region.

In Chapter 3, I showed that Tip Jets at Cape Farewell are associated with a veering east of the sea ice present on the shelf. This was only observed with the MODIS imagery, and showed very fine patterns, with sea ice breaking up as it veers off-shelf. This response of sea-ice was not visible using sea ice concentration products from satellite data, likely due to the ice being very broken up. In-situ observational datasets such as the ice bound buoys from the International Arctic Buoy Program program (Rigor et al 2002) could also be used to investigate how winds can drive sea ice export into the Greenland and Iceland Sea.

Freshwater export on the western side of Greenland and pathways through the subpolar gyre

While this study focused on freshwater exchanges between the east Greenland shelf, the Nordic Seas and Irminger Sea, our drifter deployments also provided interesting data on exchanges on the western side of Greenland. Indeed, most of the drifters deployed on the eastern side of Greenland continued downstream into the West Greenland Current, and part of them were exported into the Labrador Sea (Chapters 2 and 4). Other recent drifter deployments carried out east and west of Greenland, as well as the high density of GDP data west of Greenland allow for a thorough investigation into mechanisms driving freshwater export from the west Greenland shelf into the Labrador Sea.

In this study, I suggest that it is necessary to understand circulation over the east Greenland shelf to investigate how much freshwater is exported west of Greenland into

the Labrador Sea. Indeed, while the meltwater from West Greenland glaciers first enters the WGCC, meltwater from East Greenland glaciers and polar waters from the Arctic has already been mixed over the shelf as they arrive west of Greenland. Moreover, chapters 2 and 4 showed interactions between the coastal and shelfbreak cores as they round Cape Farewell, that could mix the fresher waters from the coast with the waters from the shelfbreak. A better understanding of the future impact of Arctic and Greenland freshwater on the upper salinity of the SPNA interior seas requires a combination of circulation and exchange studies east and west of Greenland.

Impact of freshwater exchanges on deep convection areas

This study focused on pathways for fresh shelf waters from the east Greenland shelf to deep convection regions, and on mechanisms driving cross-shelf exchanges. Further work is necessary to quantify how much freshwater is currently entering deep convection regions via these exchanges at the shelfbreak, and to what extent they impact the properties of deep convection regions. Additionally, the recent freshwater anomaly that circulated in the SPNA from the Labrador Sea (Holliday et al 2020, Bilo et al 2022) provides a good opportunity to understand the impact of a fresher upper ocean and increased stratification on deep convection in the Irminger Sea.

In this study, I investigated cross-shelf exchanges and off-shelf freshwater export under current conditions. If the shelf becomes much fresher in the future, it could lead to stronger fluxes but it is unclear whether this would only be a change of magnitude, or be more complex. A sudden salinity anomaly similar to the one from the 1960s (Dickson et al 1988), for instance associated with the release of the Beaufort Gyre (Proshuntiky et al 2019, Lin et al 2023), could lead to an abrupt freshening of the whole shelf. This would be in contrast with a slower freshening of the shelf due to Greenland melt, that initially affects the EGCC. It is unclear how these two different possible freshening mechanisms might affect freshwater export. Similarly, the presence of more freshwater and less sea ice over the shelf might affect export mechanisms as sea ice and surface freshwater respond differently to forcing.

References

Aagaard, K., & Carmack, E. C. (1989). The role of sea ice and other fresh water in the Arctic circulation. Journal of Geophysical Research, 94(C10), 14485. https://doi.org/10.1029/JC094iC10p14485

Almansi, M., Gelderloos, R., Haine, T. W. N., Saberi, A., & Siddiqui, A. H. (2019). OceanSpy: A Python package to facilitate ocean model data analysis and visualization. Journal of Open Source Software,4(39), 1506. https://doi.org/10.21105/joss.01506

Almansi, M., Haine, T. W. N., Gelderloos, R., & Pickart, R. S. (2020). Evolution of Denmark Strait overflow cyclones and their relationship to overflow surges. Geophysical Research Letters, 47. https://doi.org/10.1029/2019GL086759

Almansi, M., Haine, T. W. N., Pickart, R. S., Magaldi, M. G., Gelderloos, R., & Mastropole, D. (2017). High-frequency variability in thecirculation and hydrography of the Denmark Strait overflow from a high-resolution numerical model. Journal of Physical Oceanography, 47(12), 2999–3013. https://doi.org/10.1175/JPO-D-17-0129.1

Chen, D., M. Rojas, B.H. Samset, K. Cobb, A. Diongue Niang, P. Edwards, S. Emori, S.H. Faria, E. Hawkins, P. Hope, P. Huybrechts, M. Meinshausen, S.K. Mustafa, G.-K. Plattner, and A.-M. Tréguier, 2021: Framing, Context, and Methods. InClimate Change 2021: The Physical Science Basis. Contribution of Working Group I to the Sixth Assessment Report of the Intergovernmental Panel on Climate Change. Cambridge University Press, Cambridge, United Kingdom and New York, NY, USA, pp. 147–286, doi:10.1017/9781009157896.003.

Bacon, S. (2002). A freshwater jet on the east Greenland shelf. Journal of Geophysical Research, 107(C7). https://doi.org/10.1029/2001jc000935

Bacon, S., Marshall, A., Holliday, N. P., Aksenov, Y., & Dye, S. R. (2014). Seasonal variability of the East Greenland Coastal Current. Journal of Geophysical Research: Oceans, 119(6), 3967–3987. https://doi.org/10.1002/2013JC009279

Bakalian, F., Hameed, S., and Pickart, R. (2007), Influence of the Icelandic Low latitude on the frequency of Greenland tip jet events: Implications for Irminger Sea convection, J. Geophys. Res., 112, C04020, doi:10.1029/2006JC003807.

Bakker, P., Schmittner, A., Lenaerts, J. T. M., Abe-Ouchi, A., Bi, D., van den Broeke, M. R., Chan, W. L., Hu, A., Beadling, R. L., Marsland, S. J., Mernild, S. H., Saenko, O. A., Swingedouw, D., Sullivan, A., & Yin, J. (2016). Fate of the Atlantic Meridional Overturning Circulation: Strong decline under continued warming and Greenland melting. Geophysical Research Letters, 43(23), 12,252-12,260. https://doi.org/10.1002/2016GL070457

Bamber, J., van den Broeke, M., Ettema, J., Lenaerts, J., & Rignot, E. (2012). Recent large increases in freshwater fluxes from Greenland into the North Atlantic. Geophysical Research Letters, 39, L19501. https://doi.org/10.1029/2012GL052552

Bamber, J. L., Tedstone, A. J., King, M. D., Howat, I. M., Enderlin, E. M., van den Broeke, M. R., & Noel, B. (2018). Land Ice Freshwater Budget of the Arctic and North Atlantic Oceans: 1. Data, Methods, and Results. Journal of Geophysical Research: Oceans, 123(3), 1827–1837. https://doi.org/10.1002/2017JC013605

Bellomo, K., Angeloni, M., Corti, S. et al. Future climate change shaped by inter-model differences in Atlantic meridional overturning circulation response. Nat Commun 12, 3659 (2021). https://doi.org/10.1038/s41467-021-24015-w

Biló, T. C., Straneo, F., Holte, J., & Le Bras, I. A. (2022). Arrival of New Great Salinity Anomaly Weakens Convection in the Irminger Sea. Geophysical Re473 search Letters, 49 , e2022GL098857. https://doi.org/10.1029/2022GL098857

Böning, C. W., Behrens, E., Biastoch, A., Getzlaff, K., & Bamber, J. L. (2016). Emerging impact of Greenland meltwater on deepwater formation in the North Atlantic Ocean. Nature Geoscience, 9(7), 523–527. https://doi.org/10.1038/ngeo2740

Bourke, R. H., R. G. Paquette, and R. F. Blythe, 1992: The Jan Mayen Current of the Greenland Sea. J. Geophys. Res., 97, 7241–7250, https://doi.org/10.1029/92JC00150.

Bracco, A., J.Pedlosky, and R. S.Pickart, 2008: Eddy formation near the west coast of Greenland. J. Phys. Oceanogr., 38, 1992–2002. https://doi.org/10.1175/2008JPO3669.1

Brakstad, A., K. Våge, L. Håvik, and G. W. K. Moore, 2019: Water Mass Transformation in the Greenland Sea during the Period 1986–2016. J. Phys. Oceanogr., 49, 121–140, https://doi.org/10.1175/JPO-D-17-0273.1.

Broecker, W., Peteet, D. & Rind, D. Does the ocean–atmosphere system have more than one stable mode of operation?. Nature 315, 21–26 (1985). https://doi.org/10.1038/315021a0

Bromwich, D. H., Wilson, A. B., Bai, L., Liu, Z., Barlage, M., Shih, C.-F., et al. (2018). The Arctic System Reanalysis, version 2. Bulletin of the American Meteorological Society, 99(4), 805–828. https://doi.org/10.1175/BAMS-D-16-0215.1

Brümmer, B., Müller, G., Affeld, B., Gerdes, R., Karcher, M. and Kauker, F. (2001), Cyclones over Fram Strait: impact on sea ice and variability. Polar Research, 20: 147-152. https://doi.org/10.1111/j.1751-8369.2001.tb00050.x

Buckley, M. W., & Marshall, J. (2016). Observations, inferences, and mechanisms of the Atlantic Meridional Overturning Circulation: A review. Reviews of Geophysics, 54, 5– 63. https://doi.org/10.1002/2015RG000493

Casanova-Masjoan, M., Pérez-Hernández, M. D., Pickart, R. S., Valdimarsson, H., Ólafsdóttir, S. R., Macrander, A., et al. (2020). Along-stream, seasonal and interannual variability of the North Icelandic Irminger Current and East Icelandic Current around Iceland. Journal of Geophysical Research: Oceans, 125, e2020JC016283. https://doi.org/10.1029/2020JC016283

Centurioni LR, Turton J, Lumpkin R, Braasch L, Brassington G, Chao Y, Charpentier E, Chen Z, Corlett G, Dohan K, Donlon C, Gallage C, Hormann V, Ignatov A, Ingleby B, Jensen R, Kelly-Gerreyn BA, Koszalka IM, Lin X, Lindstrom E, Maximenko N, Merchant CJ, Minnett P, O'Carroll A, Paluszkiewicz T, Poli P, Poulain P-M, Reverdin G, Sun X, Swail V, Thurston S, Wu L, Yu L, Wang B and Zhang D (2019) Global in situ Observations of Essential Climate and Ocean Variables at the Air–Sea Interface. Front. Mar. Sci. 6:419. doi: 10.3389/fmars.2019.00419

Chafik, L., & Rossby, T. (2019). Volume, heat, and freshwater divergences in the subpolar North Atlantic suggest the Nordic Seas as key to the state of the meridional overturning circulation. Geophysical Research Letters, 46, 4799– 4808. https://doi.org/10.1029/2019GL082110

Chanut, J., B. Barnier, W. Large, L. Debreu, T. Penduff, J. M. Molines, and P. Mathiot, 2008: Mesoscale Eddies in the Labrador Sea and Their Contribution to Convection and Restratification. J. Phys. Oceanogr., 38, 1617–1643, https://doi.org/10.1175/2008JPO3485.1.

Chin, T. M., Vazquez-Cuervo, J., & Armstrong, E. M. (2017). A multi-scale high-resolution analysis of global sea surface temperature. Remote Sensing of Environment, 200 (December 2016), 154–169. https://doi.org/10.1016/j.rse.2017.07.029

Collins, M. et al., (2019). Extremes, Abrupt Changes and Managing Risks. In: IPCC Special Report on the Ocean and Cryosphere in a Changing Climate [Pörtner, H.-O., D.C. Roberts, V. Masson-Delmotte, P. Zhai, M. Tignor, E. Poloczanska, K. Mintenbeck, M. Nicolai, A. Okem, J. Petzold, B. Rama, and N. Weyer (eds.)]. In Press, pp. 589-655.

Condron, A., and P. Winsor, 2011: A subtropical fate awaited freshwater discharged from glacial Lake Agassiz. Geophys. Res. Lett., 38, L03705, https://doi.org/10.1029/2010GL046011

Copernicus Marine Service (2022), Global Ocean Gridded L 4 Sea Surface Heights And Derived Variables Reprocessed 1993 Ongoing, https://doi.org/10.48670/moi-00148, accessed [2022-12-13].

Copernicus Marine Service (2022), Global Ocean physics reanalysis [Dataset], https://doi.org/10.48670/moi-00021.

de Jong, F. M., Steur, L., Fried, N., Bol, R., & Kritsotalakis, S. (2020). Year-round measurements of the Irminger current: Variability of a two-core current system observed in 2014–2016. Journal of Geophysical Research: Oceans, 125, e2020JC016193. https://doi.org/10.1029/2020JC016193

de Jong, M. F., Bower, A. S., & Furey, H. H. (2014). Two Years of Observations of Warm-Core Anticyclones in the Labrador Sea and Their Seasonal Cycle in Heat and Salt Stratification, Journal of Physical Oceanography, 44(2), 427-444. https://doi.org/10.1175/JPO-D-13-070.1

de Jong, M. F., Oltmanns, M., Karstensen, J., & de Steur, L. (2018). Deep Convection in the Irminger Sea Observed with a Dense Mooring Array. Oceanography, 31(1), 50–59. https://doi.org/10.5670/oceanog.2018.109

de Jong, M. F., & de Steur, L. (2016). Strong winter cooling over the Irminger Sea in winter 2014-2015, exceptional deep convection, and the emergence of anomalously low SST. Geophysical Research Letters, 43, 7106– 7113. https://doi-org/10.1002/2016GL069596

de Jong, M. F., Van Aken, H. M., Våge, K., & Pickart, R. S. (2012). Convective mixing in the central Irminger Sea: 2002-2010. Deep-Sea Research Part I: Oceanographic Research Papers, 63, 36– 51. https://doi-org/10.1016/j.dsr.2012.01.003

De Steur, L., Pickart, R. S., Macrander, A., Våge, K., Harden, B., Jónsson, S., ... & Valdimarsson, H. (2017). Liquid freshwater transport estimates from the East Greenland Current based on continuous measurements north of Denmark S trait. Journal of Geophysical Research: Oceans, 122(1), 93-109. https://doi.org/10.1002/2016JC012106

Dickson R., Rudels B., Dye S., Karcher M., Meincke J., Yashayaev I. (2007). Current estimates of freshwater flux through arctic and subarctic seas. Prog. Oceanogr. 73, 210–230. doi: 10.1016/j.pocean.2006.12.003

Dickson, R. R., Meincke, J., Malmberg, S., and Lee, A. J. (1988). The “Great Salinity Anomaly” in the northern North Atlantic 1968–1982. Progress in. Oceanography, 20, 103–151. https://doi-org/10.1016/0079-6611(88)90049-3

Docquier, D., Grist, J.P., Roberts, M.J. et al. Impact of model resolution on Arctic sea ice and North Atlantic Ocean heat transport. Clim Dyn 53, 4989–5017 (2019). https://doi.org/10.1007/s00382-019-04840-y

Dodd, P. A., Heywood, K. J., Meredith, M. P., Naveira-Garabato, A. C., Marca, A. D., and Falkner, K. K. (2009). Sources and fate of freshwater exported in the East Greenland Current, Geophys. Res. Lett., 36, L19608, https://doi-org/10.1029/2009GL039663.

Doyle, J. D., and Shapiro, M. A. (1999). Flow response to large-scale topography: The Greenland tip jet. Tellus, 51A, 728–748, https://doi-org/10.1034/j.1600-0870.1996.00014.x.

Dukhovskoy, D. S., Yashayaev, I., Proshutinsky, A., Bamber, J. L., Bashmachnikov, I. L., Chassignet, E. P., et al. (2019). Role of Greenland freshwater anomaly in the recent freshening of the subpolar North Atlantic. Journal of Geophysical Research: Oceans, 124. https://doi.org/10.1029/2018JC014686

Dukhovskoy, D. S., P. G. Myers, G. Platov, M.-L. Timmermans, B. Curry, A. Proshutinsky, J. L. Bamber, E. Chassignet, X. Hu, C. M. Lee, and R. Somavilla (2016), Greenland freshwater pathways in the sub-Arctic Seas from model experiments with passive tracers, J. Geophys. Res. Oceans, 121, 877– 907, https://doi-org/10.1002/2015JC011290.

Duyck, E., & De Jong, M. F. (2021). Circulation over the South-East Greenland shelf and potential for liquid freshwater export: A drifter study. Geophysical Research Letters, 48, https://doi-org/10.1029/2020GL091948

Duyck, E., Gelderloos, R., & de Jong, M. F. (2022). Wind-Driven Freshwater Export at Cape Farewell. Journal of Geophysical Research: Oceans, 127(5), e2021JC018309. https://doi.org/10.1029/2021JC018309

Duyck, Elodie; De Jong, Marieke Femke, 2023, Full EGC-DrIFT 6h interpolated dataset, https://doi.org/10.25850/nioz/7b.b.ff, NIOZ

Fahrbach E., Meincke J., Østerhus S., Rohardt G., Schauer U., Tverberg V., & Verduin J. (2001). Direct measurements of volume transports through Fram Strait. Polar Research, 20(2), 217-224. https://doi.org/10.3402/polar.v20i2.6520

Fischer, J., Karstensen, J., Oltmanns, M., and Schmidtko, S (2018). Mean circulation and EKE distribution in the Labrador Sea Water level of the subpolar North Atlantic, Ocean Sci., 14, 1167–1183, https://doi.org/10.5194/os-14-1167-2018 .

Foukal, N. P., Gelderloos, R., Pickart, R. S., A continuous pathway for fresh water along the East Greenland shelf (2020). Science Advances, 43(6), eabc4254. https://doi.org/10.1126/sciadv.abc4254

Fox-Kemper, B., H.T. Hewitt, C. Xiao, G. Aðalgeirsdóttir, S.S. Drijfhout, T.L. Edwards, N.R. Golledge, M. Hemer, R.E. Kopp, G. Krinner, A. Mix, D. Notz, S. Nowicki, I.S. Nurhati, L. Ruiz, J.-B. Sallée, A.B.A. Slangen, and Y. Yu, 2021: Ocean, Cryosphere and Sea Level Change. In Climate Change 2021: The Physical Science Basis. Contribution of Working Group I to the Sixth Assessment Report of the Intergovernmental Panel on Climate Change. Cambridge University Press, Cambridge, United Kingdom and New York, NY, USA, pp. 1211–1362, doi: 10.1017/9781009157896.011.

Frajka-Williams, E., Bamber, J., & Vage, K. (2016). Greenland Melt and the Atlantic Meridional Overturning Circulation. Oceanography,29(4), 22-33. https://doi.org/10.5670/oceanog.2016.96

Fried, N., & de Jong, M. F. (2022). The role of the Irminger Current in the Irminger Sea northward transport variability. Journal of Geophysical Research: Oceans, 127, e2021JC018188. https://doi.org/10.1029/2021JC018188

Frierson, D. M. W., Y.-T. Hwang, N. S. Fuckar, R. Seager, S. M. Kang, A. Donohoe, E. A. Maroon, X. Liu, and D. S. Battisti (2013), Contribution of ocean overturning circulation to tropical rainfall peak in the Northern Hemisphere, Nat. Geosci., 6(11), 940– 944, doi:10.1038/ngeo1987.

Gelderloos, R., Straneo, F., & Katsman, C. A. (2012). Mechanisms behind the temporary shutdown of deep convection in the Labrador Sea: Lessons from the great salinity anomaly years 1968–71. Journal of Climate, 25(19), 6743– 6755, https://doi.org/10.1175/JCLI-D-11-00549.1

Gelderloos, R., Szalay, A. S., Haine, T. W. N., and Lemson, G. (2016). A fast algorithm for neutrally-buoyant Lagrangian particles in numerical ocean modeling. Proc. 2016 IEEE 12th Int. Conf. on e-Science, Baltimore, MD, Institute of Electrical and Electronics Engineers, 381–388, https://doi.org/10.1109/eScience.2016.7870923.

Giles, K. A., Laxon, S. W., Ridout, A. L., Wingham, D. J., & Bacon, S. (2012). Western Arctic Ocean freshwater storage increased by wind-driven spin-up of the Beaufort Gyre. Nature Geoscience, 5(3), 194– 197. https://doi.org/10.1038/NGEO1379

Gillard, L. C., X. Hu, P. G. Myers, and J. L. Bamber, 2016: Meltwater pathways from marine terminating glaciers of the Greenland ice sheet. Geophys. Res. Lett., 43, 10 873–10 882, https://doi.org/10.1002/2016GL070969.

Glessmer, M., Eldevik, T., Våge, K. et al. Atlantic origin of observed and modelled freshwater anomalies in the Nordic Seas. Nature Geosci 7, 801–805 (2014). https://doi.org/10.1038/ngeo2259

Goelzer, H., Nowicki, S., Payne, A., Larour, E., Seroussi, H., Lipscomb, W. H., Gregory, J., Abe-Ouchi, A., Shepherd, A., Simon, E., Agosta, C., Alexander, P., Aschwanden, A., Barthel, A., Calov, R., Chambers, C., Choi, Y., Cuzzone, J., Dumas, C., Edwards, T., Felikson, D., Fettweis, X., Golledge, N. R., Greve, R., Humbert, A., Huybrechts, P., Le clec'h, S., Lee, V., Leguy, G., Little, C., Lowry, D. P., Morlighem, M., Nias, I., Quiquet, A., Rückamp, M., Schlegel, N.-J., Slater, D. A., Smith, R. S., Straneo, F., Tarasov, L., van de Wal, R., and van den Broeke, M.: The future sea-level contribution of the Greenland ice sheet: a multi-model ensemble study of ISMIP6, The Cryosphere, 14, 3071–3096, https://doi.org/10.5194/tc-14-3071-2020, 2020.

Haarsma, R. J., Roberts, M. J., Vidale, P. L., Catherine, A., Bellucci, A., Bao, Q., Chang, P., Corti, S., Fučkar, N. S., Guemas, V., von Hardenberg, J., Hazeleger, W., Kodama, C., Koenigk, T., Leung, L. R., Lu, J., Luo, J.-J., Mao, J., Mizielinski, M. S., Mizuta, R., Nobre, P., Satoh, M., Scoccimarro, E., Semmler, T., Small, J., & von Storch, J.-S. (2016). High Resolution Model Intercomparison Project (HighResMIP v1.0) for CMIP6. Geoscientific Model Development, 9(11), 4185– 4208. https://doi.org/10.5194/gmd-9-4185-2016

Haine, T. W. N., Curry, B., Gerdes, R., Hansen, E., Karcher, M., Lee, C., Rudels, B., Spreen, G., de Steur, L., Stewart, K. D., & Woodgate, R. (2015). Arctic freshwater export: Status, mechanisms, and prospects. Global and Planetary Change, 125, 13– 35. https://doi.org/10.1016/j.gloplacha.2014.11.013

Hanna, E., Mernild, S.H., Cappelen, J. and Steffen, K. (2012) Recent warming in Greenland in a long-term instrumental (1881-2012) climatic context. I. Evaluation of surface air temperature records. Envionmental Research Letters, 7, 045404.

Hansen, B., & Østerhus, S. (2000). North Atlantic-Nordic seas exchanges. Progress in Oceanography, 45(2), 109– 208. https://doi.org/10.1016/S0079-6611(99)00052-X

Harden, B. E., Renfrew, I. A., and Petersen, G. N. (2011) A climatology of wintertime barrier winds off southeast Greenland. J. Climate, 24, 4701–4717. https://doi.org/10.1175/2011JCLI4113.1

Harden, B. E., Straneo, F., & Sutherland, D. A. (2014). Moored observations of synoptic and seasonal variability in the East Greenland Coastal Current. Journal of Geophysical Research: Oceans, 119(12), 8838–8857. https://doi.org/10.1002/2014JC010134

Harden, B. E., Pickart, R. S., Valdimarsson, H., Våge, K., de Steur, L., Richards, C., ... & Hattermann, T. (2016). Upstream sources of the Denmark Strait Overflow: Observations from a high-resolution mooring array. Deep Sea Research Part I: Oceanographic Research Papers, 112, 94-112., https://doi.org/10.1016/j.dsr.2016.02.007.

Hátún, H., Eriksen, C. C., and Rhines, P. B. (2007). Buoyant eddies entering the Labrador Sea observed with gliders and altimetry. J. Phys. Oceanogr., 37, 2838–2854 https://doi.org/10.1175/2007JPO3567.1

Håvik, L., & Våge, K. (2018). Wind-driven coastal upwelling and downwelling in the shelfbreak East Greenland Current. Journal of Geophysical Research: Oceans, 123(9), 6106-6115. https://doi.org/10.1029/2018JC014273

Håvik, L., K. Våge, R. S. Pickart, B. Harden, W.-J. von Appen, S. Jónsson, and S. Østerhus, 2017b: Structure and variability of the shelfbreak East Greenland Current north of Denmark Strait. J. Phys. Oceanogr., 47, 2631–2646, https://doi.org/10.1175/JPO-D-17-0062.1.

Håvik, L., R. S. Pickart, K. Våge, D. Torres, A. M. Thurnherr, A. Beszczynska-Möller, W. Walczowski, and W.-J. von Appen, 2017a: Evolution of the East Greenland Current from Fram Strait to Denmark Strait: Synoptic measurements from summer 2012. J. Geophys. Res. Oceans, 122, 1974–1994, https://doi.org/10.1002/2016JC012228.

Hersbach, H., Bell, B., Berrisford, P., Biavati, G., Horányi, A., Muñoz Sabater, J., Nicolas, J., Peubey, C., Radu, R., Rozum, I., Schepers, D., Simmons, A., Soci, C., Dee, D., Thépaut, J-N. (2023a): ERA5 hourly data on single levels from 1940 to present. [Dataset]. Copernicus Climate Change Service (C3S) Climate Data Store (CDS), https://doi.org/10.24381/cds.adbb2d47

Hersbach, H., Bell, B., Berrisford, P., Biavati, G., Horányi, A., Muñoz Sabater, J., Nicolas, J., Peubey, C., Radu, R., Rozum, I., Schepers, D., Simmons, A., Soci, C., Dee, D., Thépaut, J-N. (2023b): ERA5 monthly averaged data on single levels from 1940 to present [Dataset]. Copernicus Climate Change Service (C3S) Climate Data Store (CDS), https://doi.org/10.24381/cds.f17050d7

Hersbach, H, Bell, B, Berrisford, P, et al. The ERA5 global reanalysis. Q J R Meteorol Soc. 2020; 146: 1999–2049. https://doi.org/10.1002/qj.3803

Heuzé, C.: Antarctic Bottom Water and North Atlantic Deep Water in CMIP6 models, Ocean Sci., 17, 59–90, https://doi.org/10.5194/os-17-59-2021, 2021.

Hewitt, H. T. H. T., Bell, M. J. M. J., Chassignet, E. P. E. P., Czaja, A., Ferreira, D., Griffies, S. M. S. M., et al. (2017). Will high-resolution global ocean models benefit coupled predictions on short-range to climate timescales? Ocean Modelling, 120(October), 120– 136. https://doi.org/10.1016/j.ocemod.2017.11.002

Hirschi, J. J.-M., Barnier, B., Böning, C., Biastoch, A., Blaker, A. T., Coward, A., et al. (2020). The Atlantic meridional overturning circulation in high-resolution models. Journal of Geophysical Research: Oceans, 125, e2019JC015522. https://doi.org/10.1029/2019JC015522

Holland, M. M., J. Finnis, and M. C. Serreze, 2006: Simulated Arctic Ocean Freshwater Budgets in the Twentieth and Twenty-First Centuries. J. Climate, 19, 6221–6242, https://doi.org/10.1175/JCLI3967.1.

Holland, M. M., Finnis, J., Barrett, A. P., and Serreze, M. C. (2007), Projected changes in Arctic Ocean freshwater budgets, J. Geophys. Res., 112, G04S55, doi:10.1029/2006JG000354.

Holland, D. M., Thomas, R. H., de Young, B., Ribergaard, M. H., and Lyberth, B.: Acceleration of Jakobshavn Isbræ triggered by warm subsurface ocean waters, Nature Geosci., 1, 659–664, https://doi.org/10.1038/ngeo316, 2008.

Holliday, N. P., Meyer, A., Bacon, S., Alderson, S. G., & de Cuevas, B. (2007). Retroflection of part of the east Greenland current at Cape Farewell. Geophysical Research Letters, 34(7), L07609. https://doi.org/10.1029/2006GL029085

Holliday, N. P., Bacon, S., Cunningham, S. A., Gary, S. F., Karstensen, J., King, B. A., et al. (2018). Subpolar North Atlantic Overturning and Gyre-Scale Circulation in the Summers of 2014 and 2016. Journal of Geophysical Research: Oceans, 123, 4538– 4559. https://doi.org/10.1029/2018JC013841

Holliday, P. N., Bersch, M., Berx, B., Chafik, L., Cunningham, S., Florindo-López, C., et al. (2020). Ocean circulation causes the largest freshening event for 120 years in eastern Subpolar North Atlantic. Nature Communications, 11(1), 585. https://doi.org/10.1038/s41467-020-14474-y

Huang, J., Pickart, R.S., Huang, R.X. et al. Sources and upstream pathways of the densest overflow water in the Nordic Seas. Nat Commun 11, 5389 (2020). https://doi.org/10.1038/s41467-020-19050-y

Hurrell, J. W. (1995). Decadal trends in the North Atlantic Oscillation: Regional temperatures and precipitation. Science, 269, 676–679, https://10.1126/science.269.5224.676

Jackson, L.C., Kahana, R., Graham, T. et al. Global and European climate impacts of a slowdown of the AMOC in a high resolution GCM. Clim Dyn 45, 3299–3316 (2015). https://doi.org/10.1007/s00382-015-2540-2

Jackson, L.C. and R.A. Wood, 2018: Timescales of AMOC decline in response to fresh water forcing. Climate Dynamics, 51(4), 1333–1350, doi: 10.1007/s00382-017-3957-6.

Jackson, L.C., Roberts, M.J., Hewitt, H.T. et al. Impact of ocean resolution and mean state on the rate of AMOC weakening. Clim Dyn 55, 1711–1732 (2020). https://doi.org/10.1007/s00382-020-05345-9

Jackson, L. C., Alastrué de Asenjo, E., Bellomo, K., Danabasoglu, G., Haak, H., Hu, A., Jungclaus, J., Lee, W., Meccia, V. L., Saenko, O., Shao, A., and Swingedouw, D.: Understanding AMOC stability: the North Atlantic Hosing Model Intercomparison Project, Geosci. Model Dev., 16, 1975–1995, https://doi.org/10.5194/gmd-16-1975-2023, 2023.

Jahn, A., & Laiho, R. (2020). Forced changes in the Arctic freshwater budget emerge in the early 21st century. Geophysical Research Letters, 47, e2020GL088854. https://doi.org/10.1029/2020GL088854

Johnson, H. L., Cessi, P., Marshall, D. P., Schloesser, F., & Spall, M. A. (2019). Recent contributions of theory to our understanding of the Atlantic meridional overturning circulation. Journal of Geophysical Research: Oceans, 124, 5376– 5399. https://doi.org/10.1029/2019JC015330

Jónsson, S. (2007). Volume flux and fresh water transport associated with the East Icelandic Current. Progress in Oceanography, 73(3–4), 231– 241. https://doi.org/10.1016/j.pocean.2006.11.003

Josey, S. A., de Jong, M. F., Oltmanns, M., Moore, G. K., & Weller, R. A. (2019). Extreme variability in Irminger Sea winter heat loss revealed by ocean observatories initiative mooring and the ERA5 reanalysis. Geophysical Research Letters, 46, 293– 302. https://doi.org/10.1029/2018GL080956

JPL MUR MEaSUREs Project. 2015. GHRSST Level 4 MUR Global Foundation Sea Surface Temperature Analysis (v4.1). Ver. 4.1. PO.DAAC, CA, USA. Dataset accessed [2020-03-31] at https://doi.org/10.5067/GHGMR-4FJ04.

Katsman, C. A., Drijfhout, S. S., Dijkstra, H. A., & Spall, M. A. (2018). Sinking of dense North Atlantic waters in a global ocean model: Location and controls. Journal of Geophysical Research: Oceans, 123, 3563– 3576. https://doi.org/10.1029/2017JC013329

Kostov, Y., Armour, K. C., and Marshall, J. (2014), Impact of the Atlantic meridional overturning circulation on ocean heat storage and transient climate change, Geophys. Res. Lett., 41, 2108– 2116, doi:10.1002/2013GL058998.

Koszalka, I. M., & Lacasce, J. H. (2010). Lagrangian analysis by clustering. Ocean Dynamics, 60(4), 957–972. https://doi.org/10.1007/s10236-010-0306-2

Koszalka, I. M., Haine, T. W. N., and Magaldi, M. G., (2013). Fates and travel times of Denmark Strait overflow water in the Irminger Basin. J. Phys. Oceanogr., 43, 2611–2628, https://doi.org/10.1175/JPO-D-13-023.1.

Koszalka, I., LaCasce, J. H., Andersson, M., Orvik, K. A., & Mauritzen, C. (2011). Surface circulation in the Nordic Seas from clustered drifters. Deep Sea Research Part I: Oceanographic Research Papers, 58(4), 468-485, https://doi.org/10.1016/j.dsr.2011.01.007

Kuhlbrodt, T., Jones, C. G., Sellar, A., Storkey, D., Blockley, E., Stringer, M., Hill, R., Graham, T., Ridley, J., Blaker, A., Calvert, D., Copsey, D., Ellis, R., Hewitt, H., Hyder, P., Ineson, S., Mulcahy, J., Siahaan, A., and Walton, J.: The low-resolution version of HadGEM3 GC3.1: Development and evaluation for global climate, J. Adv. Model. Earth Sy., 10, 2865–2888, https://doi.org/10.1029/2018MS001370, 2018.

Lavender, K.L., Owens, W.B., Davis, R.E., 2005. The mid-depth circulation of the subpolar North Atlantic Ocean as measured by subsurface floats. Deep-Sea Res.I 52 (5), 767–785. http://dx.doi.org/10.1016/j.dsr.2004.12.007.

Lazier, J.R.N., 1980. Oceanographic conditions at Ocean Weather Ship Bravo, 1964–1974. Atmos. Ocean 18 (3), 227–238. doi:10.1080/07055900.1980.9649089.

Lazier, J.R.N., Hendry, R., Clarke, R.A., Yashayaev, I., Rhines, P.B., 2002. Convection and restratification in the Labrador Sea, 1990–2000. Deep-Sea Res. I 49 (10), 1819–1835. doi:10.1016/S0967-0637(02)00064

le Bras, I. A.-A., Straneo, F., Holte, J., & Holliday, N. P. (2018). Seasonality of Freshwater in the East Greenland Current System From 2014 to 2016. Journal of Geophysical Research: Oceans, 123(12), 8828–8848. https://doi.org/10.1029/2018JC014511

Le Bras, I. A.-A.; Straneo, F.; Holte, J.; Jong, M. F.; Holliday, N. P. (2020). Rapid export of waters formed by convection near the Irminger Sea's western boundary. Geophysical Research Letters, 47 (3), e2019GL085989. https://doi.org/10.1029/2019GL085989

Le Bras, I., F. Straneo, M. Muilwijk, L. H. Smedsrud, F. Li, M. S. Lozier, and N. P. Holliday, 2021: How Much Arctic Fresh Water Participates in the Subpolar Overturning Circulation?. J. Phys. Oceanogr., 51, 955–973, https://doi.org/10.1175/JPO-D-20-0240.1.

Lellouche, J. M., Greiner, E., Bourdalle-Badie, R., Garric, G., Melet, A., Drevillon, M., et al. (2021). The Copernicus global 1/12° oceanic and sea ice GLORYS12 reanalysis. Front. Earth Sci. , 9, 585, https://doi.org/10.3389/feart.2021.698876.

Li, F., Lozier, M.S., Bacon, S., Bower, A., Cunningham, S.A., de Jong, M.F., DeYoung, B., Fraser, N., Fried, N., Han, G., Holliday, N.P., Holte, J., Houpert, L., Inall, M.E., Johns, W.E., Jones, S., Johnson, C., Karstensen, J., LeBras, I.A., Lherminier, P., Lin, X., Mercier, H., Oltmanns, M., Pacini, A., Petit, T., Pickart, R.S., Rayner, D., Straneo, F., Thierry, V., Visbeck, M., Yashayaev, I., Zhou, C. (2021). Subpolar North Atlantic western boundary density anomalies and the Meridional Overturning Circulation. Nature Communications, 12, 3002 (2021). https://doi.org/10.1038/s41467-021-23350-2

Lilly, J. M. (2021), jLab: A data analysis package for Matlab, v.1.7.1, doi:10.5281/zenodo.4547006, http://www.jmlilly.net/software.

Lilly, J. M., P. B.Rhines, R.Schott, K.Lavender, J.Lazier, U.Send, and E.D'Asaro, 2003: Observations of the Labrador Sea eddy field. Prog. Oceanogr., 59, 75–176. https://doi.org/10.1016/j.pocean.2003.08.013

Lin, P., Pickart, R. S., Torres, D. J., & Pacini, A. (2018). Evolution of the Freshwater Coastal Current at the Southern Tip of Greenland. Journal of Physical Oceanography, 48(9), 2127–2140. https://doi.org/10.1175/jpo-d-18-0035.1

Lin, P., Pickart, R.S., Heorton, H. et al. Recent state transition of the Arctic Ocean's Beaufort Gyre. Nat. Geosci. 16, 485–491 (2023). https://doi-org.proxy.library.uu.nl/10.1038/s41561-023-01184-5Lozier et al 2012,

Lozier, M. S. (2012). Overturning in the north atlantic. Annual review of marine science, 4, 291-315. doi: https://doi.org/10.1146/annurev-marine-120710-100740

Lozier, M.S., Bacon, S., Bower, A. S., Cunningham, S. A., de Jong, F.M., de Steur, L., deYoung, B., Fischer, J., Gary, S. F., Greenan, B. J. W., Heimbach, P., Holliday, N. P., Houpert, L., Inall, M. E., Johns, W. E., Johnson, H. L., Karstensen, J., Li, F., Lin, X., Mackay, N., Marshall, D. P., Mercier, H., Myers, P. G., Pickart, R. S., Pillar, H. R., Straneo, F., Thierry, V., Weller, R. A., Williams, R. G., Wilson, C., Yang, J., Zhao, J., & Zika, J. D. (2017). Overturning in the Subpolar North Atlantic Program: A New International Ocean Observing System, Bulletin of the American Meteorological Society, 98(4), 737-752. doi: https://doi.org/10.1175/BAMS-D-16-0057.1

Lozier, M. S., Li, F., Bacon, S., Bahr, F., Bower, A. S., Cunningham, S. A., de Jong, M. F., de Steur, L., deYoung, B., Fischer, J., Gary, S. F., Greenan, B. J. W., Holliday, N. P., Houk, A., Houpert, L., Inall, M. E., Johns, W. E., Johnson, H. L., Johnson, C., … Zhao, J. (2019). A sea change in our view of overturning in the subpolar North Atlantic. Science, 363(6426), 516–521. https://doi.org/10.1126/science.aau6592

Lumpkin, R., and G. C. Johnson (2013), Global ocean surface velocities from drifters: Mean, variance, El Nino–Southern Oscillation response, and seasonal cycle,J. Geophys. Res. Oceans,118, 2992–3006, doi:10.1002/jgrc.20210.

Lumpkin, R., Özgökmen, T., & Centurioni, L. (2017). Advances in the Application of Surface Drifters. Annual Review of Marine Science, 9(1), 59–81. https://doi.org/10.1146/annurev-marine-010816-060641

Lumpkin, Rick; Centurioni, Luca (2019). Global Drifter Program quality-controlled 6-hour interpolated data from ocean surface drifting buoys. NOAA National Centers for Environmental Information. Dataset. https://doi.org/10.25921/7ntx-z961. Accessed [2020-03-31]

Luo, H., Castelao, R. M., Rennermalm, A. K., Tedesco, M., Bracco, A., Yager, P. L., & Mote, T. L. (2016). Oceanic transport of surface meltwater from the southern Greenland ice sheet. Nature Geoscience, 9(7), 528-532.

Lynch-Stieglitz, J. (2017). The Atlantic meridional overturning circulation and abrupt climate change. Annual review of marine science, 9, 83-104. https://doi.org/10.1146/annurev-marine-010816-060415

MacKay DJC (2003) Information theory, inference, and learning algorithms. Cambridge University Press, Cambridge

Macrander, A., Valdimarsson, H., & Jónsson, S. (2014). Improved transport estimate of the East Icelandic Current 2002–2012. Journal of Geophysical Research: Oceans, 119, 3407– 3424. https://doi.org/10.1002/2013JC009517

Malmberg, S.-A., Gade, H.G., Sweers, H.E., 1967. Report on the second joint Icelandic–Norwegian expedition to the area between Iceland and Greenland in August–September 1965. NATO Subcommittee on Oceanographic Research, Technical Report No. 41, Irminger Sea Project, 44 pp

Manabe, S., and R. J. Stouffer, 1988: Two Stable Equilibria of a Coupled Ocean-Atmosphere Model. J. Climate, 1, 841–866, https://doi.org/10.1175/1520-0442(1988)001<0841:TSEOAC>2.0.CO;2.

Manabe, S., & Stouffer, R. J. (1994). Multiple-Century Response of a Coupled Ocean-Atmosphere Model to an Increase of Atmospheric Carbon Dioxide. Journal of Climate, 7(1), 5–23. https://doi.org/10.1175/1520-0442(1994)007

Manabe, S., Stouffer, R. (1995) Simulation of abrupt climate change induced by freshwater input to the North Atlantic Ocean. Nature 378, 165–167. https://doi.org/10.1038/378165a0

Marnela, M., Rudels, B., Houssais, M.-N., Beszczynska-Möller, A., and Eriksson, P. B.: Recirculation in the Fram Strait and transports of water in and north of the Fram Strait derived from CTD data, Ocean Sci., 9, 499–519, https://doi.org/10.5194/os-9-499-2013, 2013.

Marsh, R., Desbruyères, D., Bamber, J. L., de Cuevas, B. A., Coward, A. C., and Aksenov, Y.: Short-term impacts of enhanced Greenland freshwater fluxes in an eddy-permitting ocean model, Ocean Sci., 6, 749–760, https://doi.org/10.5194/os-6-749-2010, 2010.

Marshall, J., Adcroft, A., Hill, C., Perelman, L., & Heisey, C. (1997). A finite-volume, incompressible Navier Stokes model for studies of the ocean on parallel computers. Journal of Geophysical Research, 102(C3), 5753– 5766. https://doi.org/10.1029/96JC02775

Marshall, J., Schott, F., 1999. Open-ocean convection: Observations, theory and models. Rev. Geophys. 37, 1–64. doi:10.1029/98RG02739.

Martin, T. and Biastoch, A.: On the ocean's response to enhanced Greenland runoff in model experiments: relevance of mesoscale dynamics and atmospheric coupling, Ocean Sci., 19, 141–167, https://doi.org/10.5194/os-19-141-2023, 2023.

Marzocchi, A., Hirschi, J. J. M., Holliday, N. P., Cunningham, S. A., Blaker, A. T., & Coward, A. C. (2015). The North Atlantic subpolar circulation in an eddy-resolving global ocean model. Journal of Marine Systems, 142, 126– 143. https://doi.org/10.1016/j.jmarsys.2014.10.007

Maximenko, N., Lumpkin, R., and Centurioni, L. (2013). “Ocean surface circulation,” in Ocean Circulation and Climate: A 21st Century Perspective, eds G. Siedler, S. M. Griffies, J. Gould, and J. A. Church (Cambridge, MA: Academic Press), 283–304. doi: 10.1016/b978-0-12-391851-2.00012-x

McDougall, T. J., & Barker, P. M. (2011). Getting started with TEOS-10 and the Gibbs Seawater (GSW) Oceanographic Toolbox, 28pp., SCOR/IAPSO WG127, ISBN 978-0-646-55621-5.

Medvedev, D., Lemson, G., & Rippin, M. (2016). Sciserver compute: Bringing analysis close to the data. Proceedings of the 28th international conference on scientific and statistical database management, SSDBM '16, ACM, New York, NY, USA, pp. 27:1– 27:4. https://doi.org/10.1145/2949689.2949700

Menary, M. B., Hodson, D. L. R., Robson, J. I., Sutton, R. T., Wood, R. A., and Hunt, J. A. (2015), Exploring the impact of CMIP5 model biases on the simulation of North Atlantic decadal variability, Geophys. Res. Lett., 42, 5926– 5934, doi:10.1002/2015GL064360.

Menary, M. B., Kuhlbrodt, T., Ridley, J., Andrews, M. B., Dimdore-Miles, O. B., Deshayes, J., Eade, R., Gray, L., Ineson, S., Mignot, J., Roberts, C. D., Robson, J., Wood, R. A., & Xavier, P. (2018). Preindustrial control simulations with HadGEM3-GC3.1 for CMIP6. Journal of Advances in Modeling Earth Systems, 10, 3049–3075. https://doi.org/10.1029/2018MS001495

Menary, M. B., Jackson, L. C., & Lozier, M. S. (2020). Reconciling the relationship between the AMOC and Labrador Sea in OSNAP observations and climate models. Geophysical Research Letters, 47, e2020GL089793. https://doi.org/10.1029/2020GL089793

Moore, G. W. K. (2003), Gale force winds over the Irminger Sea to the east of Cape Farewell, Greenland, Geophysical. Research Letters, 30(17), 1894, https://doi:10.1029/2003GL018012.

Moore, G. W. K., & Renfrew, I. A. (2005). Tip jets and barrier winds: A QuikSCAT climatology of high wind speed events around Greenland. Journal of Climate, 18(18), 3713–3725. https://doi.org/10.1175/JCLI3455.1

Moore, G. W. K., (2012): A new look at Greenland flow distortion and its impact on barrier flow, tip jets and coastal oceanography. Geophysical Research Letters, 39, L22806, https://doi.org/10.1029/2012GL054017.

Moore, G. W. K. (2014), Mesoscale structure of Cape Farewell tip jets, Journal of Climate, 27(23), 8956– 8965. https://doi.org/10.1175/JCLI-D-14-00299.1

Moore, G., Våge, K., Pickart, R. et al. Decreasing intensity of open-ocean convection in the Greenland and Iceland seas. Nature Clim Change 5, 877–882 (2015). https://doi.org/10.1038/nclimate2688

Moore, G.W.K., Våge, K., Renfrew, I.A. et al. Sea-ice retreat suggests re-organization of water mass transformation in the Nordic and Barents Seas. Nat Commun 13, 67 (2022). https://doi.org/10.1038/s41467-021-27641-6

Mouginot, J., Rignot, E., Bjørk, A. A., Broeke, M. van den, Millan, R., Morlighem, M., Noël, B., Scheuchl, B., and Wood, M.: Forty-six years of Greenland Ice Sheet mass balance from 1972 to 2018, P. Natl. Acad. Sci., 116, 9239–9244, https://doi.org/10.1073/pnas.1904242116, 2019.

Niiler, P. P., Sybrandy, A. S., Bi, K., Poulain, P. M., and Bitterman, D. (1995). Measurements of the water-following capability of holey-sock TRISTAR drifters. Deep Sea Res. Part I Oceanogr. Res. Pap. 42, 1951–1964. doi: 10.1016/0967-0637(95)00076-3

NOAA National Centers for Environmental Information. 2022: ETOPO 2022 15 Arc-Second Global Relief Model. NOAA National Centers for Environmental Information. DOI: 10.25921/fd45-gt74. Accessed [17-03-23].

NOAA National Geophysical Data Center. 2006: 2-minute Gridded Global Relief Data (ETOPO2) v2. NOAA National Centers for Environmental Information. https://doi.org/10.7289/V5J1012Q. Accessed 01/05/2021.

Novelli, G., Guigand, C. M., Cousin, C., Ryan, E. H., Laxague, N. J. M., Dai, H., Haus, B. K., & Özgökmen, T. M. (2017). A biodegradable surface drifter for ocean sampling on a massive scale. Journal of Atmospheric and Oceanic Technology, 34(11), 2509–2532. https://doi.org/10.1175/JTECH-D-17-0055.1

Oltmanns, M., Karstensen, J. & Fischer, J. (2018) Increased risk of a shutdown of ocean convection posed by warm North Atlantic summers. Nature Climate Change 8, 300–304, https://doi.org/10.1038/s41558-018-0105-1

Oltmanns, M., Straneo, F., Moore, G. W., & Mernild, S. H. (2014). Strong downslope wind events in Ammassalik, southeast Greenland. Journal of Climate, 27(3), 977– 993. https://doi.org/10.1175/JCLI-D-13-00067.1

Outten, S.D., Renfrew, I.A. and Petersen, G.N. (2009), An easterly tip jet off Cape Farewell, Greenland. II: Simulations and dynamics. Q.J.R. Meteorol. Soc., 135: 1934-1949. https://doi.org/10.1002/qj.531

Pacini, A., and Coauthors, 2020: Mean Conditions and Seasonality of the West Greenland Boundary Current System near Cape Farewell. J. Phys. Oceanogr., 50, 2849–2871, https://doi.org/10.1175/JPO-D-20-0086.1

Pattyn, F., Ritz, C., Hanna, E. et al. The Greenland and Antarctic ice sheets under 1.5 °C global warming. Nature Clim Change 8, 1053–1061 (2018). https://doi.org/10.1038/s41558-018-0305-8

Pennelly, C., Hu, X., and Myers, P. G. (2019). Cross-isobath freshwater exchange within the North Atlantic subpolar Gyre. Journal of Geophysical Research: Oceans, 124, 6831–6853, https://doi.org/10.1029/2019JC015144

Pérez, F. F., H. Mercier, M. Vázquez-Rodriguez, P. Lherminier, A. Velo, P. Pardo, G. Roson, and A. Rios, 2013: Atlantic Ocean CO2 uptake reduced by weakening of the meridional overturning circulation. Nat. Geosci., 6, 146–152, doi:10.1038/ngeo1680

Petit, T., Lozier, M. S., Josey, S. A., and Cunningham, S. A., (2020): A new paradigm for Atlantic Ocean deep water formation. Geophysical Research Letters, 47, https://doi.org/10.1029/2020GL091028

Pickart, R., Spall, M., Ribergaard, M. et al. Deep convection in the Irminger Sea forced by the Greenland tip jet. Nature 424, 152–156 (2003). https://doi.org/10.1038/nature01729

Piron, A., Thierry, V., Mercier, H., and Caniaux, G. (2017), Gyre-scale deep convection in the subpolar North Atlantic Ocean during winter 2014–2015, Geophys. Res. Lett., 44, 1439– 1447, https://doi.org/10.1002/2016GL071895.

Piron, A., Thierry, V., Mercier, H., and Caniaux, G., (2016). Argo float observations of basin-scale deep convection in the Irminger sea during winter 2011–2012. Deep Sea Res. Part I, 109, 76-90, https://doi.org/10.1016/j.dsr.2015.12.012.

Poulain, P. M., Gerin, R., Mauri, E., & Pennel, R. (2009). Wind effects on drogued and undrogued drifters in the eastern Mediterranean. Journal of Atmospheric and Oceanic Technology, 26(6), 1144–1156. https://doi.org/10.1175/2008JTECHO618.1

Prater, M. D., 2002: Eddies in the Labrador Sea as Observed by Profiling RAFOS Floats and Remote Sensing. J. Phys. Oceanogr., 32, 411–427, https://doi.org/10.1175/1520-0485(2002)032<0411:EITLSA>2.0.CO;2.

Proshutinsky, A., Krishfield, R., Timmermans, M.-L., Toole, J., Carmack, E., McLaughlin, F., Williams, W. J., Zimmermann, S., Itoh, M., and Shimada, K. (2009), Beaufort Gyre freshwater reservoir: State and variability from observations, J. Geophys. Res., 114, C00A10, doi:10.1029/2008JC005104.

Proshutinsky, A., Krishfield, R., Toole, J. M., Timmermans, M.-L., Williams, W., Zimmermann, S., et al. (2019). Analysis of the Beaufort Gyre freshwater content in 2003–2018. Journal of Geophysical Research: Oceans, 124, 9658– 9689. https://doi.org/10.1029/2019JC015281

Rabe, B., Karcher, M., Kauker, F., Schauer, U., Toole, J. M., Krishfield, R. A., Pisarev, S., Kikuchi, T., & Su, J. (2014). Arctic Ocean basin liquid freshwater storage trend 1992–2012. Geophysical Research Letters, 41, 961– 968. https://doi.org/10.1002/2013GL058121

Rahmstorf, S. Ocean circulation and climate during the past 120,000 years. Nature 419, 207–214 (2002). https://doi.org/10.1038/nature01090

Riser, S., Freeland, H., Roemmich, D. et al. Fifteen years of ocean observations with the global Argo array. Nature Clim Change 6, 145–153 (2016). https://doi-org.proxy.library.uu.nl/10.1038/nclimate2872

Renfrew, I.A., Outten, S.D. and Moore, G.W.K. (2009), An easterly tip jet off Cape Farewell, Greenland. I: Aircraft observations. Q.J.R. Meteorol. Soc., 135: 1919-1933. https://doi.org/10.1002/qj.513

Reverdin, G., Niiler, P. P., and Valdimarsson, H., North Atlantic Ocean surface currents, J. Geophys. Res., 108(C1), 3002, doi:10.1029/2001JC001020, 2003.

Ridley, J. K., Blockley, E. W., Keen, A. B., Rae, J. G. L., West, A. E., and Schroeder, D.: The sea ice model component of HadGEM3-GC3.1, Geosci. Model Dev., 11, 713–723, https://doi.org/10.5194/gmd-11-713-2018, 2018.

Rigor, I. G., Wallace, J. M. & Colony, R. L. Response of sea ice to the Arctic oscillation. J. Clim. 15, 2648–2663 (2002) https://doi.org/10.1175/1520-0442(2002)015<2648:ROSITT>2.0.CO;2

Roberts, M. J., Baker, A., Blockley, E. W., Calvert, D., Coward, A., Hewitt, H. T., Jackson, L. C., Kuhlbrodt, T., Mathiot, P., Roberts, C. D., Schiemann, R., Seddon, J., Vannière, B., and Vidale, P. L.: Description of the resolution hierarchy of the global coupled HadGEM3-GC3.1 model as used in CMIP6 HighResMIP experiments, Geosci. Model Dev., 12, 4999–5028, https://doi.org/10.5194/gmd-12-4999-2019, 2019.

Roberts, M. J., Jackson, L. C., Roberts, C. D., Meccia, V., Docquier, D., Koenigk, T., et al. (2020). Sensitivity of the Atlantic Meridional Overturning Circulation to model resolution in CMIP6 HighResMIP simulations and implications for future changes. Journal of Advances in Modeling Earth Systems, 12, e2019MS002014. https://doi.org/10.1029/2019MS002014

Rudels, B., Fahrbach, E., Meincke, J., Budéus, G., & Eriksson, P. (2002). The East Greenland Current and its contribution to the Denmark Strait overflow. ICES Journal of Marine Science, 59(6), 1133–1154. https://doi.org/10.1006/jmsc.2002.1284

Sampe, T., and Xie, S. P. (2007). Mapping high sea winds from space: A global climatology. Bulletin of the American Meteorological Society, 88, 1965–1978, https://doi.org/10.1175/BAMS-88-12-1965.

Schulze Chretien, L. M., & Frajka-Williams, E. (2018). Wind-driven transport of fresh shelf water into the upper 30m of the Labrador Sea. Ocean Science, 14(5), 1247–1264. https://doi.org/10.5194/os-14-1247-2018

Schyberg H., Yang X., Køltzow M.A.Ø., Amstrup B., Bakketun Å., Bazile E., Bojarova J., Box J. E., Dahlgren P., Hagelin S., Homleid M., Horányi A., Høyer J., Johansson Å., Killie M.A., Körnich H., Le Moigne P., Lindskog M., Manninen T., Nielsen Englyst P., Nielsen K.P., Olsson E., Palmason B., Peralta Aros C., Randriamampianina R., Samuelsson P., Stappers R., Støylen E., Thorsteinsson S., Valkonen T., Wang Z.Q., (2020): Arctic regional reanalysis on single levels from 1991 to present. Copernicus Climate Change Service (C3S) Climate Data Store (CDS). DOI: 10.24381/cds.713858f6 (Accessed on 05-04-2023)

Sein, D. V., Koldunov, N. V., Danilov, S., Sidorenko, D., Wekerle, C., Cabos, W., Rackow, T., Scholz, P., Semmler, T., Wang, Q., & Jung, T. (2018). The relative influence of atmospheric and oceanic model resolution on the circulation of the North Atlantic Ocean in a coupled climate model. Journal of Advances in Modeling Earth Systems, 10, 2026– 2041. https://doi.org/10.1029/2018MS001327

Shepherd, A , Ivins, E, Rignot, E et al. (86 more authors) (2020) Mass balance of the Greenland Ice Sheet from 1992 to 2018. Nature 579, 233–239 (2020). https://doi.org/10.1038/s41586-019-1855-2

Shu, Q., Qiao, F., Song, Z., Zhao, J., & Li, X. (2018). Projected freshening of the Arctic Ocean in the 21st century. Journal of Geophysical Research: Oceans, 123, 9232– 9244. https://doi.org/10.1029/2018JC014036

Sterl, M. F., & de Jong, M. F. (2022). Restratification Structure and Processes in the Irminger Sea. Journal of Geophysical Research: Oceans, e2022JC019126.

Stommel, H. (1961), Thermohaline convection with two stable regimes of flow, Tellus, 2, 224– 230. https://doi.org/10.1111/j.2153-3490.1961.tb00079.x

Storkey, D., Blaker, A. T., Mathiot, P., Megann, A., Aksenov, Y., Blockley, E. W., Calvert, D., Graham, T., Hewitt, H. T., Hyder, P., Kuhlbrodt, T., Rae, J. G. L., and Sinha, B.: UK Global Ocean GO6 and GO7: a traceable hierarchy of model resolutions, Geosci. Model Dev., 11, 3187–3213, https://doi.org/10.5194/gmd-11-3187-2018, 2018.

Stouffer, R. J., and Coauthors, 2006: Investigating the Causes of the Response of the Thermohaline Circulation to Past and Future Climate Changes. J. Climate, 19, 1365–1387, https://doi.org/10.1175/JCLI3689.1.

Straneo, F. and C. Cenedese, 2015: The Dynamics of Greenland's Glacial Fjords and Their Role in Climate. Annual Review of Marine Science, 7(1), 89–112, doi: 10.1146/annurev-marine-010213-135133.

Straneo, F., and Coauthors, 2013: Challenges to Understanding the Dynamic Response of Greenland's Marine Terminating Glaciers to Oceanic and Atmospheric Forcing. Bull. Amer. Meteor. Soc., 94, 1131–1144, https://doi.org/10.1175/BAMS-D-12-00100.1.

Sutherland, D. A., & Cenedese, C. (2009). Laboratory Experiments on the Interaction of a Buoyant Coastal Current with a Canyon: Application to the East Greenland Current. Journal of Physical Oceanography, 39(5), 1258–1271. https://doi.org/10.1175/2008jpo4028.1

Sutherland, D. A., & Pickart, R. S. (2008). The East Greenland Coastal Current: Structure, variability, and forcing. Progress in Oceanography, 78(1), 58–77. https://doi.org/10.1016/j.pocean.2007.09.006

Swift, J. H., and K. Aagaard, 1981: Seasonal transitions and water mass formation in the Iceland and Greenland seas. Deep-Sea Res., 28A, 1107–1129, https://doi.org/10.1016/0198-0149(81)90050-9.

Swingedouw D, Houssais M-N, Herbaut C, Blaizot A-C, Devilliers M and Deshayes J (2022) AMOC Recent and Future Trends: A Crucial Role for Oceanic Resolution and Greenland Melting? Front. Clim. 4:838310. doi: 10.3389/fclim.2022.838310

Talley, L. D. (2013). Closure of the Global Overturning Circulation Through the Indian, Pacific, and Southern Oceans: Schematics and Transports. Oceanography, 26(1), 80–97. http://www.jstor.org/stable/24862019

The IMBIE Team: Mass balance of the Greenland Ice Sheet from 1992 to 2018, Nature, 579, 233–239, https://doi.org/10.1038/s41586-019-1855-2, 2020

Thornalley, D.J.R., Oppo, D.W., Ortega, P. et al. Anomalously weak Labrador Sea convection and Atlantic overturning during the past 150 years. Nature 556, 227–230 (2018). https://doi.org/10.1038/s41586-018-0007-4

Timmermans, M.-L., & Marshall, J. (2020). Understanding Arctic Ocean circulation: A review of ocean dynamics in a changing climate. Journal of Geophysical Research: Oceans, 125, e2018JC014378. https://doi.org/10.1029/2018JC014378

Tonboe, R. T., Eastwood, S., Lavergne, T., Sørensen, A. M., Rathmann, N., Dybkjær, G., Pedersen, L. T., Høyer, J. L. and Kern, S., 2016: The EUMETSAT sea ice concentration climate data record, The Cryosphere, 10(5), 2275–2290, https://doi.org /tc-10-2275-2016.

Toudal Pedersen, L., Dybkjær, G., Eastwood, S., Heygster, G., Ivanova, N., Kern, S., Lavergne, T., Saldo, R., Sandven, S., Sørensen, A. and Tonboe, R., 2017: ESA Sea Ice Climate Change Initiative (Sea_Ice_cci): Sea

Ice Concentration climate data record from the AMSR-E and AMSR-2 instruments at 25km grid spacing, version 2.0, https://doi.org/10.5285/c61bfe88-873b-44d8-9b0e-6a0ee884ad95.

Trenberth, K. E., W. G. Large, and J. G. Olson, 1990: The Mean Annual Cycle in Global Ocean Wind Stress. J. Phys. Oceanogr., 20, 1742–1760, https://doi.org/10.1175/1520-0485(1990)020<1742:TMACIG>2.0.CO;2.

Trusel, L.D., Das, S.B., Osman, M.B., Evans, M.J., Smith, B.E., Fettweis, X., McConnell, J.R., Noel, B.P.Y. and van de Broeke, M.R. (2018) Nonlinear rise in Greenland runoff in response to post-industrial Arctic warming. Nature, 564, 104– 108.

UK Met Office. 2012. GHRSST Level 4 OSTIA Global Foundation Sea Surface Temperature Analysis (GDS version 2). Ver. 2.0. PO.DAAC, CA, USA. Dataset accessed [2020-06-10] at https://doi.org/10.5067/GHOST-4FK02

Våge, K., Spengler, T., Davies, H.C. and Pickart, R.S. (2009), Multi-event analysis of the westerly Greenland tip jet based upon 45 winters in ERA-40. Q.J.R. Meteorol. Soc., 135: 1999-2011, https://doi.org/10.1002/qj.488.

Våge, K., Pickart, R. S., Moore, G. W. K., & Ribergaard, M. H. (2008). Winter mixed layer development in the central Irminger Sea: The effect of strong, intermittent wind events. Journal of Physical Oceanography, 38, 541– 565. https://doi.org/10.1175/2007JPO3678.1

Våge, K., Pickart, R. S., Sarafanov, A., Knutsen, Ø., Mercier, H., Lherminier, P., van Aken, H. M., Meincke, J., Quadfasel, D., & Bacon, S. (2011). The Irminger Gyre: Circulation, convection, and interannual variability. Deep-Sea Research Part I: Oceanographic Research papers, 58, 590–614. https://doi.org/10.1016/j.dsr.2011.03.001

Våge, K., R. S. Pickart, M. A. Spall, G. Moore, H. Valdimarsson, D. J. Torres, S. Y. Erofeeva, and J. E. Ø. Nilsen, 2013: Revised circulation scheme north of the Denmark Strait. Deep-Sea Res. I, 79, 20–39, https://doi.org/10.1016/j.dsr.2013.05.007.

Våge, K., Papritz, L., Håvik, L. et al. Ocean convection linked to the recent ice edge retreat along east Greenland. Nat Commun 9, 1287 (2018). https://doi.org/10.1038/s41467-018-03468-6

Van Aken, H. M., M. F. De Jong, and I. Yashayaev (2011), Decadal and multi-decadal variability of Labrador Sea Water in the northern North Atlantic Ocean derived from tracer distributions: heat budget, ventilation, and advection, Deep Sea Res., Part I, 58, 505– 523, https://doi.org/10.1016/j.dsr.2011.02.008

Vinogradova, N., Lee, T., Boutin, J., Drushka, K., Fournier, S., Sabia, R., ... & Lindstrom, E. (2019). Satellite salinity observing system: Recent discoveries and the way forward. Frontiers in Marine Science, 243. https://doi.org/10.3389/fmars.2019.00243

Walters, D., Baran, A. J., Boutle, I., Brooks, M., Earnshaw, P., Edwards, J., Furtado, K., Hill, P., Lock, A., Manners, J., Morcrette, C., Mulcahy, J., Sanchez, C., Smith, C., Stratton, R., Tennant, W., Tomassini, L., Van Weverberg, K., Vosper, S., Willett, M., Browse, J., Bushell, A., Carslaw, K., Dalvi, M., Essery, R., Gedney, N., Hardiman, S., Johnson, B., Johnson, C., Jones, A., Jones, C., Mann, G., Milton, S., Rumbold, H., Sellar, A., Ujiie, M., Whitall, M., Williams, K., and Zerroukat, M.: The Met Office Unified Model Global Atmosphere 7.0/7.1 and JULES Global Land 7.0 configurations, Geosci. Model Dev., 12, 1909–1963, https://doi.org/10.5194/gmd-12-1909-2019, 2019.

Wang, H., Legg, S., & Hallberg, R. (2018). The effect of Arctic freshwater pathways on North Atlantic convection and the Atlantic meridional overturning circulation. Journal of Climate, 31(13), 5165-5188.

Wang Y, Bi H, Liang Y. A Satellite-Observed Substantial Decrease in Multiyear Ice Area Export through the Fram Strait over the Last Decade. Remote Sensing. 2022; 14(11):2562. https://doi.org/10.3390/rs14112562

Weijer, W., Maltrud, M. E., Hecht, M. W., Dijkstra, H. A., and Kliphuis, M. A. (2012), Response of the Atlantic Ocean circulation to Greenland Ice Sheet melting in a strongly-eddying ocean model, Geophys. Res. Lett., 39, L09606, doi:10.1029/2012GL051611.

Weijer, W., and Coauthors, (2019). Stability of the Atlantic meridional overturning circulation: A review and synthesis. Journal of Geophysical Research: Oceans, 124, 5336–5375, https://doi.org/10.1029/2019JC015083.

Weijer, W., Cheng, W., Garuba, O. A., Hu, A., & Nadiga, B. T. (2020). CMIP6 models predict significant 21st century decline of the Atlantic Meridional Overturning Circulation. Geophysical Research Letters, 47, e2019GL086075. https://doi.org/10.1029/2019GL086075

Williams, K., Copsey, D., Blockley, E. W., Bodas-Salcedo, A., Calvert, D., Comer, R., Davis, P., Graham, T., Hewitt, H. T., Hill, R., Hyder, P., Ineson, S., Johns, T. C., Keen, A. B., Lee, R. W., Megann, A., Milton, S. F., Rae, J. G. L., Roberts, M. J., Scaife, A. A., Schiemann, R., Storkey, D., Thorpe, L., Watterson, I. G., Walters, D. N., West, A., Wood, R. A., Woollings, T., and Xavier, P. K.: The Met Office Global Coupled model 3.0 and 3.1 (GC3.0 & GC3.1) configurations, J. Adv. Model. Earth Sy., 10, 357–380, https://doi.org/10.1002/2017MS001115, 2017.

Williams, K. D., Copsey, D., Blockley, E. W., Bodas-Salcedo, A., Calvert, D., Comer, R., … Xavier, P. K. (2017). The Met Office Global Coupled model 3.0 and 3.1 (GC3.0 and GC3.1) configurations. Journal of Advances in Modeling Earth Systems, 10, 357– 380. https://doi.org/10.1002/2017MS001115

Wolfe, C. L., & Cenedese, C. (2006). Laboratory experiments on eddy generation by a buoyant coastal current flowing over variable bathymetry. Journal of Physical Oceanography, 36(3), 395–411. https://doi.org/10.1175/JPO2857.1

Yang, Q., Dixon, T., Myers, P. et al. (2016). Recent increases in Arctic freshwater flux affects Labrador Sea convection and Atlantic overturning circulation. Nature Communication, 7, 10525. https://doi.org/10.1038/ncomms10525

Yeager, S., and G. Danabasoglu, 2014: The Origins of Late-Twentieth-Century Variations in the Large-Scale North Atlantic Circulation. J. Climate, 27, 3222–3247, https://doi.org/10.1175/JCLI-D-13-00125.1.

Zhang, R., Sutton, R., Danabasoglu, G., Kwon, Y. O., Marsh, R., Yeager, S. G., ... & Little, C. M. (2019). A review of the role of the Atlantic meridional overturning circulation in Atlantic multidecadal variability and associated climate impacts. Reviews of Geophysics, 57(2), 316-375.

Zhang, J., Weijer, W., Steele, M. et al. Labrador Sea freshening linked to Beaufort Gyre freshwater release. Nat Commun 12, 1229 (2021). https://doi.org/10.1038/s41467-021-21470-3

Summary

In the Atlantic, the ocean circulation transports warm and light waters northwards at the surface, and cold and dense waters southwards at depth. This large-scale circulation is called Atlantic Meridional Overturning Circulation (AMOC). Because the AMOC redistributes heat and freshwater across the Atlantic, it is a critical element of the climate system. Climate change is predicted to lead to a weakening of the AMOC in the coming century which could severely affect people and ecosystems. A key driver of the AMOC is the formation of deep waters in the Subpolar North Atlantic (SPNA). As the warm, saline surface waters from the upper branch of the AMOC reach the SPNA, they lose heat to the atmosphere, thereby getting colder and denser. In winter, strong air-sea fluxes lead to vertical mixing of the water column in the interior of the Labrador, Irminger and Nordic Seas, to depths of more than 1km. This process, called deep convection, is essential for the export of deep and cold waters to the south. In the coming decades freshwater input to the SPNA from the Greenland ice sheet and the Arctic is predicted to increase. This additional freshwater could increase the upper ocean stratification where deep convection takes place, limiting vertical mixing and potentially weakening the AMOC.

However, waters from Greenland and the Arctic do not directly enter these regions and are first advected over the Greenland continental shelf by narrow western boundary currents. On the Eastern side of Greenland, the East Greenland Current (EGC) and its coastal branch (EGCC) transport the fresh shelf waters southwards. Past Cape Farewell, at the southern tip of Greenland, they become the West Greenland Current (WGC) and West Greenland Coastal Current (WGCC). While west of Greenland, both eddies and winds are known to play a role in steering shelf waters into the Labrador Sea, possible pathways for freshwater into the Irminger and Nordic Seas east of Greenland have been less studied. As recent observations showed the importance of overturning east of Greenland for the AMOC, better understanding how Greenland and Arctic origin waters reach these regions is critical.

In this thesis, I identify regions of enhanced exchanges between the east Greenland shelf and neighbouring seas and investigate mechanisms driving these exchanges. This work primarily relies on a new observational dataset, composed of 120 surface drifters deployed in five different regions of the east Greenland shelf between 2019 and 2022. Surface drifters are floating oceanographic instruments that follow waters at a given depth, collecting GPS positions and other properties such as sea surface temperature. Two types of drifters were used, the one anchored at 15m depth, and the other at 40cm.

Trajectories from these surface drifters show very limited advection of fresh shelf waters into the Irminger Sea. Most of the drifters deployed at the east Greenland shelfbreak followed the EGC and EGCC until the southern tip of Greenland and continued into the WGC and WGCC over the west Greenland shelf. There, about two thirds of the drifters were exported into the Labrador Sea. Only limited drifter trajectories were however available over the north-east part of Greenland, and investigating exchanges between

the north-east Greenland shelf and the Nordic Seas would require further work. Some areas of the east Greenland shelf are more favourable to export: I show that at the southern tip of Greenland, strong westerly wind events can drive fresh surface waters off-shelf. This was first illustrated by the export of five of the shallow surface drifters deployed in 2019 to the Irminger Sea during a westerly wind event, and further investigated using satellite data, a high-resolution model, and trajectories from existing drifters. In particular, tip jets, strong westerly wind events occurring south of Greenland in winter, can lead to the export of freshwater to the south and east of Greenland, and drive sea-ice into the Irminger Sea.

This new drifter dataset also allowed to investigate the surface circulation over the shelf in areas where observations were so far sparse. I show that though the coastal and main branch of the EGC are distinct, they interact with each other along the east Greenland shelf. The deep Sermilik and Kangerdlussuaq troughs in particular drive bifurcations of the EGC into the EGCC, resulting in most drifters deployed at the edge of the shelf entering the coastal current as they are advected downstream. At Cape Farewell, as the EGC becomes the WGC, the coastal branch approaches the main branch and exchanges take place between the two cores. This leads to drifters from the EGCC being as likely to continue into the main branch of the WGC as into its coastal branch. Such exchanges could influence how much freshwater is exported into the Labrador Sea west of Greenland.

Finally, I investigate the representation of exchanges taking place between the east Greenland shelf and interior seas in the HadGEM3 climate model at three different horizontal resolutions. The small scale of the east Greenland shelf is a major challenge for the ability of climate models to correctly represent the circulation of fresh shelf waters and where they exit the shelf. The one-degree resolution model is unable to represent the EGC as a narrow boundary current, leading to excessive freshwater export into the Labrador Sea. Increasing the resolution to 0.25 and 0.12 degrees allows to better represent the circulation over the shelf but is not sufficient to properly represent cross-shelf exchanges, and the models we use show either excessive or too limited exchanges. This misrepresentation can lead to under or overestimation of freshwater export into the interior seas of the SPNA.

This work confirmed that only little export of freshwater takes place on the eastern side of Greenland, though local processes, driven by winds or eddies, can lead to exchanges between the shelf and neighboring seas. It also showed the importance of the circulation over the east Greenland shelf to understanding pathways for freshwater from Greenland and Arctic origin into the Labrador Sea. Further observational and modelling studies are necessary to understand exchanges between the north-east Greenland shelf and the Nordic Seas, the role of sea ice, and to quantify the input of freshwater to deep convection regions.

Samenvatting

In de Atlantische Oceaan transporteren zeestromingen warm en licht water noordwaarts aan het oppervlak en koud en zwaar water zuidwaarts in de diepte. Deze grootschalige circulatie is bekend als de Atlantic Meridionale Omwentelingsirculatie (*Atlantic Meridional Overturning Circulation, AMOC*). Omdat de AMOC warmte en zout over de Atlantische Oceaan herverdeelt, is het een kritiek onderdeel van het klimaatsysteem. Door klimaatverandering zal de AMOC naar verwachting in de komende eeuw verzwakken, wat ernstige gevolgen kan hebben voor mensen en ecosystemen. De AMOC wordt in belangrijke mate aangedreven door de vorming van diepe wateren in de Subpolaire Noord-Atlantische Oceaan (SPNA). Als het warme, zoute oppervlaktewater van de bovenste tak van de AMOC de SPNA bereikt, verliest het warmte aan de atmosfeer, waardoor het kouder en zwaarder wordt. In de winter leiden sterke lucht-zee warmtefluxen tot vertikale menging van de waterkolom, tot dieptes van meer dan 1 km in de Labrador-, Irminger- en Noorse zeeën. Dit proces, bekend als diepe convectie, is essentieel voor het zuidwaarts transport van koud water op diepte. In de komende decennia zal de zoetwaterinstroom naar de SPNA vanuit de Groenlandse ijskap en het Noordpoolgebied toenemen. Als dit extra zoete water de regio's bereikt waar diepe convectie plaatsvindt, kan het de stabiele gelaagdheid in de bovenste oceaan in deze regio's verhogen, en de AMOC mogelijk verzwakt.

Het water van Groenland en het Noordpoolgebied komt deze regio's echter niet rechtstreeks binnen. Ze worden eerst over het Groenlandse continentale plat, de ondiepe regio nabij de kust, getransporteerd door smalle grensstromen. Aan de oostkant van Groenland transporteren de Oost-Groenlandse Stroom (*East Greenland Current*, EGC) en haar kusttak (*East Greenland Coastal Current*, EGCC) het relatief zoete water van het plat zuidwaarts. Voorbij Kaap Farewell, op de zuidpunt van Groenland, gaan ze over in de West-Groenlandse Stroom (*West Greenland Current,* WGC) en de West-Groenlandse Kuststroming (*West Greenland Coastal Current*, WGCC). Ten westen van Groenland spelen zowel wervelingen als windpatronen een rol bij het verspreiden van water naar de Labradorzee. De mogelijke routes van zoet water naar de Irmingerzee en de Noorse Zeeën, ten oosten van Groenland, zijn minder goed bestudeerd, hoewel recente waarnemingen het belang van deze regio voor de AMOC hebben aangetoond.

In dit proefschrift identificeer ik regio’s waar interactie tussen het oostelijke Groenlandse kust regio en de open zee plaatsvindt, en onderzoek ik de mechanismen die deze interactie aandrijven. Dit werk is voornamelijk gebaseerd op een nieuwe observationele dataset, bestaande uit 120 drifters die tussen 2019 en 2022 zijn uitgezet in vijf verschillende regio's van het oostelijk deel van de Groenlandse plat. Drifters zijn drijvende oceanografische instrumenten die het water op een bepaalde diepte volgen en GPS-posities en andere eigenschappen zoals de temperatuur van het zeeoppervlak verzamelen. Twee types drifters werden gebruikt, verankerd op 15 m en 40 cm diepte.

De trajecten van deze oppervlakte drifters laten een zeer beperkte export van zoetwater naar de Irmingerzee zien. De meeste drifters die bij oost-Groenland werden ingezet, volgden de EGC en EGCC tot de zuidpunt van Groenland en gingen verder in de WGC en WGCC west van Groenland. Daar dreven ongeveer tweederde van de drifters af naar de Labradorzee. Er waren echter slechts beperkte trajecten van drifters beschikbaar over het noordoostelijke deel van de Groenlandse plat, en om de zoetwater routes naar de Noorse Zeeën te bestuderen is meer onderzoek nodig. Op bepaalde plaatsen op het Oost-Groenlandse plat zijn de omstandigheden gunstiger voor export: Ik toen aan dat op de zuidpunt van Groenland sterke westenwinden zoet oppervlaktewater van het continentale plat kunnen stuwen. Dit werd voor het eerst geïllustreerd door vijf van de ondiepe drifters die tijdens een westelijk windsysteem naar de Irmingerzee gevoerd werden. Dit heb ik verder onderzocht met behulp van satellietgegevens, een hoge-resolutie model, en trajecten van bestaande drifters. Met name tip jets, sterke westenwinden die ’s winters voorkomen in het zuiden van Groenland, kunnen ter plekke zoetwater verplaatsen, en duwen daarmee zeeijs tot in de Irmingerzee.

Deze nieuwe drifter-dataset maakte het ook mogelijk om de oppervlaktecirculatie over het plat te onderzoeken in gebieden waar tot nu toe weinig waarnemingen waren. Ik toon aan dat, hoewel de kust- en hoofdstroom van de EGC apart zijn, er uitwisselingen zijn tussen beide. Met name de diepe troggen van Sermilik en Kangerdlussuaq veroorzaken splitsingen van de EGC in de EGCC, waardoor de meeste drifters die aan de rand van het plat worden ingezet in de kuststroming terechtkomen als ze stroomafwaarts worden meegevoerd. Bij Kaap Farewell, waar de EGC overgaat in de WGC, nadert de kusttak de hoofdtak en vindt uitwisseling plaats tussen de twee kernen. Dit leidt ertoe dat drifters van de EGGC even waarschijnlijk in de hoofdtak van de WGC terechtkomen als in de kusttak. Dergelijke uitwisselingen zouden de export van zoet water naar de Labradorzee ten westen van Groenland kunnen beïnvloeden.

Tot slot onderzoek ik hoe de uitwisselingen tussen de oostelijke Groenlandse plat en de open zeeën in het HadGEM3-klimaatmodel worden gerepresenteerd, op drie verschillende horizontale resoluties. Het zeer smalle oostelijke Groenlandse plat is een uitdaging voor klimaatmodellen. Bij een modelresolutie van één graad kan de EGC niet juist worden weergeven, wat leidt tot overmatige zoetwaterexport naar de Labradorzee. Door de resolutie te verhogen naar 0,25 en 0,12 graden wordt de circulatie over het plat realistischer, maar dit is niet voldoende om de uitwisseling goed te simuleren. Dit kan leiden tot een onder- of overschatting van de zoetwaterexport naar de open oceaan.

Dit werk bevestigt dat er weinig zoetwaterexport plaatsvindt aan de oostkant van Groenland, hoewel lokale processen, aangedreven door windsystemen of wevelingen, kunnen leiden tot uitwisselingen tussen de kust regio en aangrenzende zeeën. Het onderzoek toonde ook het belang aan van de circulatie over het oostelijke deel van de Groenlandse plat voor het begrijpen van de routes van zoet water uit Groenland en het Noordpoolgebied naar de Labradorzee. Verdere waarnemings- en modelstudies zijn nodig om de uitwisseling tussen de noordoostelijke Groenlandse plaat en de Noorse Zeeën, en de rol van zeeijs te begrijpen, en om de toevoer van zoet water naar diepe convectiegebieden te kwantificeren.

Résumé

Les grands courants marins de l'océan Atlantique Nord transportent des eaux chaudes des tropiques vers le pôle en surface, et des eaux froides du pôle vers les tropiques en profondeur. Cette circulation est appelée Circulation Méridienne de Retournement Atlantique *(Meridional Overturning Circulation,* AMOC). Le changement climatique devrait entraîner un affaiblissement de l'AMOC au cours du siècle à venir, ce qui pourrait avoir de graves répercussions sur les populations humaines et les écosystèmes. L'un des principaux éléments de l'AMOC est la formation d'eaux profondes dans l'Atlantique Nord subpolaire (SPNA). Lorsque les eaux chaudes et salines de la branche supérieure de l'AMOC atteignent l'Atlantique Nord subpolaire, elles perdent de la chaleur, devenant ainsi plus froides et plus denses. En hiver, d'importants flux air-mer entraînent un mélange vertical de la colonne d'eau dans les mers du Labrador, d'Irminger et Nordiques, atteignant des profondeurs de plus de 1 km. Ce mécanisme, appelé convection profonde, est essentiel à la formation des eaux qui sont exportées vers le sud par la branche inférieure de l'AMOC. Au cours des prochaines décennies, de plus en plus d'eaux douce entrera dans l'Atlantique depuis le Groenland et de l'Arctique. Si elles atteignent les mers où la convection profonde a lieu, la stratification de la colonne d'eau y augmentera, limitant la formation d'eaux profondes et potentiellement affaiblissant l'AMOC.

Toutefois, les eaux du Groenland et de l'Arctique ne pénètrent pas directement dans ces régions mais sont d'abord transportées le long du plateau continental du Groenland. Du côté est du Groenland, le courant est du Groenland (*East Greenland Current,* EGC) et sa branche côtière (*East Greenland Coastal Current*, EGCC) transportent ces eaux vers le sud. Au cap Farewell, à l'extrémité sud du Groenland, ces courants deviennent le courant ouest du Groenland (*West Greenland Current,* WGC) et le courant côtier ouest du Groenland (*West Greenland Coastal Current*). À l'ouest du Groenland, les vents et les instabilités du courant exportent des eaux douces vers la mer du Labrador. À l'Est, vers la mer d'Irminger et les mers Nordiques, ces échanges ont été moins étudiés, alors que de récentes observations ont démontré l'importance de ces régions pour l'AMOC.

Dans cette thèse, j'identifie les régions d'échanges entre la côte du Groënland et les mers adjacentes, et étudie les mécanismes à l'origine de ces échanges. Ce travail s'appuie principalement sur des observations effectuées à l'aide de 120 bouées dérivantes déployées dans cinq régions de l'est du Groenland entre 2019 et 2022. Les bouées dérivantes de surface (*surface drifters*) sont des instruments océanographiques flottants qui suivent les eaux à une profondeur donnée, collectant leur position et d'autres informations telles que la température de l'eau. Deux types de bouées ont été utilisées, ancrées à 40 cm et à 15 m de profondeur.

Les trajectoires de ces bouées dérivantes montrent que très peu des eaux douces se trouvant sur le plateau continental du Groënland entrent dans la mer d'Irminger. La plupart des bouées suivent l'EGC et l'EGCC jusqu'à la pointe sud du Groenland et

continuent à l'ouest du Groënland dans le WGC et le WGCC. Environ deux tiers d'entre elles sont ensuite exportées dans la mer du Labrador. Très peu de données sont cependant disponibles dans la partie nord-est du Groenland, limitant l'étude des échanges entre cette région et les mers Nordiques. Dans certaines zones du plateau est du Groenland des échanges locaux avec les mers voisines ont lieu. Par exemple je montre qu'à l'extrémité sud du Groenland de forts vents d'ouest peuvent entraîner les eaux de surface à l'extérieur du plateau. Ce phénomène a d'abord été observé par cinq bouées dérivantes de surface peu profondes, exportées vers la mer d'Irminger lors d'un épisode de vents d'ouest, puis étudié plus en détail à l'aide de données satellitaires, d'un modèle à haute résolution et d'autres bouées dérivantes. En particulier, les « tip jets », de forts vents d'ouest se produisant au sud du Groenland en hiver, peuvent conduire à l'exportation d'eau douce et de glace de mer au sud et à l'est du Groenland.

Ce nouvel ensemble de données dérivantes m'a également permis d'étudier les courants de surface dans des zones où les observations étaient jusqu'à présent rares. Je montre que, bien que la branche côtière et la branche principale de l'EGC soient distinctes, elles interagissent l'une avec l'autre le long du plateau continental de l'Est du Groenland. En particulier les profondes dépressions de Sermilik et de Kangerdlussuaq entraînent des bifurcations de l'EGC vers l'EGCC, ce qui fait que la plupart des bouées dérivantes déployées dans l'EGC entrent dans le courant côtier. Au cap Farewell, le courant côtier se rapproche de l'EGC, et des échanges ont lieu entre les deux branches. Ainsi, les bouées dérivantes se trouvant dans l'EGCC avant d'atteindre le cap ont autant de chances de continuer dans la branche principale du WGC que dans sa branche côtière. De tels échanges pourraient influencer la quantité d'eau douce exportée dans la mer du Labrador à l'ouest du Groenland.

Pour finir, j'utilise le modèle climatique HadGEM3 à différents degrés de résolution spatiale pour comprendre l'impact de la résolution du modèle sur la représentation des échanges entre le plateau continental de l'est du Groenland et les mers adjacentes. Le modèle à résolution d'un degré ne peut représenter l'EGC comme un courant étroit longeant la côte du Groënland, ce qui entraîne une exportation excessive d'eau douce dans la mer du Labrador. L'augmentation de la résolution à 0,25 et 0,12 degré permet de mieux représenter la circulation sur le plateau mais n'est pas suffisante pour représenter correctement les échanges avec les mers adjacentes. Les modèles utilisés dans cette étude produisent des échanges excessifs ou trop limités, ce qui peut entraîner une sous-estimation ou une surestimation de l'exportation d'eau douce dans les mers intérieures du SPNA.

Cette thèse confirme que l'exportation d'eau douce depuis l'est du Groenland vers la mer d'Irminger est faible, bien que des vents importants ou des instabilités du courant puissent causer des échanges locaux. Elle montre également l'importance de la circulation sur le plateau continental est du Groenland pour l'export d'eaux douces vers la mer du Labrador. D'autres études d'observation et de modélisation seront toutefois nécessaires pour comprendre les échanges entre le plateau du nord-est du Groenland et les mers nordiques, le rôle de la glace de mer, et pour quantifier l'apport d'eau douce dans les régions de convection profonde.

Acknowledgements

I have been both impatient and nervous about writing this section. After more than four years of intense work, high and lows, pandemic, doubts, fieldwork, activism, working from the office and from home, broken technological devices and other adventures, there are so many people to thank, so many words to write, that I fear I cannot do justice to the countless ways I found support, the countless people I relied on during my PhD.

Before thanking all the people who kept me going through the years, I want to acknowledge those without whom this research would never have been possible: The crews and science teams of the research ships from which the drifters used in this study were deployed. In 2019, we sailed with the Adolph Jansen from the island of Kulusuk to the edge of the Greenland continental shelf, where we deployed our first batch of drifters. I got pretty seasick on that small boat, but that memory is outshined by the one of the icebergs, glaciers and the whale we saw from close when getting back at the Greenland coast. That same year, we deployed another batch of drifters in Fram Strait, from the research icebreaker R/V Kronprins Haakon. I will never forget my first walk on sea ice, the sound of the boat making its way through it, and the sighting of a polar bear next to the boat, wondering where this nice food smell came from. In 2020, despite the pandemic, we were able to board the R/V Pelagia, that brought us from Texel all the way to Cape Farewell, where we deployed our third batch of drifters. It was a very special experience to be onboard with a very small science team, working only during the day, but still managing to do everything we planned. In 2021, the last batch of drifters was deployed at Scoresby Sund and at Denmark Strait by Rob, during his own expedition to the Subpolar North Atlantic. A very important aspect for keeping motivation when being at sea for several weeks is food, and I want to extend a special thanks to the cooks who strived to provide good vegan options onboard!

Femke, I feel like this PhD is also an adventure we embarked on together (quite literally, given that we've been on four field campaigns). Thank you for giving me the opportunity to work on such an essential topic, and for all the work we did together in these 4+ years. It was maybe not always smooth sailing (and with the pandemic, we had bad weather coming our way!), but I could always rely on your advice and support, whether my existential anxiety regarded the direction of a paper, or the wording of an e-mail. The fieldwork we went on together in Greenland will remain one of the dearest memories of my PhD, despite my (I maintain, not so irrational) fear of encountering a polar bear. I am also very grateful for the opportunity you gave me to work mostly from Amsterdam in the last 2 years, as well as your trust in my ability to combine writing my PhD with getting heavily involved in climate activism.

Very little would have been possible without my PhD partner in crime, Nora. I still remember when we met at the hotel in Den Burg before the interviews for the position. I thought I had very little chance to get it with you in the game. Luckily, there was space for us both! Thank you for the time we spent together at NIOZ, on ships, at conferences

and in Den Helder, for the science discussions, the feedbacks on writings, and all the healthy ranting. Sasha, Miriam, Nick, Peter, Sjoerd, it was great to see the physical oceanography group at NIOZ grow and get more opportunities to discuss science (or eat cake) together. Florine, Erika, it was a pleasure to work with you, and the studies you did during your internship and Masters' thesis really contributed to my thinking and research ideas.

Eleanor, Nick, Ilona, thank you for our drifter discussions. Knowing that similar experiments were being carried out in different regions of Greenland, and being able to discuss issues we faced, or ideas we had, share our results and inspire each other, was very valuable. Renske, thanks for the work we did together on the impact of tip jet events at Cape Farewell.

A PhD is much more than 4+ years of research. It is a chunk of life, it is countless people we met, who influence our work, but also us as a person, and who keep us going through the years and beyond. The isolation of NIOZ on Texel can sometimes feel a bit much, as there seems to be hardly anything else than our research work. Without the strong-knit community of PhD students, it would be impossible to go on. Even though I moved further and further away from the institute, I am eternally grateful for the time spent together (rollerskating, surfing, talking about everything and nothing all at once), and for the support and advice I found in the PhD student community. In particular I want to thank Laura. You really kept me afloat during the pandemic. Our weekly walks around Den Helder (the waterfront or the park?) were a breath of air in an increasingly suffocating world, and I am extremely happy to count you as a good friend.

Living in another country can make it complicated to keep strong ties with old friends back home. Laure-Anne, Céline, Ségo, even as we have been seeing each other less and less frequently, I know I can always rely on your presence at the other end of a WhatsApp conversation, which was especially important during the deepest months of the pandemic. Thank you for still being around despite the distance and the sometimes very long times spent without talking to each other (it only makes the next call longer).

One month into my PhD, my climate anxiety and anger had become so strong that I could not anymore soothe it by reading about other people entering coal mines and disrupting oil companies' annual meetings. Even though (and maybe because) the topic of my PhD was relevant for climate science, I could not anymore sit at my desk the whole day to produce some more (even though essential) details of very specific processes, while knowing that the huge body of knowledge already amassed about the climate crisis and its disastrous consequences was not pushing policymakers to take necessary action. I had to get involved, not only with the production of knowledge, but with the people actually pushing for change. This is when I found the people from Extinction Rebellion, and I cannot imagine a world where I'd have gone through my PhD without the strength and the connections I found in the climate movement. Every single person I met gave me an inch more hope, an inch more will to fight every single day that we are delaying our response to the climate crisis. I could never mention and individually thank all the wonderful people I got to know through these 4 years, from the old PSC crew, XR Alkmaar

and Castricum, tthe Klimaatkamp, Rebellion teams I've been involved with, the program team of the Klimaatrebellie, XR Amsterdam, Behoud Lutkemeer, S4XR, De Sering, and of course Awesomesauce. From the people who have been with me since day one, to the people I met in the most recent waves of actions. Thank you.

This last year, my main involvement has been with Scientist Rebellion, a network of academics who believe that our community has a role to play in the climate movement, that the time is so late, the case so strong, that scientists and scholars should organize, join protests and civil disobedience actions, using their position in society to heighten the sense of emergency on the climate crisis. I met incredible people, who showed me all the nuances academic activism could take, who opened doors I never even knew where there, from organizing colleagues to get universities to cut ties with the fossil fuel industry to legitimizing activism in academia by discussing it at scientific conferences. This new network of academics was also a strong help in the last stage of my PhD as I could profit from their own experience with finishing their thesis (and share an unofficial office in Amsterdam). Again, there is no way I'd be able to thank everyone, but I do want to make a shout out to the people who first started S4XR with me, Miriam, Federico, Ernst, you were really an inspiration for me when I felt uncertain about being a climate activist and a scientist, to Fabian, without whose drive (and optimism?), Scientist Rebellion Netherlands would never have been a thing, Paulina, with whom I organized so much, before and in SR, Nicole, who became my activist rock at NIOZ.

Some of the wonderful people I met through activism became close friends, and an integral part of my life in Amsterdam. Thanks to Koen and Marthe, for supporting me through the last phases of my thesis, when I could sometimes not see how I would ever manage to finish it. To Akelei, for the work sessions and the gym sessions, the long chats around ginger tea and the parties. Ismani, for being around for so long, and still my favourite person to talk politics and strategy with (even when we disagree), Ruerdje for the always listening ear and the deep chats. And many, many others. Amsterdam, and the Netherlands more generally, would have been way less fun without you.

Thank you finally to everyone who proof-read, commented, translated parts of this thesis: Nora and Femke for a lot of what is here, Miriam and Anneke for the introduction, Niels and Ismani for the Dutch version of the summary.

As I finish writing these acknowledgments (I do need to send the thesis to the printer!), I feel so many names, so many highlights are still missing. So, one last time, I want to thank everyone who has been around in the last years, whether at NIOZ or in XR, in Amsterdam, on Texel, or back in France.

Je veux adresser ces dernières lignes de remerciements à ma famille, qui m'a tôt donné une fascination pour l'océan. Qu'est ce qui m'a donné cette sensibilité et proximité pour la mer, ce désir d'embarquer, sur des expéditions océanographiques ou autres navires ? Peut être était-ce Dunkerque où le passé et le présent s'entrelacent avec l'océan, peut être Thalassa, tous les vendredis soirs sur France 3, ou peut être votre propre fascination

que vous m'avez transmise? Au moment où j'écris ces lignes, j'ai une pensée pour Mamie Marie, qui a certainement contribué à cet intérêt et je pense aurait été très fière de me voir devenir océanographe. Papy, Mamie, marraine, et tout le monde, je suis désolée de ne pas vous avoir plus vus ces dernières années. Je sais que vous avez suivi avec intérêt mon travail et mes expéditions, et je pense à vous. Et bien sûr, papa, maman, merci de m'avoir soutenue pendant toutes ces années, d'avoir toujours été là dans les moments compliqués, ou les moments importants. De Brest à Oban, de Texel à Amsterdam, et maintenant à Hambourg, vous ne vous attendiez peut-être pas à ce que j'ai autant la bougeotte, mais vous m'avez accompagnée dans tous mes changements de décor et déménagements, maitrisant à perfection l'art du Tetris dans le Scénic et du (dé)montage de lit mezzanine.

Merci.

Elodie

List of publications

Duyck, E*., &* De Jong, M. F. *(*2021*).* Circulation over the south-east Greenland shelf and potential for liquid freshwater export: A drifter study*. Geophysical Research Letters,* 48*, e2020JB020886.* https://doi.org/10.1029/2020GL091948

Duyck, E., Gelderloos, R., & de Jong, M. F. (2022). Wind-Driven Freshwater Export at Cape Farewell. Journal of Geophysical Research: Oceans, 127(5), e2021JC018309. https://doi.org/10.1029/2021JC018309

Duyck, E., & De Jong, M. F. (2023). Cross-shelf exchanges between the east Greenland shelf and interior seas. Journal of Geophysical Research: Oceans, 128, e2023JC019905. https://doi.org/10.1029/2023JC019905

About the author

Elodie Duyck was born in 1994 in Villeneuve d'Ascq and grew up in Northern France. She always had a fascination for the ocean, and knew she wanted to work with the sea. In 2017, she graduated from the ENSTA Bretagne engineering school and the university of Brest, with a double Masters, in ocean mapping and practical oceanography, and in ocean and climate physics. During her studies, she was able to join two fieldwork expeditions on oceanographic vessels, which strengthened her decision to work on, and with, the ocean.

She wrote her Master Thesis at the IUEM in Brest and SAMS in Oban (Scotland) about Subpolar Mode Waters in the Subpolar North Atlantic. After graduation, she worked for a dredging company, helping with sea floor mapping for the installation of cables for offshore wind farms. In February 2019, she started her PhD at NIOZ, under the supervision of Femke de Jong. She is now working as a post-doctoral researcher at the university of Hamburg, with Eleanor Frajka Williams, where she investigates pathways for fresh Greenland and Arctic waters into the Labrador Sea.

Driven by sadness, anger and frustration at the lack of action on the climate crisis, at its injustice, and by the realization that producing new knowledge is utterly insufficient to push political actors to take necessary climate measures, she has been involved in climate activism since the start of her PhD. Active in Extinction Rebellion for several years, she contributed to starting the Dutch branch of Scientist Rebellion, a group of worried scientists and academics that engage in climate activism and civil disobedience, and push for their universities and research institutes to act more in line with the climate and ecological emergency.

"Any further delay in concerted anticipatory global action on adaptation and mitigation will miss a brief and rapidly closing window of opportunity to secure a liveable and sustainable future for all (very high confidence)"

IPCC AR6 Synthesis report, 2023
Section 3.4.2

"Dear friends, humanity is on thin ice –
and that ice is melting fast"

UN Secretary general Antonio Guterres, May 2023
speech for the press conference launching the IPCC AR6 synthesis report